THE UNIVERSITY OF CHICAGO

REGULATION OF MYOFIBROBLAST DIFFERENTIATION AND PULMONARY FIBROSIS BY CARDIAC GLYCOSIDES

A DISSERTATION SUBMITTED TO

THE FACULTY OF THE DIVISION OF THE BIOLOGICAL SCIENCES

AND THE PRITZKER SCHOOL OF MEDICINE

IN CANDIDACY FOR THE DEGREE OF

DOCTOR OF PHILOSOPHY

DEPARTMENT OF PATHOLOGY

BY

JENNIFER LA

CHICAGO, ILLINOIS

DECEMBER 2016

Table of contents

List of Figures

List of Abbreviations

Ad-GFP……..Adenoviral-Green Fluorescent Protein
Ad-LacZ……...Adenoviral-LacZ
Ad-TGFBR2……..……..Adenoviral-transforming growth factor β receptor type 2
Ad-Truncated
TGFBR2…….Adenoviral- Truncated transforming growth factor β receptor type 2
AEC…….Alveolar epithelial cell
ATP…….Adenosine triphosphate
cAMP…….Cyclic adenosine monophosphate
COX-2……..Cyclooxygenase-2
ECM……Extracellular matrix
FGF……Fibroblast growth factor
HLF……Human lung Fibroblasts
IL-5……..Interleukin-5
IL-8……..Interleukin-8
IL-10……..Interleukin-10
IL-13……..Interleukin-13
ILD……Interstitial lung disease
IP……..Intraperitoneal
IPF……..Idiopathic pulmonary fibrosis
IV……..Intravenous
LTBP……..Latent Transforming growth factor β binding protein
METS……Metabolic equivalent
MKL1……Megakaryoblasitc leukemia 1
mRNA……messenger Ribonucleic Acid
PBS……Phosphate-buffered saline
PCR……quantitative Polymerase Chain Reaction
PDGF/R……..Platelet derived growth factor / receptor
PGE2……Prostaglandin E2
PKA……...Protein Kinase A
SMA……..Smooth Muscle-α-actin
SRF……Serum Response Factor
TGF-β……...Transforming Growth Factor-β 1
VASP ……Vasodilator-stimulate phosphoprotein

Abstract

Transforming growth factor β-1(TGFβ1) plays a central role in the induction of myofibroblast differentiation and the development of pulmonary fibrosis. Cardiac glycosides (ouabain, digoxin) inhibit the Na^+/K^+-ATPase and thus increase the intracellular $[Na^+]/[K^+]$ ratio within cells. Previous microarray analysis showed cyclooxygenase 2 (COX-2), the rate limiting enzyme required for the synthesis of prostaglandins, was upregulated upon ouabain treatment in multiple cell lines. Given the anti-fibrotic effects of prostaglandins through the activation of protein kinase A (PKA), we examined if cardiac glycosides stimulate COX-2 expression in human lung fibroblasts (HLF) and how they affect myofibroblast differentiation. Ouabain dramatically upregulated COX-2 expression in HLF and induced a sustained activation of PKA, which was inhibited with NS-398 (COX-2 inhibitor) and COX-2 knockdown. Ouabain induced COX-2 expression was lost with treatment of KB-R4943, a Na^+/Ca^{2+} exchanger inhibitor. Furthermore, ouabain inhibited TGFβ1 stimulated RhoA activation, stress fiber formation, SRF activation and myofibroblast differentiation (measured by expression of smooth muscle α-actin, collagen-1, and fibronectin), which were tightly coupled with the change in the intracellular $[Na^+]/[K^+]$ ratio. Although the expression of COX-2 and activation of PKA were highly associated with these effects, neither the inhibition of COX-2 enzymatic activity by NS-398 nor the inhibition of COX-2 expression by siRNA or KB-R4943, rescued the effects of ouabain on TGFβ1 stimulated myofibroblast activation.

When looking directly at the canonical TGFβ1 signaling pathway, we found the inhibition of the Na^+/K^+-ATPase by K^+-free media/ouabain, resulted in a dramatic

downregulation of TGFβR2 mRNA and protein. The downregulation of TGFβR2 was accompanied with the inhibition of TGFβ1-induced Smad2 phosphorylation and myofibroblast differentiation. Given the essential role of TGFβR2 in the initiation TGFβ1-induced signaling and the fibrotic response, we tested if overexpression of TGFβR2 could reverse the effects of ouabain on myofibroblast activation. Overexpression of TGFβR2, by multiple mechanisms, was unable to abolish the inhibitory actions of ouabain on myofibroblast differentiation. Nonetheless, the impedance of the Na^+/K^+-ATPase activity by ouabain dramatically suppressed TGFβ1-induced myofibroblast differentiation at nanomolar concentrations as a result we investigated if ouabain exhibited anti-fibrotic properties in vivo, using the bleomycin model of pulmonary fibrosis in cardiac glycoside sensitive mice ($\alpha1^{S/S}$ mice). To confirm the sensitivity to cardiac glycosides in these mutant mice, we examined the effects of ouabain on both wild-type and $\alpha1^{S/S}$ fibroblasts. Isolated wild-type mouse lung fibroblasts showed no change in TGFβR2 mRNA levels after ouabain treatment, while $\alpha1^{S/S}$ mouse lung fibroblasts showed a drastic downregulation of TGFβR2 mRNA in the presence of ouabain, further indicating the inhibition of the Na^+/K^+-ATPase is required for the downregulation of TGFβR2. Moreover, mice treated with 50 μg/kg per day of ouabain after bleomycin injury demonstrated decreased collagen deposition in the lung as compared to injured PBS controls via the hydroyproline assay.

Together, these data show that ouabain, through the increase in intracellular $[Na^+]/[K^+]$ ratio, drives the induction of COX-2 expression and PKA activation, which is accompanied by decreased Rho activation and myofibroblast differentiation in response to TGFβ1. Furthermore, nanomolar concentrations of ouabain profoundly

downregulated TGFβR2, an important player in the initiation of TGFβ1signaling and the fibrotic response. However, COX-2 expression, PKA activation, and downregulation of TGFβR2 were not sufficient for inhibition of the fibrotic effects of TGFβ1 by ouabain, suggesting additional mechanisms must exist. However, we have demonstrated ouabain potently inhibited TGFβ1-induced myofibroblast differentiation and attenuated pulmonary fibrosis in the bleomycin model, indicating an important role of the Na^+/K^+-ATPase in fibrogenesis in vitro and in vivo.

Chapter 1: Introduction

Idiopathic Pulmonary Fibrosis

Idiopathic pulmonary fibrosis (IPF) is a chronic, progressive, and lethal disease. Grossly, diseased lungs present with fibrosis along the periphery of the lobes in a "honeycombing" pattern (Wolters et al., 2014). Fibroblastic foci, aggregates of actively proliferating myofibroblasts and fibroblasts, are typically found in the fibrotic lungs, and are good indicators of a poor prognosis and decreased survival (Katzenstein and Myers, 1998; Tiitto et al., 2006). Radiographic and clinical syndromes of IPF share many similarities with other interstitial lung diseases (ILD), thus diagnosis poses a significant clinical challenge (Gross and Hunninghake, 2001). Typically, diagnoses are based on exclusion of other possible ILDs and obtaining a surgical lung biopsy is required to confirm suspected IPF (2000a). The estimated prevalence of IPF varies, but an epidemiological study of all ILDs from 1988 to 1990 in Bernalillo County, NM suggested that IPF is more common than previously estimated. In fact, the study showed IPF was the most common form of ILDs, attributing to almost 50% of all ILDs diagnosed (Coultas et al., 1994). The current estimated prevalence is 50 per 100,000, which dramatically increases with age (Raghu et al., 2006a). There are no geographical, racial, or ethnical links to this disorder, however it is more commonly found in men (Raghu et al., 2004). IPF is an age-related disease with most patients falling between the ages of 50-70. From the onset of symptoms, most patients usually present with slow and gradual decline of lung function, with some patients exhibiting acute exacerbations, defined by rapid progression of disease (King Jr et al., 2011). The mean survival time for patients with pulmonary fibrosis is 3-5 years after diagnosis (King et al., 2001; Raghu et al., 2011) and this poses a vexing clinical challenge given the lack of efficacious therapy.

Currently, Pirfenidone and Nintedanib are the only two FDA approved drugs for this disease. Pirfenidone demonstrated anti-fibrotic effects via dietary intake in hamsters with bleomycin-induced pulmonary fibrosis (Iyer et al., 1995, 1998). Its mechanism of action was thought to be through the suppression of pro-inflammatory and pro-fibrotic cytokines, like IL-5, IL-10,IL-13, platelet derived growth factor(PDGF), fibroblast growth factor(FGF), and transforming growth factor β1 (Hirano et al., 2006; Liu et al., 2005; Oku et al., 2008). Pirfendione entered three phase 3, randomized, controlled trials for the treatment of pulmonary fibrosis (Noble et al., 2011). The first trial was conducted over a 52 week period on Japanese patients diagnosed with IPF, following the guidelines of the American Thoracic Society/European Respiratory society Consensus statement (2000b). Eligible participants were given 1,800 mg/day Pirfenidone, 1,200mg/day Pirfendione, or placebo, and after 52 weeks of treatment forced vital capacity, change in the lowest arterial oxygen saturation after a 6 minute exercise, and progression-free survival was measured, where progression was defined by death or decline in more than 10% of baseline forced vital capacity. Both high and lose doses of drug significantly improved forced vital capacity over placebo, but no significant difference was found in the changes in the lowest arterial oxygen saturation after a 6 minute exercise or progression-free survival (Taniguchi et al., 2010). The following clinical trials, studies 004 and 006, took place in Australia, Europe, and North America. Over a 72 week period, patients were given 2403, 1197, or 0 mg/day of drug in study 004, and 2403 or 0mg/day of drug in study 006. The primary endpoint was the change in forced vital capacity. The mean change in forced vital capacity between the highest drug dose and placebo was -8.0% and -12.4% respectively in study 004, while study 006 did not

show any significant difference between the treated and placebo group (Noble et al., 2011). Nintedanib, also known as BIBF 1120, is a small molecule that inhibits vascular endothelial growth factor receptor (VEGFR), fibroblast growth factor receptor (FGFR), and platelet-derived growth factor (PDGFR) (Hilberg et al., 2008). Promising results in a phase 2 trial, which showed improved forced vital capacity, fewer acute exacerbations, and preserved quality of life (Richeldi et al., 2011), led to the start of two phase 3 clinical trials, INPULSIS-1 and INPULSIS-2. The trials were performed in 24 different countries in the Americas, Europe, Asia, and Australia. To qualify, patients must have been diagnosed with IPF within the last 5 years and had to be at least 40 years of age. Eligible participants received either 150mgs of Nintedanib or placebo twice a day for 52 weeks. The primary end point analysis was assessing the rate of decline in forced vital capacity with secondary endpoints being time of onset for the first acute exacerbation and change in quality of life based on the St. George's Respiratory Questionnaire (SGRQ). Similarly to Pirfenidone, both INPULSIS-1 and INPULSIS-2 demonstrated Nintedanib significantly improve forced vital capacity as compared to placebo after 52 weeks of treatment. However, only INPULSIS-2 reported to find significant differences between the time of onset of the first acute exacerbation and the SGRQ scores (Richeldi et al., 2014). Importantly, neither Pirfenidone nor Nintedanib promoted increased survival. Together, these clinical trials suggest that Pirfenidone and Nintedanib significantly improved forced vital capacity without definitively showing improvements in acute exacerbations, quality of life, or survival time. Given Pirfenidone and Nintedanib are the only two FDA approved drugs for IPF, a therapeutic that prolongs survival and maintains quality of life, still requires further investigation.

Idiopathic Pulmonary Fibrosis: The Abnormal Wound Healing Hypothesis and the role of Myofibroblasts.

Pulmonary fibrosis is known to arise from injury to the lung via radiation therapy (Gross, 1977) or administration of certain types of medications (Hay et al., 1991), however the etiology of this disease for most patients is unknown. Studies have divulged that gastroesophageal reflux (Raghu et al., 2006b; Tobin et al., 1998) and exposure to certain environmental (Baumgartner et al., 1997; Hubbard et al., 1996; Iwai et al., 1994) and microbial agents (Lok et al., 2001; Tsukamoto et al., 2000; Ueda et al., 1992) are associated with IPF. Initially it was hypothesized that IPF stems from chronic inflammation (Keogh and Crystal, 1982), where insults to the lung results in continuous and non-resolving inflammation, therefore leading to fibrogenesis of the lung. However, this school of thought has proven to be controversial, given many studies refute the role of inflammation in the pathogenesis of IPF. Huaux and colleagues demonstrated that, although mice deficient in IL-10 produced a greater inflammatory response upon silica injury, they developed less fibrosis than their wild-type littermates (Huaux et al., 1998). Furthermore, in contrast to wild-type mice, αvβ6 knockout mice exhibited an exaggerated inflammatory response after intratracheal bleomycin instillation, but they were protected from fibrosis (Munger et al., 1999). Clinical IPF patients also show little or no response to high doses of glucocorticoid treatment, even in the presence of potent immunosuppressive drugs (Gauldie, 2002; Mason et al., 1999). Evidence now supports that IPF derives from aberrant alveolar epithelial re-epithelialization after injury (Selman et al., 2001; Thannickal et al., 2004)(Figure 1.1). Briefly, the alveolar epithelium is composed of type 1 and type 2 alveolar epithelial cells. The majority of the alveolar

surface area is lined with type 1 alveolar epithelial cells, which act as a barrier for foreign microbes and also facilitate gas exchange (Williams, 2003). Type 2 alveolar epithelial cells secrete surfactant protein to help decrease alveolar surface tension (Clements, 1997). Importantly, damage to the alveolar epithelium is restored by type 2 alveolar epithelial cells. Their capacity to differentiate and proliferate allows for the replenishment of damaged type 1 and type 2 alveolar epithelial cells respectively (Fehrenbach, 2001; Witschi, 1990). When the injured lung fails to properly re-epithelize, due to constant injury or malfunctions of the alveolar epithelial cells, non-resolving wound-healing and fibrogenesis occurs. Studying the early mechanisms involved in alveolar epithelial repair in vivo has proven to be difficult, thus this hypothesis still remains under investigation. However, there are many studies in support of this theory. Ultrastructural studies of fibrotic lungs show abnormalities in the alveolar epithelium (Coalson, 1982; Kawanami et al., 1982) and type II alveolar epithelial cells in a fibrotic lung have a reduced capacity to proliferate and differentiate into type I alveolar epithelial cells after injury (Kasper and Haroske, 1996). Furthermore, continuous injury to type II alveolar epithelial cells induces pulmonary fibrosis and is used as a model of pulmonary fibrosis (Sisson et al., 2010).

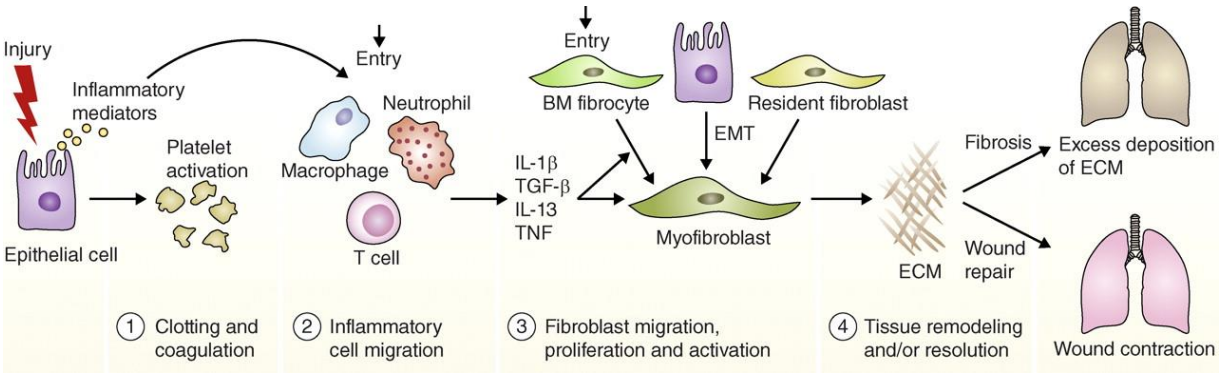

Figure 1.1 Dysregulation of wound healing may result in fibrosis.
Upon injury, alveolar epithelial cells secrete pro-inflammatory cytokines to recruit immune cells. Recruited immune cells remove dead cell debris, foreign organisms, and secrete proinflammatory and profibrotic cytokines. Fibroblasts, which may arise from bone marrow fibrocytes, resident fibroblasts, or EMT of epithelial cells, differentiate into myofibroblasts in response to these pro-fibrotic mediators. Activated myofibroblasts help facilitate wound repair by inducing wound contraction. Dysregulation of any stage in the wound healing process may result in fibrosis. (Wynn et al. 2011)

Myofibroblasts are thought to contribute to the pathogenesis and progressive nature of IPF. They are described as smooth muscle (SM)-like fibroblasts, and display a phenotype which is in an intermediate state between fibroblasts and smooth muscle cells (Desmoulière et al., 2005; Hinz et al., 2007). In 1971, Gabbiani and colleagues first characterized the myofibroblasts, which they called 'modified fibroblasts'. Similar to smooth muscle cells, these 'modified fibroblasts' presented with bundles of fibrils throughout the cytoplasm, as well as dense areas of fibrils resembling 'attachment sites' of smooth muscle. These observations are now appreciated as stress fibers and focal adhesions respectively (Gabbiani et al., 1971). After these initial findings, the expression of cytoskeletal and smooth muscle proteins are now accepted markers of myofibroblasts, smooth muscle (SM) α-actin (SMA) being the most established marker of myofibroblast activation (Hinz et al., 2007; Tomasek et al., 2002). Importantly, under normal conditions, the myofibroblast machinery is essential for wound healing (Darby et al., 2014; Gabbiani, 2003). The expression of smooth muscle α-actin provides the myofibroblast with the ability to produce a strong contractile force to induce wound closure (Gabbiani, 2003; Hinz et al., 2001) and the secretion of extracellular matrix proteins (collagen isoforms, cellular fibronectin, etc.) gives structural integrity and promotes matrix remodeling during the wound healing response. Once the wound is resolved, myofibroblasts undergo apoptosis (Desmoulière et al., 1995) and pathogenesis occurs when fibroblasts/myofibroblasts are signaled to survive and proliferate. A brief description of events after injury is as follows: 1. upon injury, alveolar epithelial cells release pro-inflammatory, pro-coagulant, and pro-fibrotic mediators, to initiate a wound healing response. Amongst these cytokines, transforming growth factor

β1 (TGFβ1) is the most established inducer of myofibroblast differentiation (Sime et al., 1997). 2. Fibroblasts, under stimulation of TGFβ1, differentiate into myofibroblasts, indicated by de novo expression of cytoskeletal, contractile, and extracellular matrix proteins (Biernacka et al., 2011; Hinz, 2006; Leask and Abraham, 2004), all of which facilitate wound healing. 3. After the wound is resolved, myofibroblasts undergo apoptosis (Wynn and Ramalingam, 2012). During aberrant wound healing, it is thought that epithelial cells continue to secrete pro-fibrotic mediators, resulting in increased activation and survival of myofibroblasts. The continuous contraction and deposition of extracellular matrix proteins by myofibroblasts leads to distortion of the alveolar architecture and excessive scarring of the lung respectively. Moreover, the myofibroblast phenotype is associated with secretion of pro-fibrotic factors (connective tissue growth factor (CTGF), insulin-like growth factor (IGF-1) etc.), thus perpetuating the ongoing tissue remodeling and fibrosis. Interestingly, myofibroblasts are invariably found in histologic sections of human lung specimens from patients with pulmonary fibrosis and are thought to be a critical pathogenic cell responsible for the progressive nature of IPF (Leask and Abraham, 2004). Therefore, disrupting cellular mechanisms, which induce and maintain the myofibroblast phenotype, may be a potential strategy to attenuate the ongoing fibrotic response in pulmonary fibrosis.

Transforming Growth Factor B-1: Ligand and Signaling

TGFβ1 is involved in the initiation and progression of pulmonary fibrosis (Bartram and Speer, 2004; Broekelmann et al., 1991; Fernandez and Eickelberg, 2012; Wolters et al., 2014). The Gauldie lab has demonstrated transient overexpression of active TGFβ1 is sufficient to induce pulmonary fibrosis in rats (Sime et al., 1997) and thus the

overexpression of TGFβ1 is now used as a model of pulmonary fibrosis (B Moore et al., 2013). Moreover, lungs of patients with pulmonary fibrosis display upregulated TGFβ1 expression (Bartram and Speer, 2004; Khalil et al., 1996) , therefore it is conceivable that inhibiting TGFβ1 signaling could be a possible approach to treating fibrotic disease. Importantly, disruption of TGFβ1 signaling has demonstrated to be effective in ameliorating fibrosis in vitro and in vivo. In vivo, a specific inhibitor of TGFβR1, SD-209, attenuated TGFβ1 induced pulmonary fibrosis in female sprague-dawley rats (Bonniaud et al., 2005). In vitro, expression of kinase-defective TGFβR2 alone was enough to weaken TGFβ1 stimulated tenascin and fibronectin production in rat lung fibroblasts (Zhao, 1999), and in parallel, treatment with soluble TGFβR2 diminished liver fibrosis in mice (Yata et al., 2002). Although numerous studies have shown restricting the initiation of TGFβ1 signaling hinders myofibroblast differentiation in vitro and attenuates fibrosis in vivo, there still remains a concern that TGFβ1 also plays a key role in regulating inflammation (Sanjabi et al., 2009; Wahl, 1992) and tumor suppression (de Caestecker et al., 2000; Jakowlew, 2006; Massagué, 2008). Therapies interfering with global TGFβ1 signaling may carry out undesirable side effects and an efficacious TGFβ1 inhibitor in humans needs further investigation.

There are 3 mammalian transforming growth factor β isoforms, TGFβ1 being the most potent inducer of myofibroblast differentiation (Massagué, 1992) . TGFβ1 is tightly regulated and initially translated as a large latent complex composed of the latent transforming growth factor β binding protein (LTBP), the latent associated peptide, and the mature TGFβ1 (Rifkin, 2005). The LTBP anchors the biologically inactive dimer (also known as latent TGFβ1), made up of the latent associated peptide and the mature

TGFβ1, to the extracellular matrix. In addition to anchoring the dimer, LTBP is thought to play a role in assembly, secretion, and activation of latent TGFβ1 (Annes et al., 2004; Miyazono et al., 1991). Proteolytic cleavage of the large complex releases the inert dimer, which needs to be further processed to produce the biologically active TGFβ1 (Taipale et al., 1994). The mature TGFβ1 binds an array of receptors, but the canonical signaling involves binding of TGFβ1 to TGFβR1 and TGFβR2 to initiate the Smad pathway (Massagué, 2012) (Figure 1.2). In this pathway, active TGFβ1 binds to TGFβR2 homodimer, a serine threonine receptor kinase. Upon binding, TGFβ1 assumes a conformational change, which allows for binding of a TGFβR1 homodimer, thus resulting in the formation of a hetero-tetramer of TGFβR1 and TGFβR2. When TGFβR1 and TGFβR2 tetradimerize, TGFβR2 phosphorylates and activates TGFβR1. Binding of ligand also triggers receptor internalization into endosomes via clathrin coated pits, which is required for TGFβ1 signaling (Figure 1.3); and disruption of clathrin coated pit formation is associated with loss of TGFβ1 signaling (Di Guglielmo et al., 2003; Penheiter et al., 2002). Smad2/3, a regulatory-Smad, is a substrate for TGFβR1. Under basal conditions, Smad2/3 remains in the cytosol bound to SARA (Smad anchor for receptor activation) via the FYVE domain (Tsukazaki et al., 1998). SARA is important for localizing Smad2/3 near TGFβR1 for Smad2/3 phosphorylation/activation. Once phosphorylated, Smad2/3 dissociates from SARA, heterodimerizes with Smad4 (co-Smad), and translocates into the nucleus. The Smad complex preferentially binds to Smad binding elements (SBE) (Jonk et al., 1998; Zawel et al., 1998) to initiate Smad-dependent gene transcription (Derynck and Zhang, 2003; Feng and Derynck, 2005).

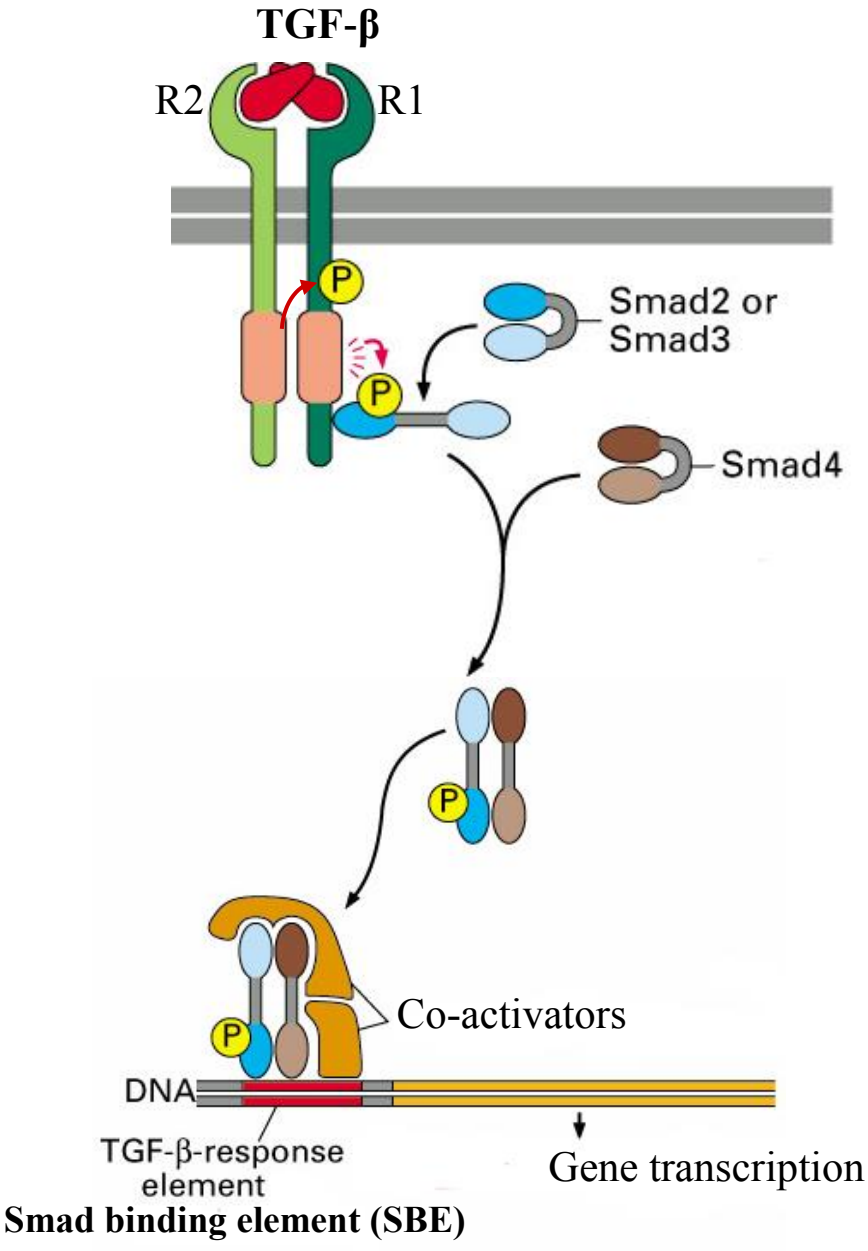

Figure 1.2 Transforming Growth Factor-beta 1 signaling. Simplified scheme of TGFβ1 signaling through the canonical Smad pathway. (Alberts et al., 2002)

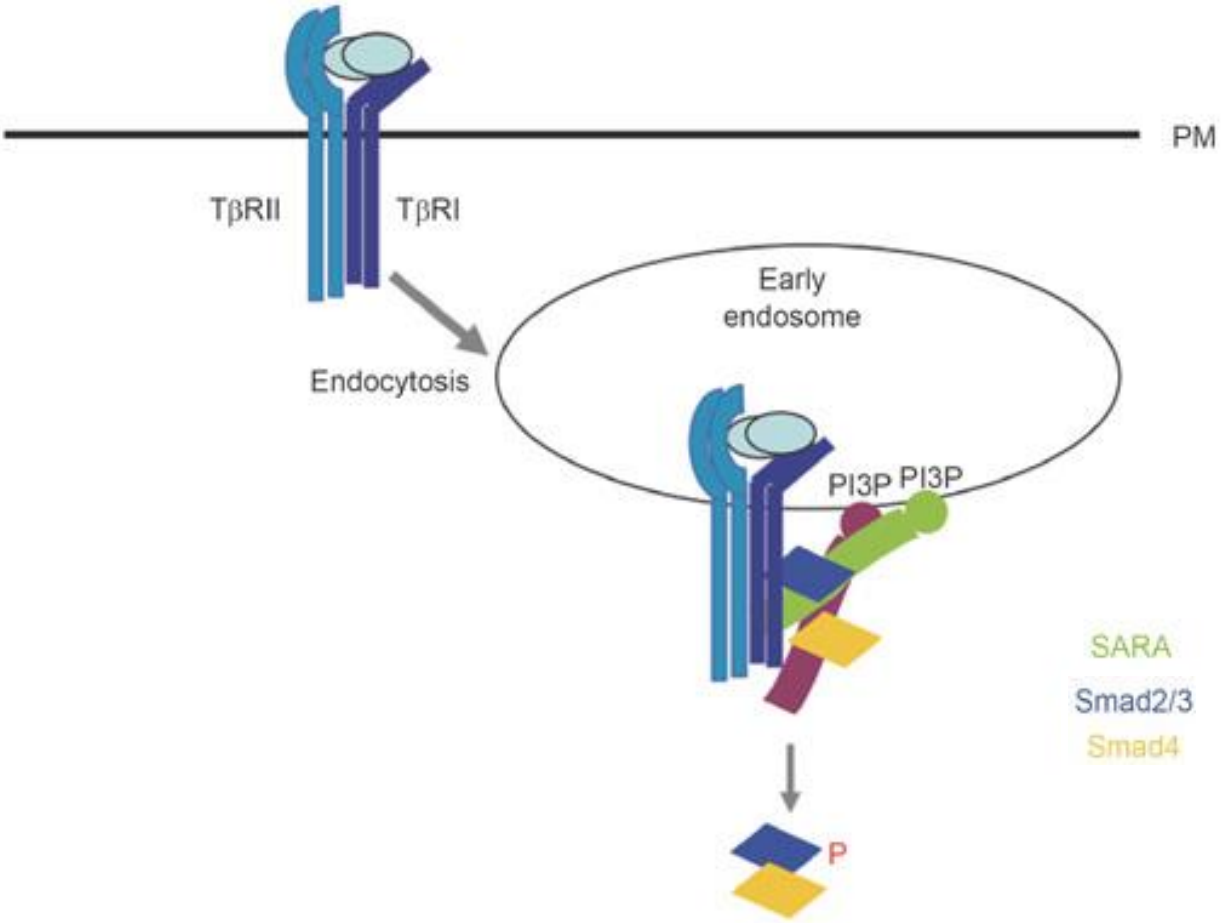

Figure 1.3. Endocytosis of Transforming Growth Factor beta Receptors by clathrin coated pits is required for initiation of TGFβ1 signaling.
The high concentration of phosphatidylinositol-3 phosphate in early endosomes allows for the recruitment of SARA via the FYVE domain. SARA brings SMAD2/3 close to TGFβR1 for receptor-mediated Smad phosphorylation. (Chen, 2009)

As a negative feedback mechanism, Smad2/3 promotes the transcription of Smad7, an inhibitory Smad (von Gersdorff et al., 2000), which competes for binding of TGFβR1, blocking further phosphorylation of regulatory Smads (Briones-Orta et al., 2011).

Regulation of TGFβ1 induced myofibroblast differentiation.

The mechanism of myofibroblast differentiation by TGFβ1 has been studied by many groups (Midgley et al., 2013; Serini et al., 1998; Thannickal et al., 2003). In our laboratory, we found the activation of serum response factor (SRF) by TGFβ1 is required for myofibroblast differentiation in pulmonary fibroblasts (Sandbo et al., 2009). We showed fibroblasts upregulated the expression of SRF in response to 24 and 48 hours stimulation of TGFβ1, which was accompanied with increased expression of smooth muscle actin, indicative of myofibroblast differentiation. Suppression or downregulation of SRF through pharmacological inhibitor CCG-1423 or ad-shSRF, blocked TGFβ1 induced myofibroblast activation, suggesting the activity of SRF is necessary for differentiation (Figure 1.4). Interestingly, activation of PKA via various mechanisms, potently inhibited myofibroblast differentiation, and was coupled with the loss of TGFβ1 induced SRF expression (Figure 1.5). A following study of ours revealed TGFβ1 induced myofibroblast differentiation by SRF relied on the following series of events; 1. Smad-dependent activation of RhoA, 2. stress fiber formation, 3. nuclear accumulation of megakaryoblastic leukemia 1 (MKL1), a coactivator of SRF, and 4. induction of SRF dependent genes (Sandbo et al., 2011).

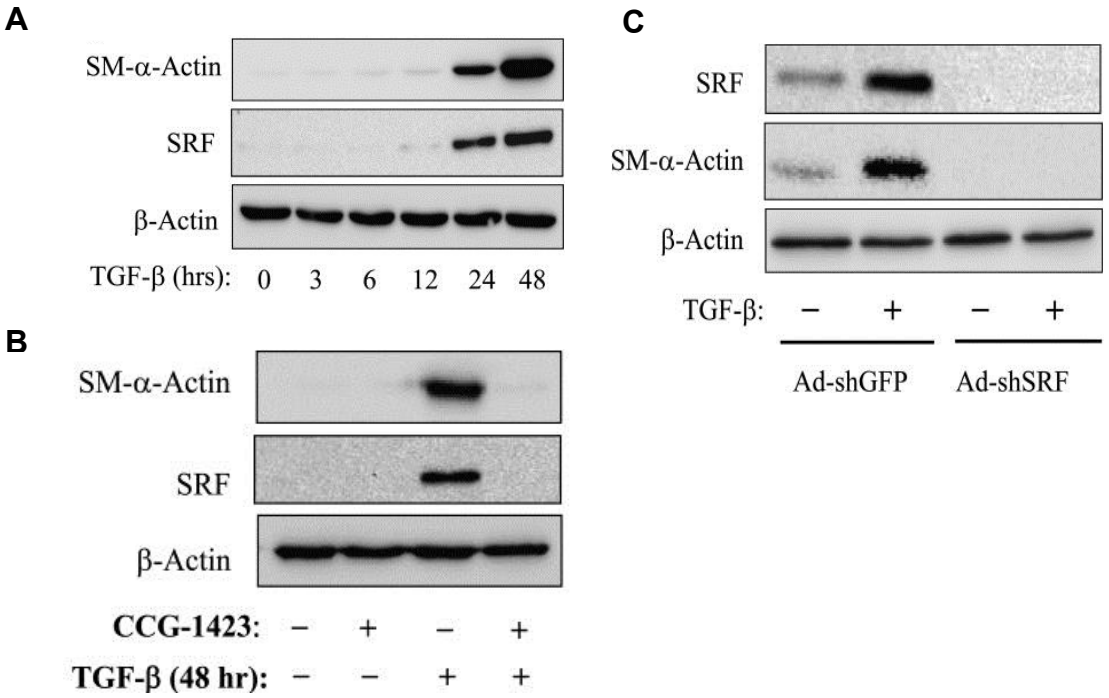

Figure 1.4. Pulmonary Myofibroblast differentiation is dependent on Serum Response Factor (SRF).
(**A**) Human lung fibroblasts were grown to subconfluence, serum-starved overnight, and stimulated with 2 ng/ml TGFβ1 for the indicated times. (**B**) Serum-starved human lung fibroblasts were pretreated with 10 μM CCG-1423 for 1 hour, followed by stimulation with 2 ng/ml TGFβ1 for 48 hours. (**C**) Subconfluent human lung fibroblasts were transduced with recombination-deficient adenovirus expressing short hairpin RNA against SRF (Ad-shSRF), or with control adenovirus expressing shRNA against GFP (Ad-shGFP) in 0.1% bovine serum albumin for 48 hours, followed by stimulation of cells with 2 ng/ml TGFβ1 for an additional 48 hours. All cell extracts were analyzed by Western blotting with antibodies against SRF, SM–α-actin, or β-actin as indicated. (Reprinted with permission of the American Thoracic Society. Copyright © 2016 American Thoracic Society. Sandbo.N, Kregel S, Taurin S, Bhorade S, Dulin NO. 2009. Critical role of serum response factor in pulmonary myofibroblast differentiation induced by TGF-beta. 41. 332-338 The *American Journal of Respiratory Cell and Molecular Biology* is an official journal of the American Thoracic Society.)

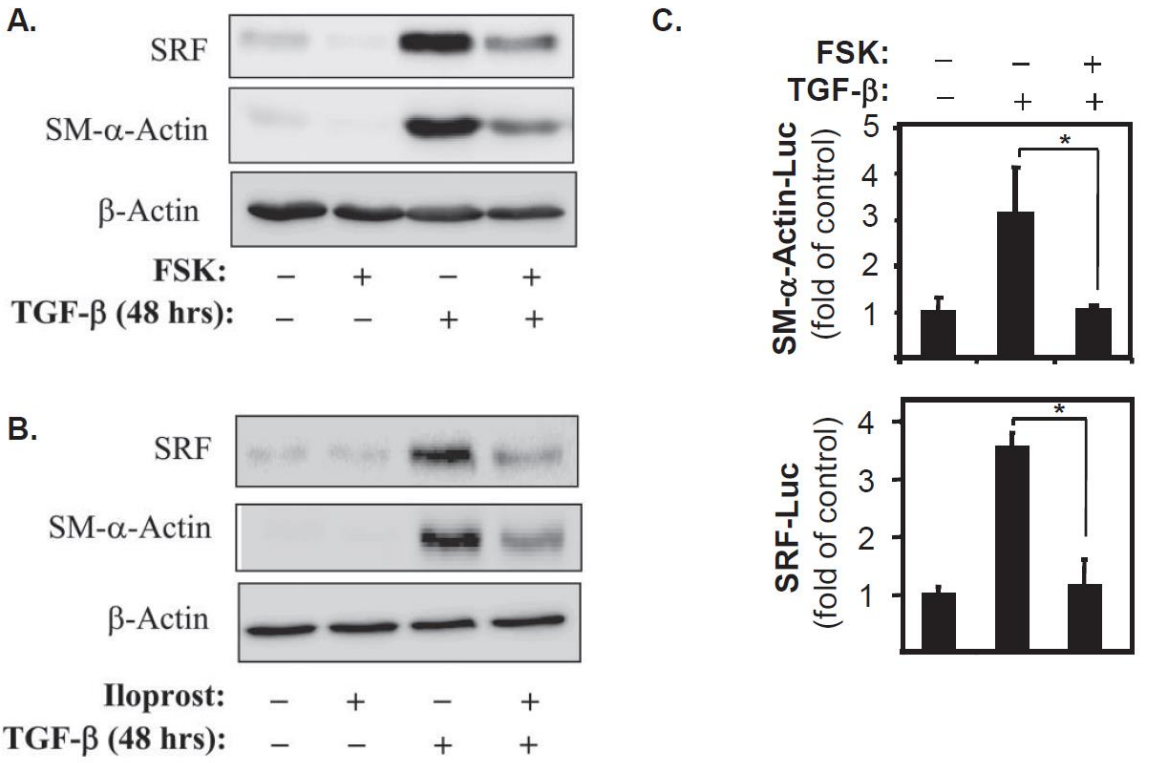

Figure 1.5. Inhibition of Myofibroblast differentiation by protein kinase A (PKA) Activators.

(**A**) Serum-starved human lung fibroblasts were pretreated with 10 μM forskolin (FSK) for 15 minutes, followed by stimulation with 2 ng/ml TGFβ1 for 48 hours. The cell extracts were analyzed by Western blotting with antibodies against SRF, SM–α-actin, or β-actin as indicated. (**B**) Serum-starved human lung fibroblasts were pretreated with 10 μM Iloprost for 15 minutes, followed by stimulation with 2 ng/ml TGFβ1 for 48 hours. The cell extracts were analyzed by Western blotting with antibodies against SRF, SM–α-actin, or β-actin as indicated. (**C**) Human lung fibroblasts were transfected with luciferase reporters (SM–α-actin promoter or SRF-luciferase reporter), along with thymidine kinase-driven renilla (TK-RL) control reporter. Serum-starved cells were pretreated with 10 μM FSK for 15 minutes, followed by stimulation with 2 ng/ml TGFβ1 for 24 hours. The activity of luciferase was then measured in cell lysates and normalized to the activity of renilla. Data represent the results of at least three experiments performed in triplicate (*$P < 0.05$). (Reprinted with permission of the American Thoracic Society. Copyright © 2016 American Thoracic Society. Sandbo.N, Kregel S, Taurin S, Bhorade S, Dulin NO. 2009. Critical role of serum response factor in pulmonary myofibroblast differentiation induced by TGF-beta. 41. 332-338 The *American Journal of Respiratory Cell and Molecular Biology* is an official journal of the American Thoracic Society.)

Fibroblasts, in response to TGFβ1, formed stress fibers and induced the SRF luciferase reporter gene in a RhoA and Smad-dependent manner. Disruption of the actin cytoskeleton by latrunculin-B, a toxin that depolymerizes actin, efficiently blocked TGFβ1 stimulated stress fiber formation and SRF luciferase, suggesting actin polymerization is required for SRF-dependent transcription. Miralles et al., demonstrated actin dynamics regulate SRF activity through MKL1 (Miralles et al., 2003), as a result we investigated the effects of actin polymerization on MKL1 nuclear accumulation in human lung fibroblasts in response to TGFβ1. In addition to promoting stress fiber formation and myofibroblast activation, TGFβ1 triggered nuclear accumulation of MLK1, both of which were blocked by latrunculin-b, indicating anti-fibrotic effects of latrunculin-b. Unfortunately, the toxicity of latrunculin B limits the therapeutic value of this drug as a treatment for pulmonary fibrosis. Alternatively, the activation of PKA potently suppressed TGFβ1-stimulated stress fiber formation and myofibroblast differentiation. Together, these data suggests actin polymerization is required for TGFβ1-induced myofibroblast differentiation and latrunculin-b/activation of PKA inhibits myofibroblast differentiation by blocking stress fiber formation. The following model is proposed: TGFβ1 induces Smad-dependent gene transcription which contributes to the activation of RhoA. RhoA stimulates the polymerization of filamentous-actin (f-actin) from globular-actin (g-actin). In its monomeric form, g-actin binds to MKL1, thus sequestering the co-activator from binding to SRF. Induction of f-actin formation reduces the pool of available g-actin, and as a result frees MLK1 and allows it to partner with SRF.

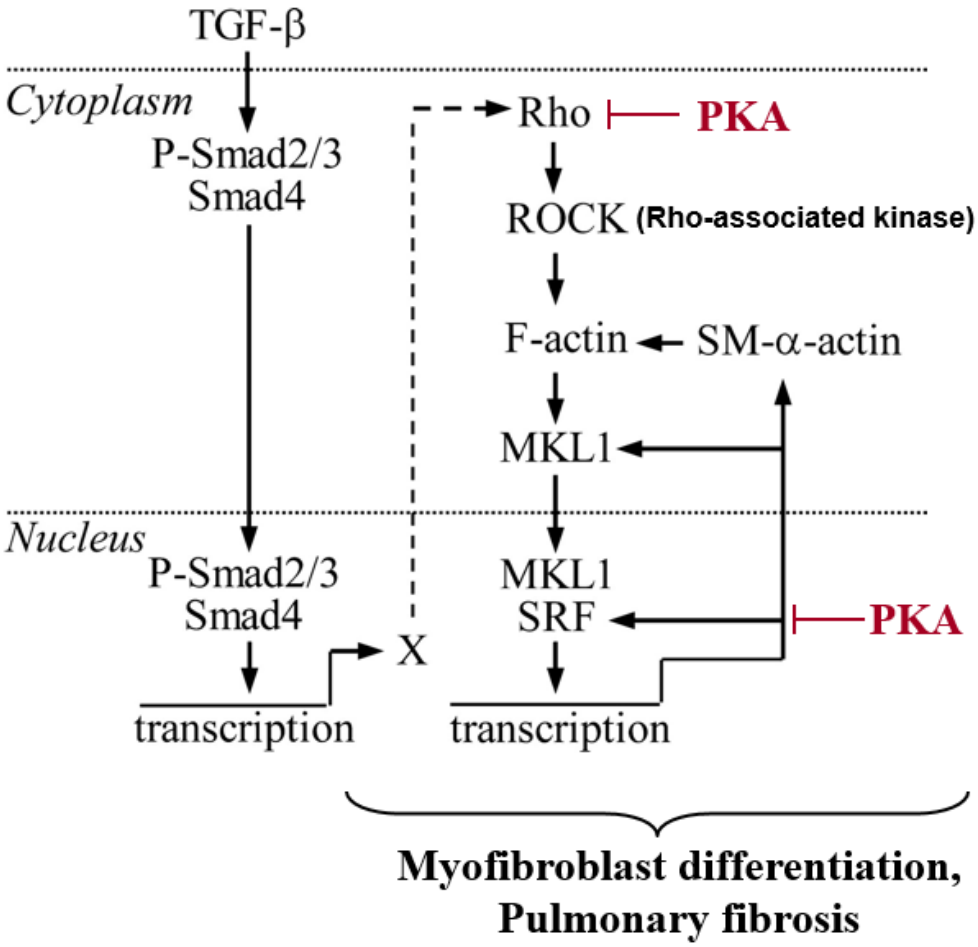

Figure 1.6. Alternative mechanism to inhibit myofibroblast differentiation: The proposed model for TGFβ1 induced differentiation markers is as follows: *1*) TGFβ1 stimulates a Smad-dependent expression of signaling molecules (X) driving activation of RhoA; *2*) RhoA-induced stress fiber formation promotes MKL1 nuclear accumulation and SRF-dependent transcription of SM α-actin, as well as *3*) of SRF itself and MKL1, both driving the SRF-dependent gene transcription further. Activation of PKA inhibits RhoA and SRF, thus myofibroblast differentiation. Inhibiting the SRF axis via stimulation of PKA activity may be a potential therapeutic for fibrotic disease. (Sandbo et al. 2011)

The activated SRF-MKL1 complex binds to serum response elements (SRE) to promote transcription of fibrotic genes, including production of extracellular matrix components and smooth muscle α-actin (Sandbo et al., 2009, 2011) (Figure 1.6). Importantly, studies have confirmed inhibiting SRF dependent gene transcription elicits anti-fibrotic effects in vitro and in vivo. Blocking the transient receptor potential vanilloid 4 (TRPV4) channel modulates actin remodeling and inhibits myofibroblast differentiation (Rahaman et al., 2014). CCG-203971, a pharmacological inhibitor of SRF/MKL1 dependent transcription, attenuated pulmonary fibrosis in both the bleomycin and the type II alveolar epithelial cell injury model of pulmonary fibrosis (Sisson et al., 2015). Thus, targeting SRF, an axis downstream of TGFβ1 signaling, may be an approach to treating pulmonary fibrosis and may eliminate the concern of deleterious side effects from global inhibition of TGFβ1 (Sandbo et al., 2009, 2011).

COX-2 is an inducible protein upregulated in response to an inflammatory stimuli (Hla and Neilson, 1992; O'Banion et al., 1991). Importantly, it is the rate limiting enzyme required for converting arachidonic acid to prostaglandin E2 (PGE2) (Smith et al., 1996), a lipid compound that modulates inflammation (Figure 1.7). PGE2 has been shown to mediate inflammation by stimulating the production of IL-8 (Yu and Chadee, 1998) and monocyte chemoattractant protein-1(MCP-1) (Nakayama et al., 2006), resulting in the migration of neutrophils and monocytes/macrophages respectively. On the contrary, another study demonstrated PGE2 promoted the secretion of IL-10 by macrophages, leading to an anti-inflammatory response (MacKenzie et al., 2013). The paradoxical characteristics of this lipid may be attributed to its multiple receptors, the G protein coupled receptors, EP1, EP2, EP3, and EP4, (Ricciotti and FitzGerald, 2011).

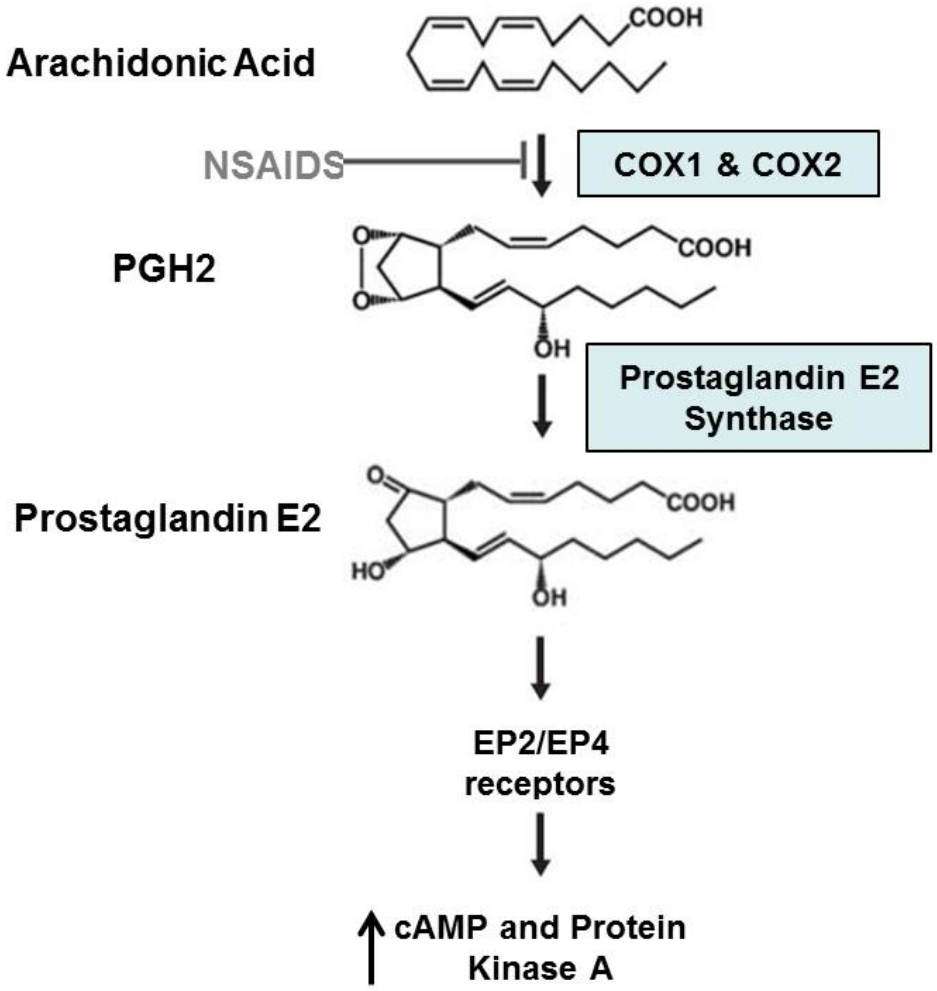

Figure 1.7. Prostaglandin E2 Biosynthesis by Cycoloxygenase-2. Cyclocoxygenase-1 and 2 (COX-1 & COX-2) are enzymes involved in the rate limiting step of converting arachidonic acid to prostaglandin E (PGE2). COX-1 is a constitutively expressed protein required for producing basal levels of prostaglandins. COX-2 is an inducible protein which is upregulated during an inflammatory response. The induction of COX-2 protein results in increased PGE2 synthesis. PGE2 can bind to four G-protein coupled receptors (EP1-4), and activation of EP2/EP4 receptors results in increased cAMP levels and activation of protein kinase A.

Stimulation of EP2 and EP4, G_s receptors, boost intracellular cAMP production and thus drives the activation of PKA. On the other hand, activation of EP1 and EP3, G_i receptors, reduces intracellular cAMP and increases Ca^{2+} levels (Sugimoto and Narumiya, 2007). Given PGE2 has the capacity to activate PKA via the EP2/EP4 receptors; it may modulate the fibrotic response. Interestingly, multiple observations in the field have recorded IPF patients have decreased COX-2 and PGE2 expression. Immunostaining and lung lavage fluid revealed IPF lungs displayed significantly lower COX-2, (Petkova et al., 2003) prostaglandin E1, and prostaglandin E2 levels (Borok et al., 1991) when compared to healthy controls. Further, Wilborn and colleagues discovered fibroblasts isolated from IPF patients have a reduced capacity to induce COX-2 expression and have a decreased ability to synthesize PGE2. Serum-starved normal lung fibroblasts produced 5 fold more PGE2 than IPF fibroblasts. Given COX-2 is required for efficient synthesis of PGE2 from arachidonic acid, the lack of PGE2 production by IPF fibroblasts may be due to abnormal COX-2 induction. In the same study, Wiborn et al found fibroblasts from patients with IPF have a lower capacity to induce COX-2 expression upon lipopolysaccharide (LPS) stimulation (Wilborn et al., 1995). Epigenetic modification of the COX-2 gene is thought to contribute to the observed lack of COX-2 expression in IPF cells. Coward and colleagues demonstrated IPF fibroblasts transcribe COX-2 mRNA at a significantly slower rate in comparison to normal lung fibroblasts. However, treatment of IPF fibroblasts with histone deacetylase inhibitors or overexpression of histone acetyltransferases, in conjunction with stimulation with pro-inflammatory cytokines, enhanced the induction of COX-2 protein expression, suggesting IPF fibroblast may have a more closed chromatin due to

malfunction in histone acetylation (Coward et al., 2009). In addition, 5-aza-2'-deoxycytidine, a DNA methylation inhibitor, restored expression of COX-2 mRNA in fibrotic lung fibroblasts, allowing fibrotic fibroblast to synthesize PGE2 at a similar capacity to control fibroblasts (Evans et al., 2016). Importantly, COX-2 and PGE2 have demonstrated to exhibit anti-fibrotic effects in vivo and in vitro, and it is thought that the lack of these two macromolecules may contribute to the onset and/or progression of IPF. In vivo, COX-2 knockout mice developed worse fibrosis than wild type mice upon bleomycin injury (Bonner et al., 2002) and administration of PGE2 attenuated pulmonary fibrosis in the bleomycin model (Dackor et al., 2011). In vitro, PGE2 induces fibroblast apoptosis (Huang et al., 2009), suppresses fibroblast proliferation (Lama et al., 2002), and inhibits myofibroblast differentiation (Thomas et al., 2007). Further, there is evidence to support the inhibition of myofibroblast differentiation by PGE2 was through the activation of PKA (Huang et al., 2007, 2008; Kolodsick et al., 2003). As previously mentioned, PKA negatively regulates SRF activity (Davis et al., 2003; Hogarth et al., 2004), and we and others have shown PKA activators are inhibitors of myofibroblast differentiation in vitro (Kach et al., 2013, 2014, Sandbo et al., 2009, 2011). Further, given the potent antifibrotic effects of prostaglandins, iloprost, a prostacyclin analogue, was brought to clinical trials. Unfortunately its therapeutic value was limited due to its negative side effects such as vasodilatation of pulmonary vascular beds. Therefore, identifying PKA-activating molecules without such side effects remains unaccomplished.

Animal Models

Animal models serve as the basis for understanding the pathogenesis of IPF. The lung injury (asbestosis, silica, bleomycin), cytokine overexpression (TGFB, TGFA, IL-13, IL-1B, TNFA overexpression), and familial models (SFTPC, SFTPA2, TERT, TERC, and HPS mutations) are some examples of animals models used to study IPF (B Moore et al., 2013). Unfortunately, none of these existing models fully recapitulate IPF; moreover, most models instead generally resemble models of interstitial lung diseases. Despite that, animal research has been important in providing insight on the roles of other factors that contribute to fibrosis in vivo. Currently, the bleomycin model is the most established and frequently used model (Moore and Hogaboam, 2008). Bleomcyin has been employed for decades as a treatment for various types of cancers and its mechanism of action is thought to be through inducing DNA strands breaks, thus interrupting cell replication (Chen et al., 2008; Stubbe and Kozarich, 1987). Notably, an adverse side effect of bleomycin treatment is pulmonary fibrosis, which triggered the use of bleomycin in animal models. Intratracheal delivery of bleomycin in mice is the most commonly applied technique (B Moore et al., 2013); however multiple routes of administration (intravenous, intraperitoneal, subcutaneous, intratracheal, and intramuscular) can induce pulmonary fibrosis in a variety of animal species, including rodents, dogs, and monkeys (Muggia et al., 1983). The time course of bleomycin-induced lung fibrosis via intratracheal instillation has been characterized in mice (Izbicki et al., 2002). The initial single dose of bleomycin directly damages alveolar epithelial cells. Inflammatory cells migrate to the damage alveoli within the first week (Janick-Buckner et al., 1989) and signs of fibrosis start at day 14 with maximal fibrosis seen at

day 21-28 (Izbicki et al., 2002; Schrier et al., 1983). The ease of delivery and short time line for fibrosis manifestation are amongst the major advantages of this bleomycin model. However, this model does have its shortcomings and fails to recapitulate many characteristics of IPF. In contrast to IPF found in humans, mice lungs injured by bleomycin lack fibroblastic foci, develop diffuse and centralized fibrosis, and exhibit resolving fibrosis (Degryse and Lawson, 2011). Moreover, the development of fibrosis in response to bleomycin in rodents is strain, age, and gender dependent, thus it is important to have age, sex, and strain matched controls when using the bleomycin model (Redente et al., 2011; Schrier et al., 1983).

The Na/K ATPase/ Cardiac Glycosides

The Na^+/K^+-ATPase is an integral plasma protein required for maintaining the electro-chemical gradient. The pump is made up of the catalytic α subunit and the regulatory β subunit. The α subunit hydrolyzes ATP to pump 3 Na^+ out of the cell and 2 K^+ ions into the cell against their concentration gradient. Briefly, when the enzyme is in the E1-ATP state, it has a high affinity for Na^+ ions. Upon binding of 3 Na^+ ions, ATP phosphorylates the pump, occluding the Na^+ ions. A conformational change occurs, resulting in the release of the 3 Na^+ ions extracellularly, and allowing for extracellular K^+ ions to bind. Binding of the K^+ ions is followed by dephosphorylation of the protein by aqueous hydrolysis, thus occluding the K^+ ions. Then ATP binds to the complex, induces a conformational change, and releases the K^+ ions intracellularly. The enzyme returns to the original E1-ATP state and repeats the process (Kaplan, 2002). The end result is the maintenance of a high K^+ and low Na^+ intracellular concentration, which is important in regulating osmotic balance, cell volume, and the resting potential.

Furthermore, the concentration gradient established by the pump fuels many secondary transporters, like the Na^+/Ca^{2+}, Na^+/H^+, and Na^+/Cl^- exchanger. The β subunit stabilizes the enzyme (Ackermann and Geering, 1990; Geering et al., 1989, 1996) and acts as a molecular chaperone to assist in the transport and insertion of the α subunit to the plasma membrane (Geering, 2001). Studies have shown the α subunit is unable to perform its catalytic function alone and the expression of both the α and β subunit is required for a functional Na^+/K^+-ATPase (Noguchi et al., 1987). The dimerization of the α subunit with the β subunit stimulates structural changes in the α subunit, transforming it from a trypsin sensitive to a trypsin resistant protein, suggesting the β subunit is involved in structural stabilization and maturation of the α subunit (Geering et al., 1996). There are 4 known α and 3 known β mammalian isoforms, and the combination of the α and β dimerization is cell and tissue specific (Levenson, 1994; Tokhtaeva et al., 2012). However, the α1β1 dimer has been shown to be present in most tissues.

Schatzmann identified cardiac glycosides as specific inhibitors of the Na^+/K^+-ATPase (Schatzmann and Räss, 1965), and later studies established these molecules bind to the α subunit to inhibit its function (Laursen et al., 2013; Lingrel et al., 1997; Yatime et al., 2011). In 1785, William Withering, an English physician, discovered the active ingredient in the foxglove plant, digoxin (cardiac glycoside), improved symptoms of congestive heart failure (Silverman, 1989). Since then, digoxin has been used for treatment of congestive heart failure and cardiac arrhythmias in the states (Aronow and Aranow, 1992). Ouabain, a cardiac glycoside isolated from Strophanthus gratus (Pubchem, 2016)**,** is prescribed in Europe for similar cardiac dysfunctions. The major mechanism contributing to the positive inotropic effects of the heart by cardiac

glycosides is through the regulation of intracellular Ca^{2+}. Inhibition of the Na^{+}/K^{+}-ATPase leads to an increase in the intracellular $[Na^{+}]/[K^{+}]$ ratio and depolarization of cells, resulting in the activation of the Na^{+}/Ca^{2+} exchangers and of the voltage-gated Ca^{2+} channels, both leading to an increase in the intracellular Ca^{2+} concentrations, which stimulates a stronger cardiac muscle contraction (Blaustein and Lederer, 1999).

The use of cardiac glycosides has been well established as a therapeutic for cardiac dysfunctions for decades, however new research has suggested they may regulate other signaling pathways, and can be repurposed for new therapeutic applications. As mentioned previously, Na^{+}/K^{+}-ATPase controls many other secondary transporters, thus playing an important role as a signal transducer (Aperia, 2007; Scheiner-Bobis and Schoner, 2001; Xie and Askari, 2002). During the last two decades, a number of studies reported that along with inhibition of the Na^{+}/K^{+}-pump and modulation of the canonical Na_i^{+}/K_i^{+} -dependent cell functions, cardiac glycosides may have Na_i^{+}/K_i^{+}–independent effects, like activation of Ras/Raf/ERK1/2, phosphatidylinositol 3-kinase (PI(3)K), PI(3)K-dependent protein kinase B, phospholipase C, Ca_i^{2+} oscillations, promoting the interaction of Na^{+}/K^{+} -ATPase with the membrane-associated nonreceptor tyrosine kinase Src, and augmenting the production of reactive oxygen species (for review, see Aperia, 2007; Liu and Xie, 2010). Studies unveiling such new findings have led cardiac glycosides to enter preclinical studies for cancer therapy (Menger et al., 2013; Slingerland et al., 2013). However, the first observation of possible anti-cancer effects of cardiac glycosides was noted in 1979 by Dr. Stenkvist. He noticed breast cancer tumor-cells in breast cancer patients taking cardiac glycosides showed more benign characteristic as compared to patients not

taking cardiac glycosides (Stenkvist et al., 1979). Moreover, breast cancer patients on digitalis were ~10 times less likely to have recurring cancer 5 years after mastectomy, suggesting cardiac glycosides may play a role in regulating aggressiveness of breast cancer (Stenkvist et al., 1982). A 20 year follow-up showed that 6% versus 34% of patients died from breast cancer when on digitalis versus not on digitalis (Stenkvist, 1999). Interestingly, our findings indicate cardiac glycosides may have anti-fibrotic properties. We discovered the inhibition of the Na^+/K^+-ATPase by cardiac glycosides dramatically upregulates COX-2 expression and PKA activation while potently downregulating TGFβR2 mRNA and protein. Furthermore these effects were accompanied with the inhibition of TGFβ1 induced myofibroblast activation in pulmonary fibroblasts. In vivo, ouabain exhibited anti-fibrotic effects in the bleomycin model, suggesting cardiac glycosides may also be repurposed for treatment of fibrotic disease.

Hypothesis and Specific Aims

Pulmonary fibrosis, defined by excessive scarring of the lung, is a fatal disease with a survival rate of 3 to 5 years. The prevailing hypothesis is that abnormal wound healing is the root cause of this disease. Myofibroblasts, smooth muscle like cells activated in the presence of pro-fibrotic cytokines, are commonly found in the lung of patients with pulmonary fibrosis, and are thought play a significant role in the onset and progression of IPF. Therefore it is hypothesized that the inhibition of myofibroblast differentiation may be important in treating this fibrotic disease. We have found that ouabain and digoxin, part of the family of cardiac glycosides, inhibit myofibroblast differentiation in response to TGFβ1. No research has been conducted to examine the role of cardiac glycosides in the regulation of myofibroblast differentiation or pulmonary fibrosis. Based

on my preliminary data, I propose an innovative hypothesis that cardiac glycosides regulate myofibroblast differentiation and pulmonary fibrosis through a dual mechanism involving the induction of cyclooxygenase-2 (COX-2) expression and activation of PKA, and through downregulation of TGFβ receptor-2 (TGFβR2). To test this hypothesis I propose the following aims:

Specific Aim # 1. Examine the mechanism of by which cardiac glycoside induced COX-2 expression to regulate myofibroblast activation in vitro.

Specific Aim #2. Examine the mechanism of by which cardiac glycosides regulate myofibroblast activation through the downregulation of TGFβR2. I will also investigate the effect of ouabain administration on the development and progression of pulmonary fibrosis in the bleomycin mouse model of the disease.

Significance. Idiopathic pulmonary fibrosis (IPF) is a detrimental disease with a mean survival rate of 3-5 years (Ley et al., 2011; 2000a)**.** Currently there are no effective FDA approved treatments for IPF and a novel therapeutic target is needed. This study may lead to the development of new strategies for treatment of IPF. Fundamentally, this study will uncover new roles of the Na^+/K^+-ATPase in the control of myofibroblast differentiation and a novel mode of action of cardiac glycosides.

Chapter 2

Regulation of myofibroblast differentiation by cardiac glycosides

Abstract

Myofibroblast differentiation is a key process in pathogenesis of fibrotic diseases. Cardiac glycosides (ouabain, digoxin) inhibit the Na^+/K^+-ATPase, resulting in the increase of the intracellular $[Na^+]/[K^+]$ ratio in cells. A microarray analysis suggested that elevation of the intracellular $[Na^+]/[K^+]$ ratio may promote the expression of cyclooxygenase-2 (COX-2), a critical enzyme in the synthesis of prostaglandins. Given the anti-fibrotic effects of prostaglandins through the activation of protein kinase A (PKA), we examined if cardiac glycosides stimulate COX-2 expression in human lung fibroblasts and how they affect myofibroblast differentiation. The cardiac glycoside, ouabain, stimulated a profound COX-2 expression and a sustained PKA activation, which was blocked by COX-2 inhibitor or by COX-2 knockdown. Ouabain-induced COX-2 expression and PKA activation were abolished by the inhibitor of the Na^+/Ca^{2+} exchanger, KB-R4943. Ouabain inhibited TGFβ1 induced RhoA activation, stress fiber formation, SRF activation, and myofibroblast activation. These effects were recapitulated by the increase in intracellular $[Na^+]/[K^+]$ ratio through the treatment of cells with K^+-free media or with digoxin. Although the inhibition of COX-2 or of the Na^+/Ca^{2+} exchanger blocked ouabain-induced PKA activation, this failed to reverse the inhibition of TGFβ1-induced RhoA activation or myofibroblast differentiation by ouabain. Together, these data demonstrate that ouabain, through the increase in intracellular $[Na^+]/[K^+]$ ratio, drives the induction of COX-2 expression and PKA activation, which is accompanied by decreased RhoA activation and myofibroblast differentiation in

response to TGFβ1. However, COX-2 expression and PKA activation are not sufficient for inhibition of the fibrotic effects of TGFβ1 by ouabain.

Results

Ouabain increases COX-2 expression and activates PKA in human lung fibroblasts. As shown in figure 2.1, quiescent human lung fibroblasts (HLFs) do not express detectable levels of COX-2. Treatment of HLF with 100 nM ouabain resulted in a profound and sustained expression of COX-2 of both mRNA and protein levels (Figure 2.1A). Given the established role of COX-2 in the production of prostanoids, which act through receptor-mediated activation of cAMP/PKA signaling, we assessed PKA activation in HLFs by examining phosphorylation of the PKA substrate, vasodilator-stimulated phosphoprotein (VASP), using electrophoretic mobility shift assay as a reporter for PKA activity (Davis et al., 2003). As shown in figure 2.1B, 100 nM ouabain stimulated a sustained VASP phosphorylation at 24-48 hours, which paralleled COX-2 expression in HLF cells. Furthermore, the specific inhibitor of COX-2, NS-398, completely abolished ouabain-induced VASP shift, while increasing COX-2 expression (Figure 2.1B). To confirm the specificity of NS-398, we performed a knockdown of COX-2 mRNA. Figure 2.1C demonstrates a highly efficient knockdown of COX-2 expression in HLF, resulting in suppression of VASP shift triggered by ouabain. Together, these data demonstrate that ouabain induces the expression of COX-2 in HLF, which functionally translates to activation of PKA.

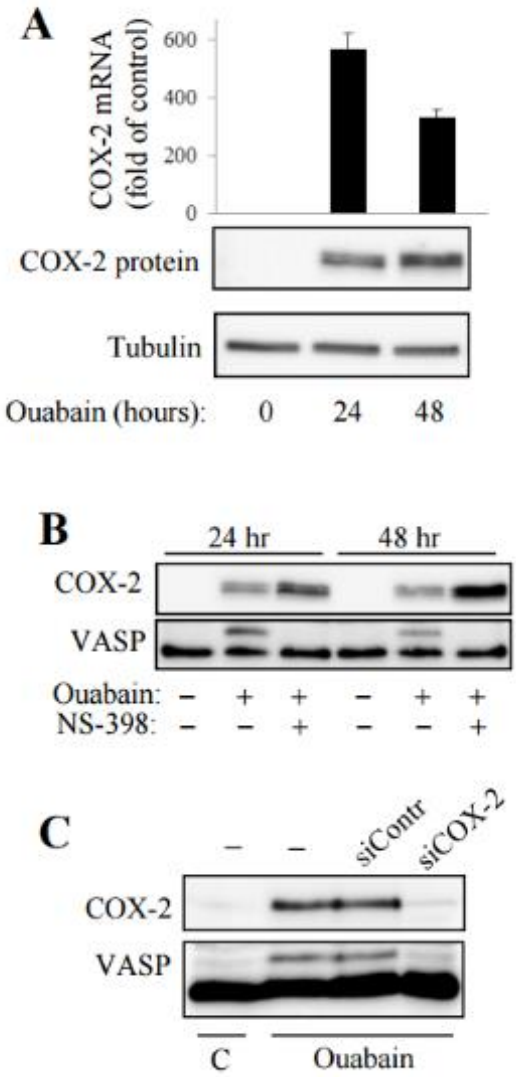

Figure 2.1. Ouabain-induced COX-2 expression and PKA activation in human lung fibroblasts (HLF).
Serum-starved HLFs were treated with 100 nM ouabain with or without 1 μM NS-398 for the times indicated. Cells were analyzed by real time qPCR for COX-2 mRNA levels (**A**), or by Western blotting for COX-2 expression and VASP shift (**A-C**). **C**. HLFs were transfected with a scramble or COX-2 siRNAs, serum-starve for 24 hours, and treated with 100 nM ouabain for 24 hours. Shown are the Western blots for COX-2 and VASP. (La et al. 2016)

Activation of Na^+/Ca^{2+}-exchanger mediates COX-2 expression and PKA activation in HLF. It is well-documented that elevation of the $[Na^+]_i/[K^+]_i$ ratio, as a result of inhibition of Na^+/K^+-ATPase, typically leads to increases in $[Ca^{2+}]_i$ via activation of the reverse mode of the Na^+/Ca^{2+} exchanger (Blaustein and Lederer, 1999) and/or of voltage-gated Ca^{2+} channels (McDonald et al., 1994) – a phenomenon termed excitation-transcription coupling (Orlov and Hamet, 2015). It has been shown also that agonist-induced COX-2 expression is mediated by intracellular Ca^{2+} (Nakao et al., 2001; Zhu et al., 2002). To explore the role of Ca^{2+} in COX-2 expression triggered by ouabain, we used inhibitors of the voltage-gated L-type Ca^{2+} channels, nicardipine, and of the Na^+/Ca^{2+} exchanger, compound KB-R4943. We found that exposure of HLF to 100 nM ouabain increased the rate of $^{45}Ca^{2+}$ influx by ~50% (Figure 2.2A). These differences were preserved in the presence of nicardipine but were abolished by KB-R4943. Figure 2.2B shows that KB-R4943 sharply decreases COX-2 expression and VASP shift in response to ouabain. Neither COX-2 expression nor VASP phosphorylation were affected by nicardipine.

Disruption of actin stress fibers by ouabain in HLF. Microscopy analysis showed that ouabain treatment resulted in a cell shape transition of human lung fibroblasts (Figure 2.3A), an effect that was observed at long-term treatment (24-48hours), but not at short-term treatment (up to 6 hours).

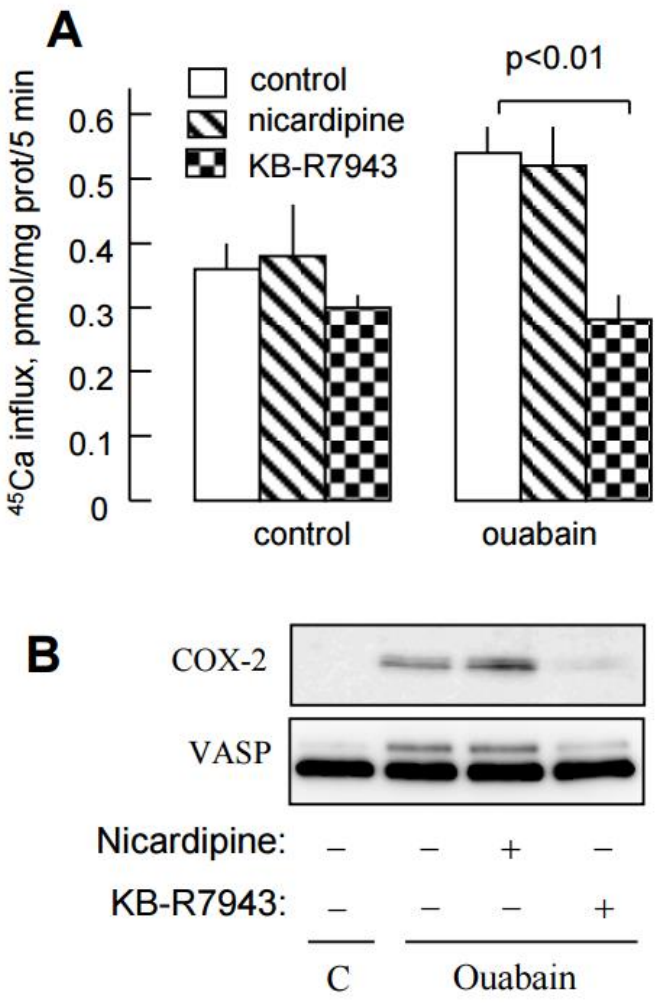

Figure 2.2. Effect of ouabain, nicardipine and KB-R7943 on $^{45}Ca^{2+}$ influx, and on COX-2 expression and VASP shift. **A**. HLFs were pre-incubated for 24 hours in the presence of 100 nM ouabain, 1 mM nicardipine or 3 mM KB-R7943, and the rate of $^{45}Ca^{2+}$ influx was measured as described in Methods. Means ± S.E. from experiments performed in triplicate are shown. **B**. HLFs were treated with 100 nM ouabain, 1 mM nicardipine or 3 mM KB-R7943 for 24 hours, and cell extracts were examined by Western blotting for COX-2 expression and VASP shift. (La et al. 2016)

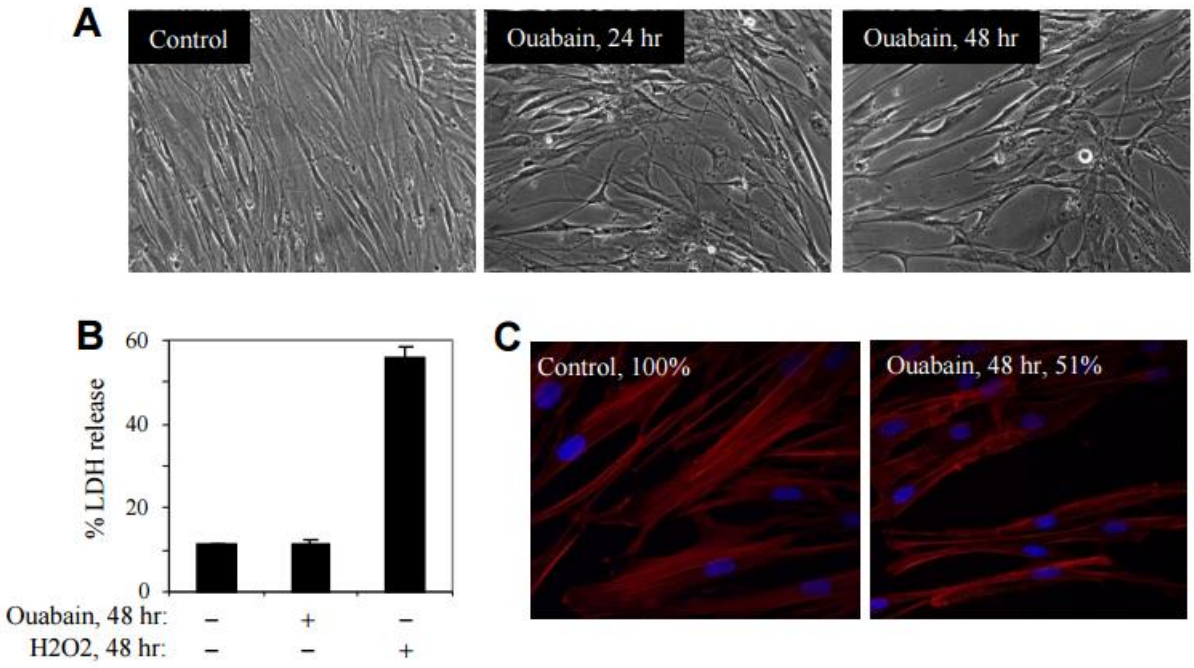

Figure 2.3. Ouabain distorts actin stress fibers without affecting HLF viability.

A. Serum-starved HLFs were treated with or without 100 nM ouabain for times indicated. Shown are the phase-contrast microscopy images of the cells. **B.** Effect of 100 nM ouabain or 1 mM H_2O_2 on HLF viability as assessed by LDH release. **C**. Phalloidin staining of HLFs treated with or without 100 nM ouabain for 48 hours. Percentile intensity of phalloidin is indicated. (La et al. 2016)

Because such cell shape changes may be associate with cell death, and because ouabain is known to induce apoptosis of various but not all cell types (Akimova et al., 2006; Orlov and Hamet, 2015), we examined potential cytotoxic effects of ouabain on HLF by measuring the release of lactate dehydrogenase (LDH). As shown in figure 2.3B, 100 nM ouabain had no significant cytotoxic effect for up to 48 hours, whereas the positive control, H_2O_2, drove a drastic increase in LDH release. We also did not observe membrane blebbing or accumulation of apoptotic bodies (commonly found with apoptosis) in ouabain-treated HLF (Figure 2.3A). On the other hand, a similar shape change in ouabain-treated HLF was previously described as “arborisation” or “stellation” in vascular smooth muscle cells treated with agents that disrupt actin filaments or activate PKA (Chaldakov et al., 1989; Orlov et al., 1996a). Given that, we examined a potential effect of ouabain on stress fibers in HLF. As shown in figure 2.3C, ouabain treatment halved the total content of polymerized actin and clearly disrupted the structure of stress fibers, as assessed by phalloidin staining.

Ouabain and digoxin inhibited TGF-β1-induced myofibroblast differentiation. We and others have demonstrated that myofibroblast differentiation is regulated by activators of PKA (Huang et al., 2008; Sandbo et al., 2009). Given the activation of PKA by ouabain in HLF, we examined its effect on myofibroblast differentiation in response to TGFβ1. As shown in figure 2.4A, treatment of HLF with TGFβ1 resulted in a profound induction of myofibroblast differentiation markers, such as smooth muscle α-actin (SM-α-actin), fibronectin and collagen-1. Ouabain inhibited the expression of myofibroblast markers in response to TGFβ1, which paralleled to its effect on COX-2 expression.

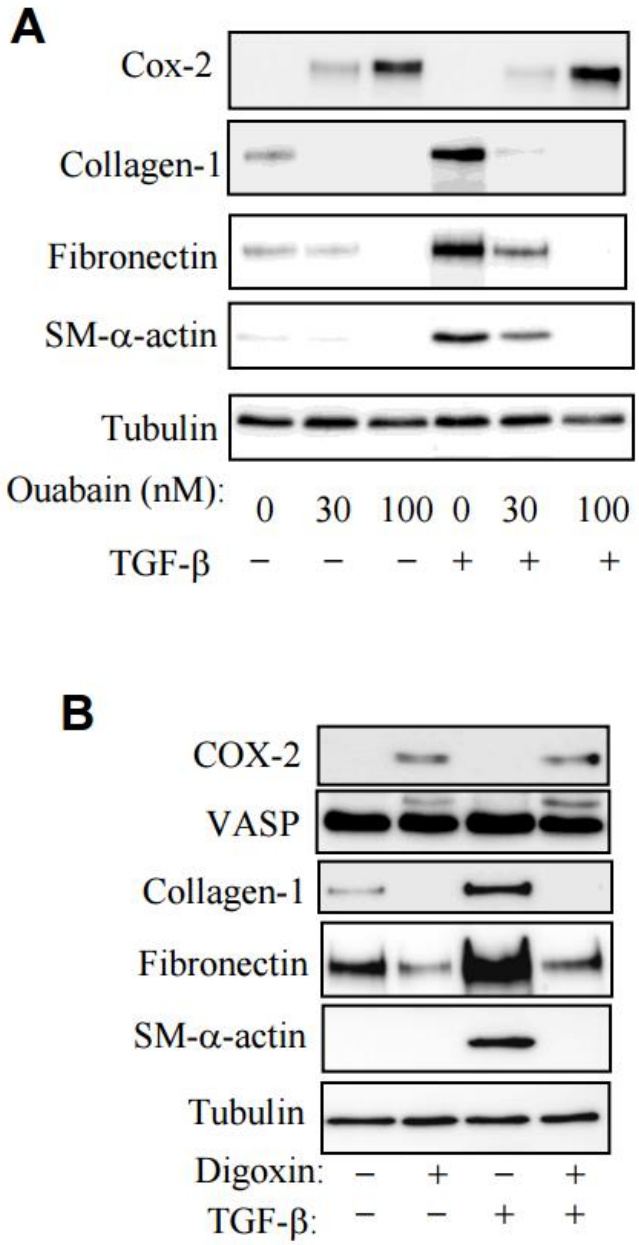

Figure 2.4. Ouabain and digoxin inhibit myofibroblast differentiation.
Serum-starved HLFs were treated with or without 1 ng/ml TGFβ1 in the presence or absence of 30 or 100 nM ouabain (**A**) or 100 nM digoxin (**B**) for 48 hours. Cell extracts were assessed by Western blotting for COX-2 expression, VASP shift, and myofibroblast differentiation markers as indicated. (La et al. 2016)

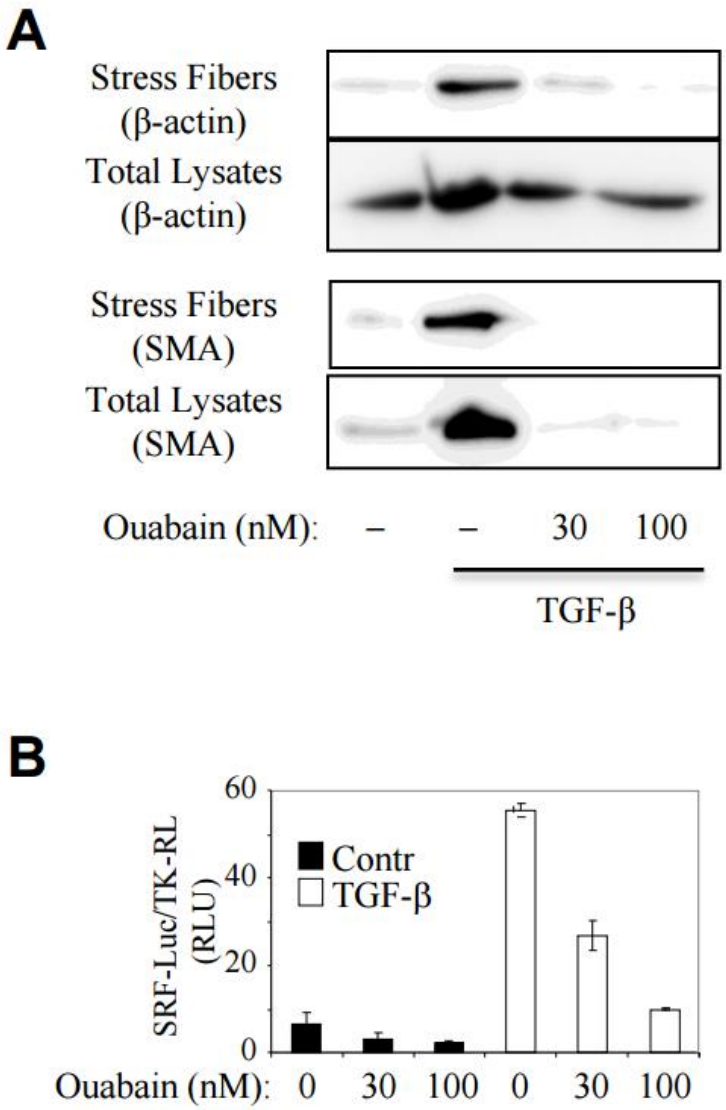

Figure 2.5. Ouabain inhibits TGFβ1-induced stress fiber formation and SRF activation.

A. Serum- starved HLF cells were treated with 1 ng/ml TGFβ1 in the presence or absence of ouabain for 48 hours. Cell extracts were either lysed (total) or were processed for isolation of stress fibers, followed by Western blotting with desired antibodies. **B.** Effect of increasing concentrations of ouabain (100 nM, 48 hours) on SRF-luciferase reporter activity. (La et al. 2016)

We also examined the effect of clinically relevant cardiac glycoside, digoxin, on myofibroblast differentiation. As shown in figure 2.4B, digoxin similarly stimulated expression of COX-2, phosphorylation of VASP, and completely blocked myofibroblast differentiation in response to TGFβ1. Upon stimulation with TGFβ1, fibroblasts respond by altering their ultrastructure by formation of actin stress fibers and modified focal adhesion complexes, which provide mechanical coupling to the surrounding matrix, and increases contractility of myofibroblasts (Hinz, 2006; Vaughan et al., 2000). Furthermore, actin stress fiber formation drives the activation of Serum response factor (SRF) and SRF-dependent expression of several myofibroblast markers including SM-α-actin (Sandbo et al., 2009, 2011). Therefore, we examined the effect of ouabain on this pathway. Consistently with previous data (Sandbo et al., 2011), a 48 hour exposure to TGFβ1 resulted in stress fiber formation, as quantitatively examined by biochemical isolation of stress fibers (Figure 2.5A). Importantly, ouabain decreased TGFβ1 induced stress fiber formation. Furthermore, ouabain attenuated TGFβ1 induced SRF-luciferase reporter activity (Figure 2.5B). Together, these data suggest that ouabain attenuates TGFβ1 induced myofibroblast differentiation through a disruption of actin stress fibers and inhibition of SRF activity.

Role of intracellular monovalent cations in regulation of COX-2 expression and myofibroblast differentiation. The roles of Na_i^+/K_i^+-mediated and Na_i^+/K_i^+-independent signaling mechanisms in cellular responses triggered by cardiac glycosides are widely-disputed (Orlov and Hamet, 2015). Keeping this in mind, we (i) employed K^+ -free media as an alternative approach for Na^+/K^+-ATPase inhibition, and (ii) compared dose-dependent action of ouabain on the $[Na^+]_i/[K^+]_i$ ratio, COX-2 content, and expression of

myofibroblast markers. As expected, inhibition of Na^+/K^+-ATPase in K^+-free media resulted in the same elevation of intracellular Na^+ content as it was detected in HLFs subjected to Na^+/K^+-ATPase inhibition by 100 nM ouabain (Figure 2.6A). Importantly, similarly to ouabain-treated cells, inhibition of the Na^+/K^+ -ATPase by K^+-free media was accompanied by the expression of COX-2, phosphorylation of VASP, and downregulation of TGFβ1 induced expression of myofibroblast markers (Figure 2.6B). Figure 2.7A shows that at 3 nM, ouabain did not change $[K^+]_i$ and slightly but not significantly increased $[Na^+]_i$ (p=0.6). At higher concentrations (10-100 nM), ouabain dose-dependently increased $[Na^+]_i$ and decreased $[K^+]_i$ by 8- and 7-fold, respectively. A similar dose-response analysis of the effect of ouabain on TGFβ1 induced myofibroblast differentiation revealed the following (Figures 2.7B, 2.7C): (i) Ouabain, at doses of 30-100 nM, induced COX-2 expression, which paralleled to inhibition of SM-α-actin expression; and (ii) 10 nM ouabain, resulting in 3-fold gain of $[Na^+]_i$ and 2-fold loss of $[K^+]_i$ (Figure 2.7A), had no detectable effect on COX-2 expression, but significantly inhibited the expression of SM-α-actin (p=0.047) , collagen-1 (p=0.025) or fibronectin (p=0.006) (Figures 2.7B, 2.7C).

COX-2 expression is not sufficient for inhibition of HLF differentiation by ouabain. Lastly, we examined the role of COX-2-dependent PKA activation in the inhibitory effect of ouabain on myofibroblast differentiation, first using COX-2 inhibitor NS-398. As shown above, this compound at concentration of 1 μM completely blocked ouabain-induced VASP phosphorylation as an indicator of PKA activity in HLF (Figure 2.1B).

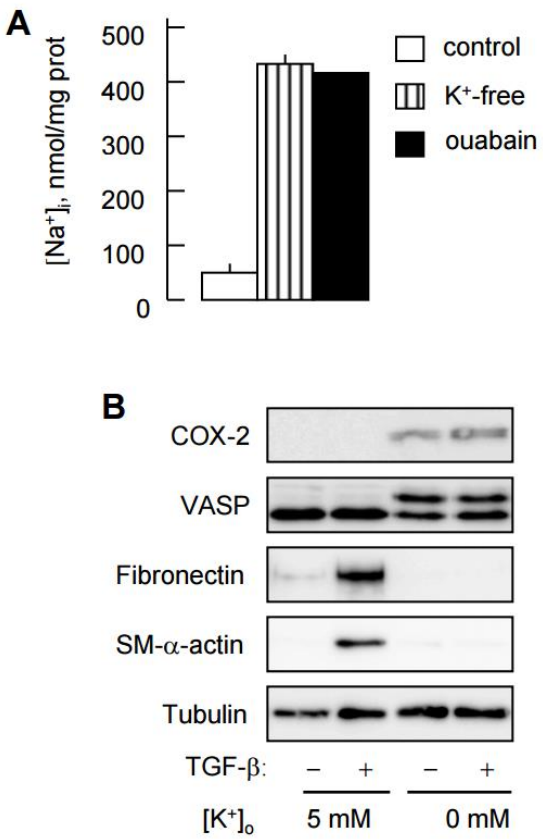

Figure 2.6. Effect of K^+-free medium on intracellular Na^+ content and on COX-2 expression, VASP phosphorylation and myofibroblast differentiation. HLFs were treated with a control medium ($[K^+]_o$=5 mM), K^+ -free medium, or with 100 nM ouabain in a control medium for 48 hours, with or without 1 ng/ml TGFβ1 for 48 hours as indicated. **A.** intracellular Na^+ concentration was measured as described in Methods. **B.** Cell extracts were analyzed by Western blotting with desired antibodies as indicated.

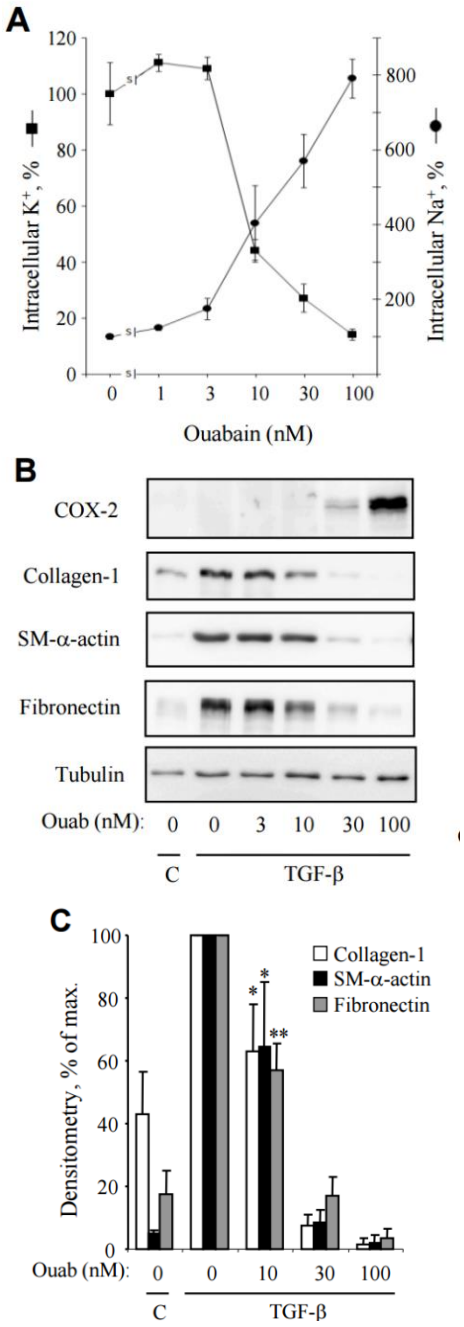

Figure 2.7. Dose-dependent actions of ouabain on intracellular Na^+ and K^+ content, COX-2 expression, and expression of myofibroblast differentiation markers.

A. HLFs were treated with ouabain for 48 hours and assessed for intracellular Na^+ and K^+ content. Means ± S.E. from experiments performed in triplicate are shown. **B.** HLFs were treated with 1 ng/ml TGFβ1 in the presence of increasing doses of ouabain for 48 hours. Cell extracts were examined by Western blotting for COX-2 expression, and myofibroblast differentiation markers. Shown are the representative images from three independent experiments. **C.** Densitometry of ECL for Collagen-1, SM-a-actin and fibronectin Western blots (mean ± SD from three independent experiments). * p<0.01) (La et al. 2016)

However, NS-398 failed to abolish the inhibitory effect of ouabain on myofibroblast differentiation (Figure 2.8A). We, and others, have demonstrated that Rho/Rho kinase (ROCK) signaling is critical for TGFβ1-induced stress fiber formation and SRF-dependent expression of myofibroblast marker proteins. Therefore, we examined the contribution of COX-2 expression on the regulation of this signaling pathway by ouabain, by assessing phosphorylation of cofilin as a downstream target of ROCK and a reporter of its activity, as we performed previously (Sandbo et al., 2011). As shown in figure 2.8A, ouabain inhibited TGFβ1 induced phosphorylation of cofilin; however, NS-398 failed to reverse this effect. Considering the possibility of prostaglandin-independent effects of COX-2, we then used the knockdown approach. As shown in figure 2.8B, transfection of HLF with COX-2 siRNA resulted in a complete attenuation of ouabain induced COX-2 expression. However, this did not affect the ability of ouabain to inhibit TGFβ1-induced myofibroblast differentiation or cofilin phosphorylation as a reporter of Rho signaling. Finally, we considered the role of elevated $[Ca^{2+}]_i$ via the activation of the reverse transport of the Na^+/Ca^{2+} exchanger in the action of ouabain (Figure 2.2). As shown in figure 2.8C, the inhibitor of Na^+/Ca^{2+} exchanger, KB-R4943, while inhibiting the effect of ouabain on COX-2 expression, failed to reverse the inhibition of TGFβ1 induced Rho activation (cofilin phosphorylation) and myofibroblast differentiation by ouabain.

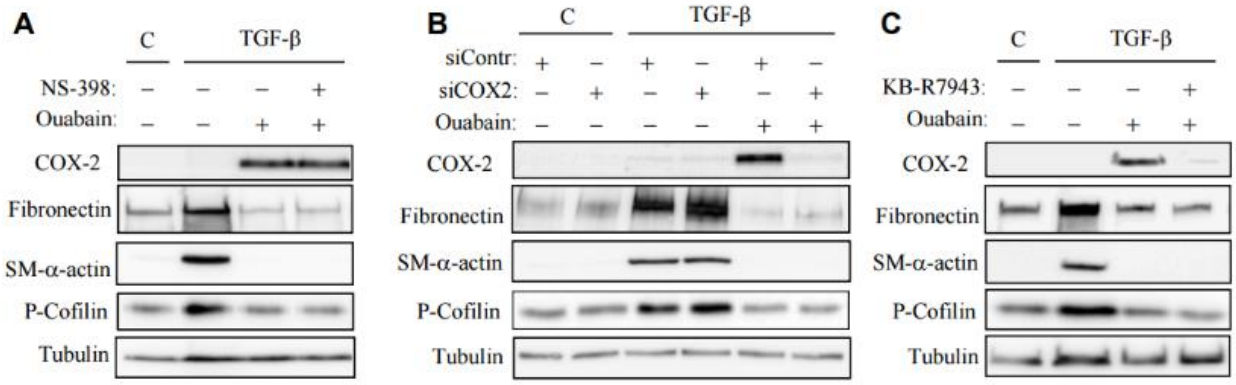

Figure 2.8. Inhibition of COX-2 or of Na+/Ca2+ exchanger does not abolish the inhibitory action of ouabain on TGF-β-induced myofibroblast differentiation. HLFs were treated with 1 μM NS-398 (**A**), or pre-transfected with a control or COX-2 siRNA (**B**), or treated with 3 μM KB-R7943 (**C**), followed by incubation with 100 nM ouabain, or 1 ng/ml TGFβ1 for 48 hours as indicated. Cells were lysed and the cell extracts were analyzed by Western blotting with the desired antibodies as indicated. (La et al. 2016)

Chapter 3

Inhibition of Na/K-ATPase results in attenuated TGFβ1 signaling and fibrosis through the downregulation of TGFβ receptor-2 expression.

Abstract

Transforming growth factor β1 (TGFβ1) plays a central role in the induction of myofibroblast differentiation and the development of pulmonary fibrosis. We found the inhibition of the Na^+/K^+-ATPase by K^+-free media or the cardiac glycoside, ouabain, resulted in a dramatic downregulation of TGFβR2 mRNA and protein levels in HLF. Considering this, we examined the effect of ouabain/ K^+-free media on TGFβ1-induced signaling and fibrosis. The loss of TGFβR2 in response to ouabain/ K^+-free media was tightly coupled with the inhibition of TGFβ1-stimulated Smad2 phosphorylation and myofibroblast differentiation. However, the over-expression of TGFβR2 was unable to rescue the inhibitory actions of ouabain, suggesting the downregulation of TGFβR2 was not sufficient for the inhibition of Smad2 phosphorylation and myofibroblast differentiation by ouabian. Nonetheless, given ouabain potently downregulated myofibroblast differentiation in nanomolar concentrations, we investigated if ouabain displayed anti-fibrotic effects in vivo. Transgenic $\alpha1^{S/S}$ mice, with a knock-in of cardiac glycoside sensitive Na^+/K^+ -ATPase, were utilized in the bleomycin model to assess the anti-fibrotic properties of ouabain. The use of transgenic mice was important because the alpha 1 subunit in wild-type rodents is insensitive to cardiac glycosides. First, wild-type and $\alpha1^{S/S}$ mouse lung fibroblast were isolated and subjected to ouabain treatment to verify their sensitivity to cardiac glycosides. Isolated wild-type mouse lung fibroblasts showed no change in TGFβR2 mRNA after ouabain treatment, while $\alpha1^{S/S}$ mouse lung fibroblasts demonstrated a drastic decrease in TGFβR2 mRNA in the presence of

ouabain. This further validated the downregulation of TGFβR2 by ouabain is Na^+/K^+-ATPase dependent. Lastly, mice treated with 50 µg/kg per day of ouabain exhibited decreased collagen deposition in the lung as compared to PBS controls. Together these data suggest an important role of the Na^+/K^+-ATPase in fibrogenesis in vitro and in vivo.

Results

Inhibition of the Na^+/K^+-ATPase results in the downregulation of TGFβR2 mRNA and protein. Treatment of quiescent human lung fibroblasts (HLF) with 100 nM ouabain resulted in a profound downregulation of TGFβR2 mRNA (Figure 3.1A) and protein (Figure 3.1B) levels in a time dependent manner. Taking into account this response may be specific to the current primary cell line used; we assessed if the loss of TGFβR2 by ouabain could be reproduced in three different primary IPF and normal lung (NL) fibroblasts. We found the loss of TGFβR2 in response to ouabain was recapitulated in both IPF and NL fibroblasts (Figure 3.1C), suggesting this effect was a universal response of fibroblasts to ouabain. Although cardiac glycosides have been established as inhibitors of the Na^+/K^+-ATPase we also utilized K^+-free media, which directly inhibits this ATPase, in order to confirm the effects of ouabain were due to Na^+/K^+-ATPase-specific effects. Serum starved HLF were placed in K^+-free media for 3, 6, and 24 hours before cells were analyzed for TGFβR2 mRNA via qPCR. The kinetics of TGFβR2 downregulation by K^+-free media were similar to what was seen after ouabain treatment (Figure 3.2A).

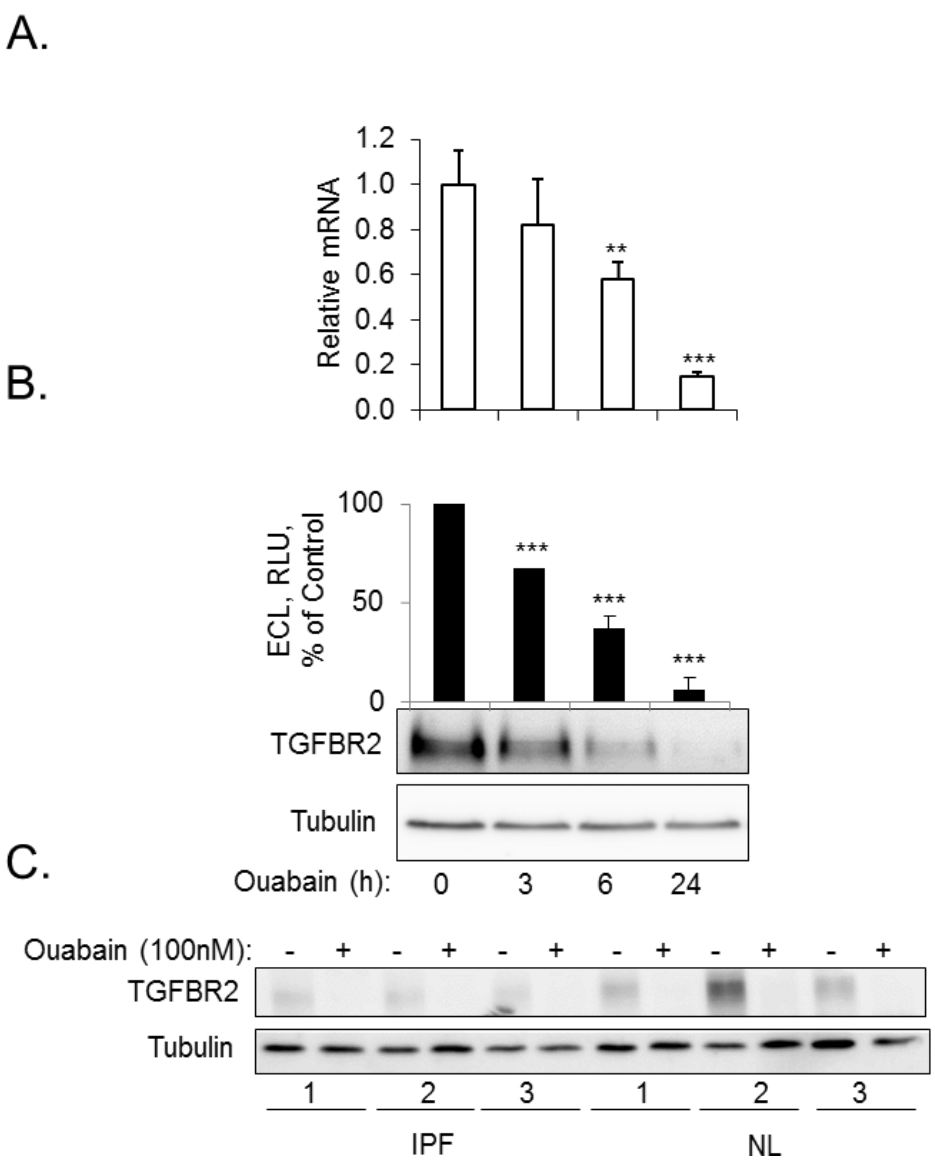

Figure 3.1. Ouabain down-regulates TGFβR2 mRNA and protein levels in human lung fibroblasts (HLF).

A and **B**. Serum-starved HLF were treated with 100nM ouabain for 3, 6, and 24 hours. Cells were analyzed by real-time qPCR for TGFβR2 mRNA levels (**A**) and by Western blotting for TGFβR2 protein levels (**B**). Shown are the representative images and the quantitative analysis of ECL from at least three independent experiments. *Error bars*, S.E. *, $p < 0.05$, **$p < 0.005$, ***$p < 0.005$ **C.** HLF isolated from IPF and non-IPF lungs were treated with or without 100nM ouabain. Cells lysates were analyzed for TGFβR2 protein via Western blotting.

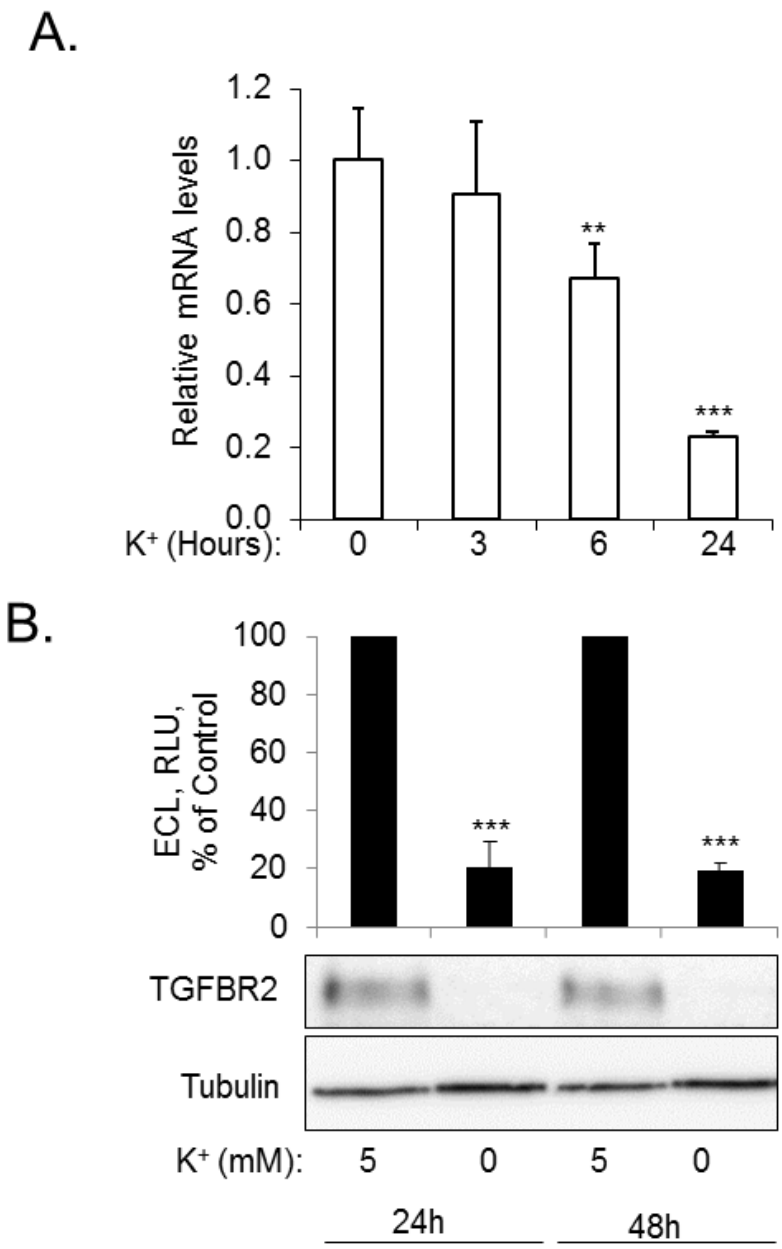

Figure 3.2. Inhibition of Na^+/K^+ ATPase by potassium free media results in the down-regulation of TGFβR2 mRNA and protein levels in human lung fibroblasts.

A. HLFs were placed in potassium free media for 3, 6, and 24 hours, and then analyzed for TGFβR2 mRNA levels via qPCR. **B**. HLFs were placed in either 5mM or 0mM potassium for 24 or 48 hours. Cell extracts were examined by Western blotting for TGFβR2 expression. Shown are the representative images and the quantitative analysis of ECL from at least three independent experiments. S.E; *, $p < 0.05$, **$p < 0.005$, ***$p < 0.005$

Cell extracts examined by Western blotting displayed loss of TGFβR2 protein after long term (24-48h) placement of HLF in K^+-free media as compared to their 5 mM K^+ media controls (Figure 3.2B).

The downregulation of TGFβR2 by inhibiting the Na^+/K^+-ATPase was accompanied with the loss of TGFβ1-induced Smad phosphorylation, myofibroblast differentiation, and epithelial-to-mesenchymal transition (EMT). Given the vital role of TGFβR2 on the initiation TGFβ1 signaling and in turn the fibrotic response, we investigated the effects of ouabain/K^+-free media on 1. TGFβ1 signaling and 2. TGFβ1 induced myofibroblast differentiation and EMT. The phosphorylation of Smad2, an event which occurs directly downstream of TGFβR1 activation, was used to evaluate the role of the Na^+/K^+-ATPase on TGFβ1 signaling. First, HLFs were treated with 0, 10, 30, and 100 nM of ouabain for 24 hours before stimulation with TGFβ1 for 1 hour. TGFβ1 promoted Smad2 phosphorylation in cells with no drug treatment, but, ouabain blocked TGFβ1-induced Smad2 phosphorylation in conjunction with downregulation of TGFβR2, in a dose dependent manner (Figure 3.3A). Similar experiments were performed using 0 mM K^+ media. HLF were placed in either 5 mM K^+ or 0 mM K^+ media for 24 hours then stimulated with TGFβ1 for an hour. As predicted, cells plated in 5 mM K^+ media displayed induction of Smad2 phosphorylation in response to TGFβ1. Importantly, cells in 0 mM K^+ media demonstrated inhibition of TGFβ1-induced Smad2 phosphorylation, which was associated with the downregulation of TGFβR2 protein (Figure 3.3B). Both ouabain and 0 mM K^+ media did not affect Smad2 expression (Figures 3.3A and 3.3B), therefore the loss in Smad2 phosphorylation was not due to decrease a in Smad2 protein. Given phosphorylation of

Smad2 is essential for Smad-dependent gene transcription, we further explored the effects of ouabain/K^+-free media on Smad-dependent gene transcription using a luciferase reporter assay. A plasmid containing both the Smad binding element (SBE), a consensus sequence in which Smad2 binds (Zawel et al., 1998), and the luciferase gene, was transiently transfected into HLFs, followed by 24 hour treatment of ouabain with or without 1 hour stimulation of TGFβ1. TGFβ1 stimulation alone drove the SBE-luciferase reporter. In parallel with the inhibition of Smad2 phosphorylation, ouabain blunted TGFβ1-induced luciferase expression in a dose dependent manner (Figure 3.3C), suggesting a significant role of the Na^+/K^+-ATPase in the initiation of TGFβ1 signaling. Considering Smad-dependent gene transcription is required for TGFβ1 induced myofibroblast differentiation, we examined the regulation of myofibroblast activation by ouabain/K^+-free media (Sandbo et al., 2011). HLFs were co-treated with ouabain and TGFβ1 for 24 hours and then cell lysates were examined for myofibroblast differentiation markers via Western blotting. TGFβ1 promoted myofibroblast differentiation in the absence of ouabain as shown by the increase in the differentiation markers fibronectin, collagen-1, and smooth muscle α-actin. Notably, ouabain inhibited myofibroblast differentiation and downregulated TGFβR2 in a dose dependent manner (Figure 3.4A). Correspondingly, HLF were treated with TGFβ1 for 24 hours in either 5 mM or 0 mM K^+ and then assessed for differentiation. Primary fibroblasts treated with TGFβ1 in 5 mM K^+ differentiated to myofibroblasts, indicated by the presence of differentiation markers collagen-1, fibronectin, and smooth muscle α-actin.

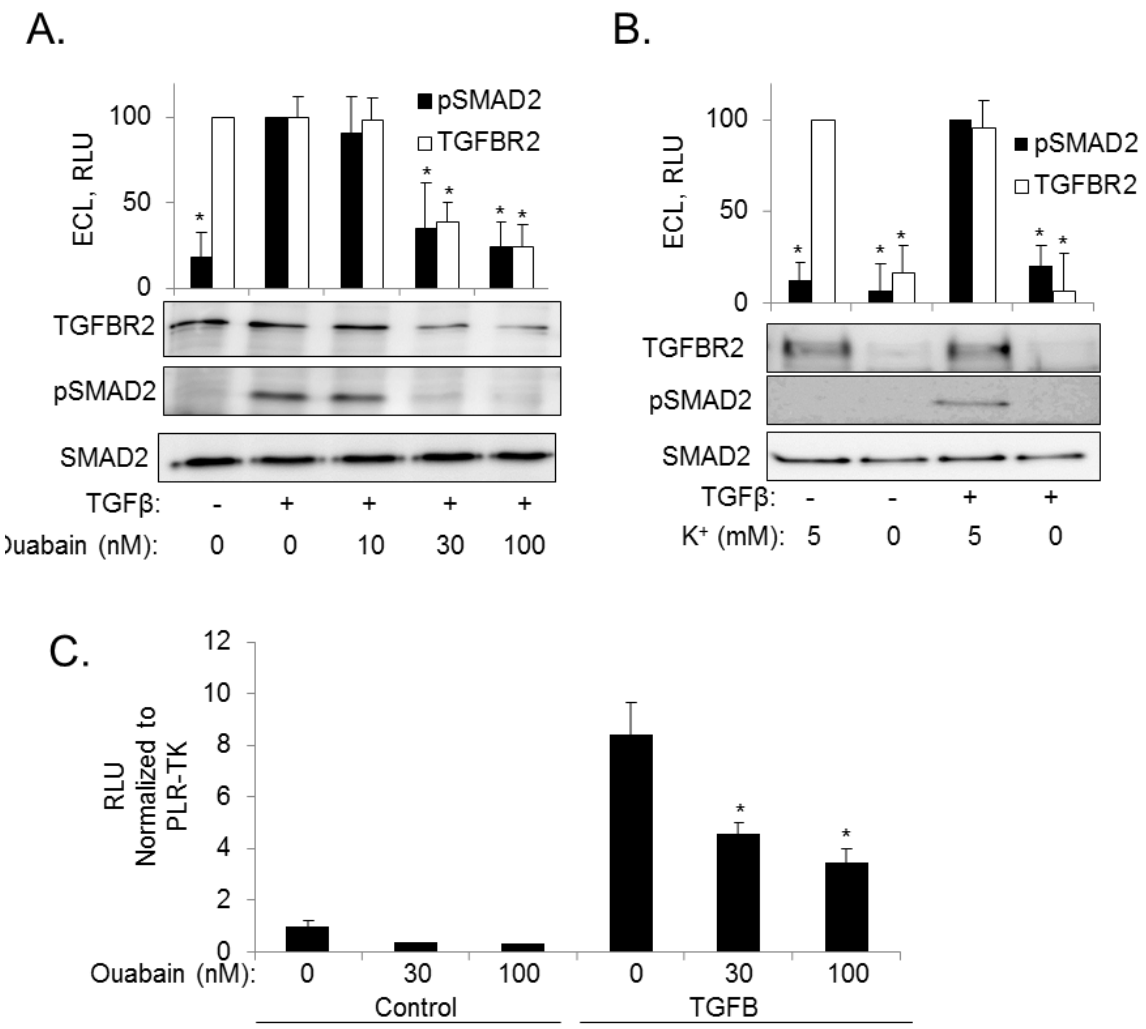

Figure 3.3. Inhibition of the Na,K-ATPase, by potassium free media and ouabain, blocks TGFβ1-induced SMAD2 phosphorylation and SBE luciferase.

HLF were pretreated with ouabain at 10, 30,100nM (**A**) or placed in 5mM or 0mM potassium (**B**) for 24 hours. Cells were then stimulated with 1ng/ml of TGFβ1 for 1 hour. Cell lysates were extracted for Western blotting to examine the effect of ouabain or potassium free media on TGFβ1-induced Smad2 phosphorylation (**A** and **B**). Shown are the representative images and the quantitative analysis of ECL from at least three independent experiments. Black bar represents pSmad and white bar represents TGFβR2 . S.E. *, $p < 0.05$, **$p < 0.005$, ***$p < 0.005$. **C.** HLF were transiently transfected with Smad-binding element (SBE) luciferase, along with thymidine kinase-driven renilla (TK-RL) control reporter, then serum starved for 24 hours. Afterwards cells were treated with increasing doses of ouabain overnight before being stimulated with TGFβ1 for 1 hour. The activity of luciferase was then measured in cell lysates and normalized to the activity of renilla. Data represent the results of at least three experiments performed in triplicate (*$P < 0.05$).

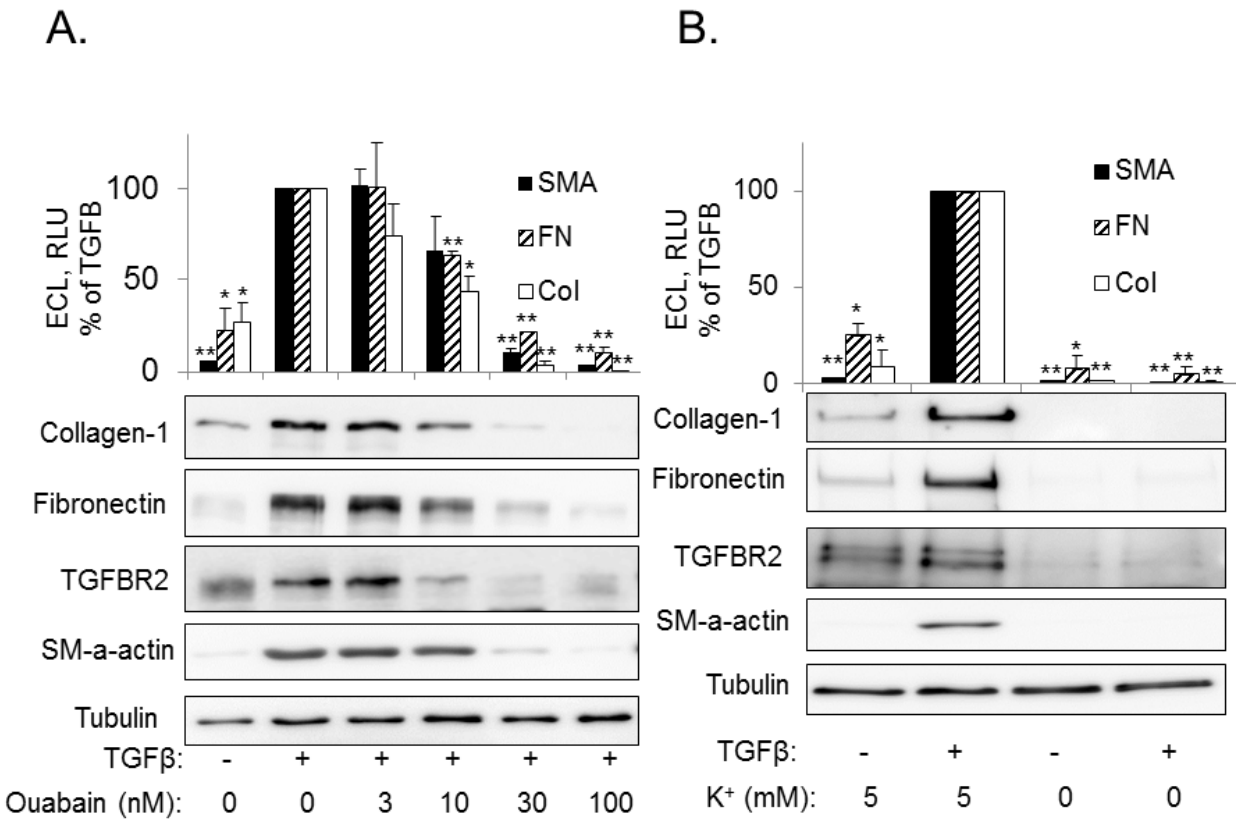

Figure 3.4. Inhibition of the Na,K-ATPase, by potassium free media and ouabain blocks, TGFβ1 myofibroblast differentiation.
HLF were treated with increasing doses of ouabain (**A**) or placed in 5mM or 0mM potassium (**B**) and stimulated with or without 1ng/ml of TGFβ1 for 24 hours. Western blotting was used to visualize differentiation makers. Shown are the representative images and the quantitative analysis of ECL from at least three independent experiments. S.E.; *$p < 0.005$, **$p < 0.0005$

In contrast, fibroblasts placed in 0 mM K^+ were blocked from differentiation in response to TGFβ1, demonstrated by the lack of differentiation markers (Figure 3.4B).

There is evidence to support alveolar epithelial cells undergoing epithelial to mesenchymal transition may be a source of fibroblast progenitor cells (Willis et al., 2005). Given myofibroblasts contribute to the pathogenesis of pulmonary fibrosis; it is conceivable to conclude that limiting the available fibroblast population for myofibroblast activation would attenuate the progression of this disease. As a result, we investigated whether ouabain plays a role in EMT. As previously demonstrated by other groups, we confirmed stimulation of A549 cells with TGFβ1 induced the expression of mesenchymal markers vimentin and n-cadherin, suggesting A549 cells have the capacity to undergo EMT (Kasai et al., 2005). Similarly to HLF, TGFβR2 protein decreased in response to ouabain (Figure 3.5A), which was coupled with inhibition of TGFβ1-induced Smad2 phosphorylation and mesenchymal markers in A549 cells (Figures 3.5A and 3.5B).

TGFβR2 overexpression was unable to rescue the effects of ouabain on TGFβ1-induced signaling and fibrosis. Taking into account the inhibition of the Na^+/K^+-ATPase by ouabain/K^+-free media profoundly downregulates TGFβR2, which was highly associated with the inhibition of TGFβ1 induced signaling and fibrosis, we investigated if overexpression of TGFβR2 could reverse these effects. Serum starved human lung fibroblasts were infected with ad-TGFβR2, ad-GFP, and ad-truncated-TGFβR2. As shown previously, TGFβ1 stimulation resulted in Smad2 phosphorylation which was blocked by ouabain treatment.

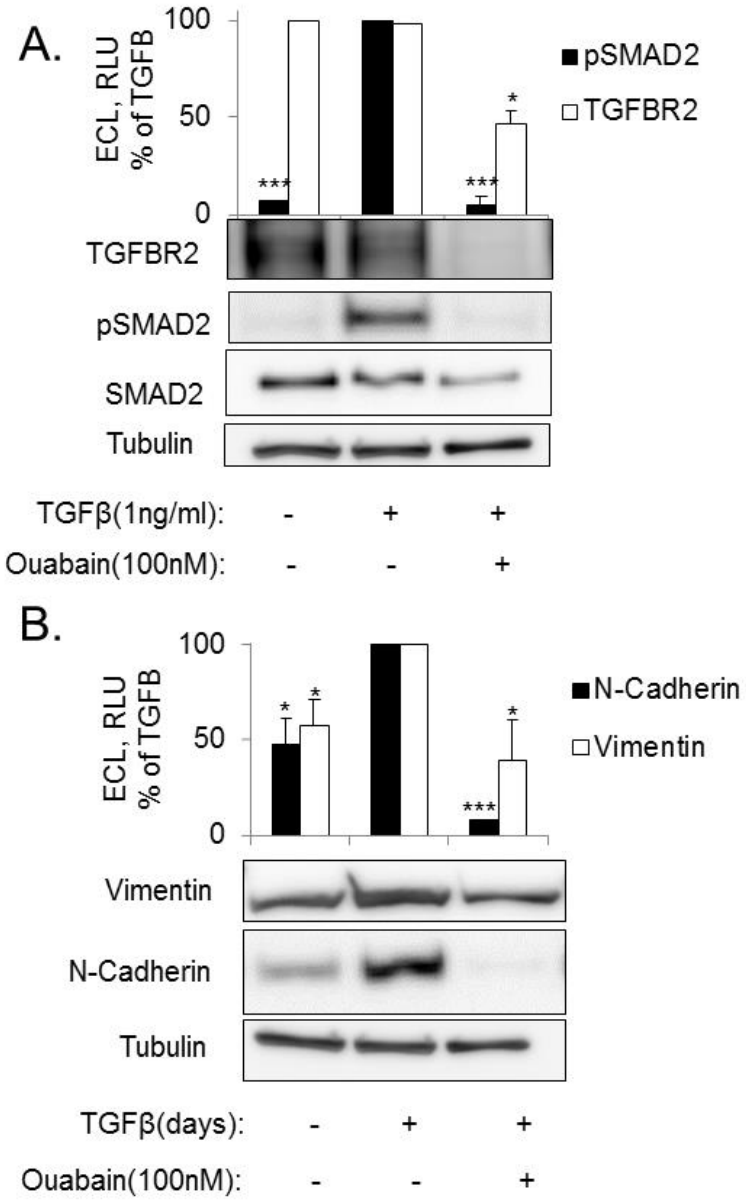

Figure 3.5. The downregulation of TGFβR2 by ouabain was accompanied with the loss of TGFβ1-induced Smad2 phosphorylation and mesenchymal markers in A549 cells.

Serum starved A549 cells were pretreated with increasing doses of ouabain for 24 hours followed by stimulation with 1ng/ml of TGFβ1 for 1 hour (**A**) or simultaneously treated with ouabain and TGFβ1 for 24 hours (**B**). Cell lysates were used to examine Smad2 phosphorylation (**A**) and mesenchymal markers (**B**). Shown are the representative images and the quantitative analysis of ECL from at least three independent experiments. S.E.; **, $p < 0.05$, **$p < 0.005$, ***$p < 0.005$

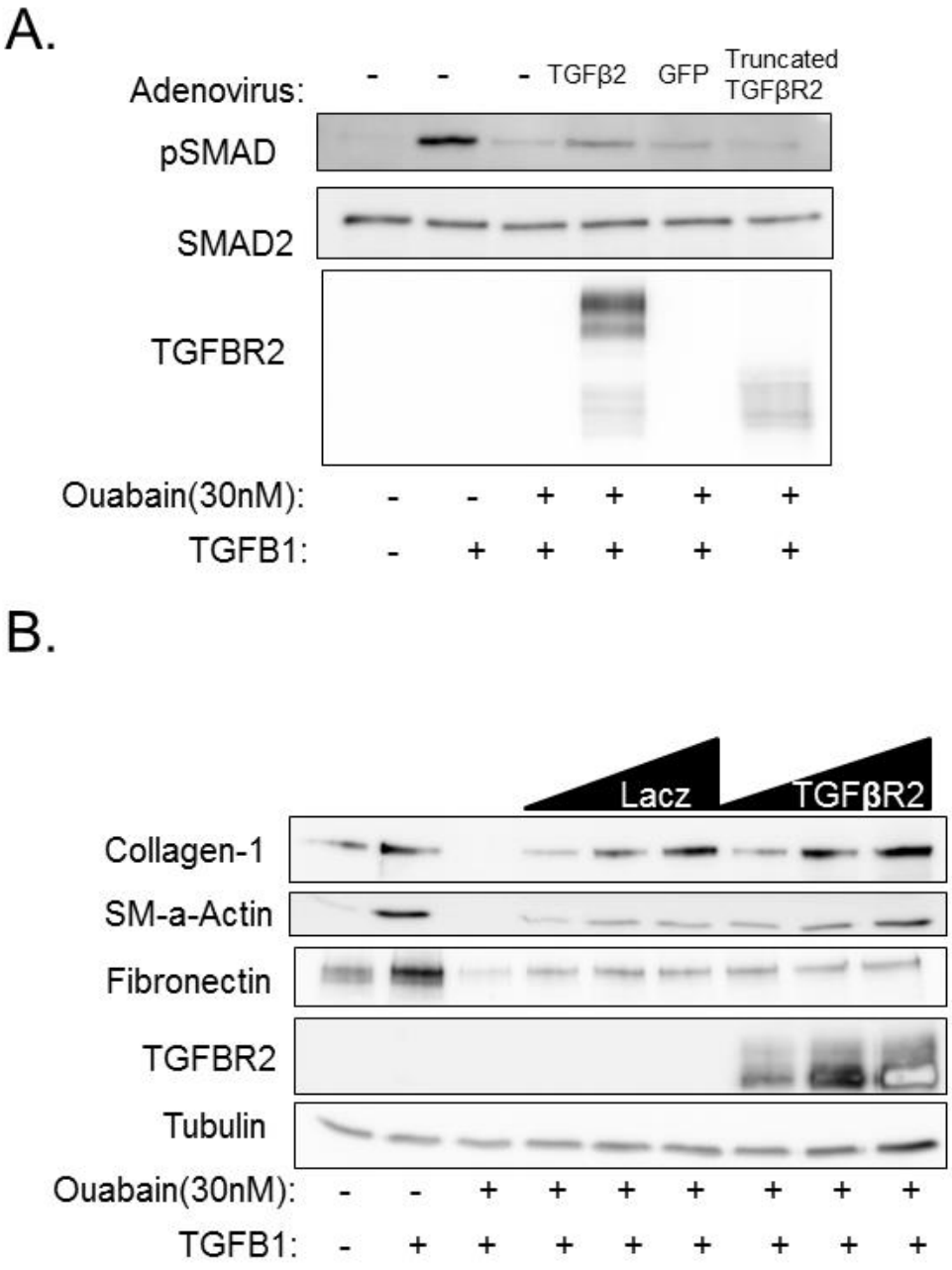

Figure 3.6. Overexpression of TGFβR2 via adenovirus does not rescue the effects of ouabain.
HLF were infected with LacZ and TGFβR2 adenovirus. Afterwards cells were treated with ouabain for 24 hours followed by 1 hour stimulation with TGFβ1 (**A**) or cells were simultaneous stimulation with ouabain (30nm) and TGFβ1 for 24 hours (**B**). Cells were lysed and analyzed via Western blotting.

TGFβR2 overexpression slightly reversed the effects of ouabain, while ad-GFP and ad-truncated-TGFβR2 did not, suggesting some rescue of the inhibitory actions by ouabain with TGFβR2 overexpression (Figure 3.6A). Next, we investigated the effect of TGFβR2 overexpression on myofibroblast differentiation. As demonstrated before, ouabain treatment alone inhibited TGFβ1-induced myofibroblast differentiation. The effects of the adenoviral overexpression on differentiation markers were the following: i) ad-LacZ and ad-TGFβR2 reversed the effects of ouabain on collagen-1 expression in a dose dependent manner; ii) all three doses of ad-LacZ slightly increased smooth muscle α-actin levels compared to ouabain treatment alone while ad-TGFβR2 showed rescue in a dose dependent manner; and iii) both ad-LacZ and ad-TGFβR2 increased fibronectin protein expression above ouabain treatment alone. Given both ad-LacZ and ad-TGFβR2 slightly reversed the effects of ouabain on TGFβ1-induced myofibroblast differentiation, it was unclear if these results were adenovirus dependent or protein overexpression dependent (Figure 3.6B). To bypass the possible nonspecific consequences on myofibroblast differentiation by adenovirus infection, transfection of TGFβR2 mRNA was employed as an alternative mode of homogenous TGFβR2 overexpression. HLF were transfected with TGFβR2 mRNA and treated with TGFβ1 with or without ouabain. Transfection of TGFβR2 mRNA increased TGFβR2 protein levels in a dose dependent manner. Comparably to previous observations, ouabain in all conditions downregulated TGFβR2 protein and myofibroblast differentiation markers, suggesting, TGFβR2 overexpression was unable to rescue the effects of ouabain on myofibroblast differentiation. Interestingly, higher doses of TGFβR2 mRNA transcript also resulted in the inhibition of myofibroblast differentiation.

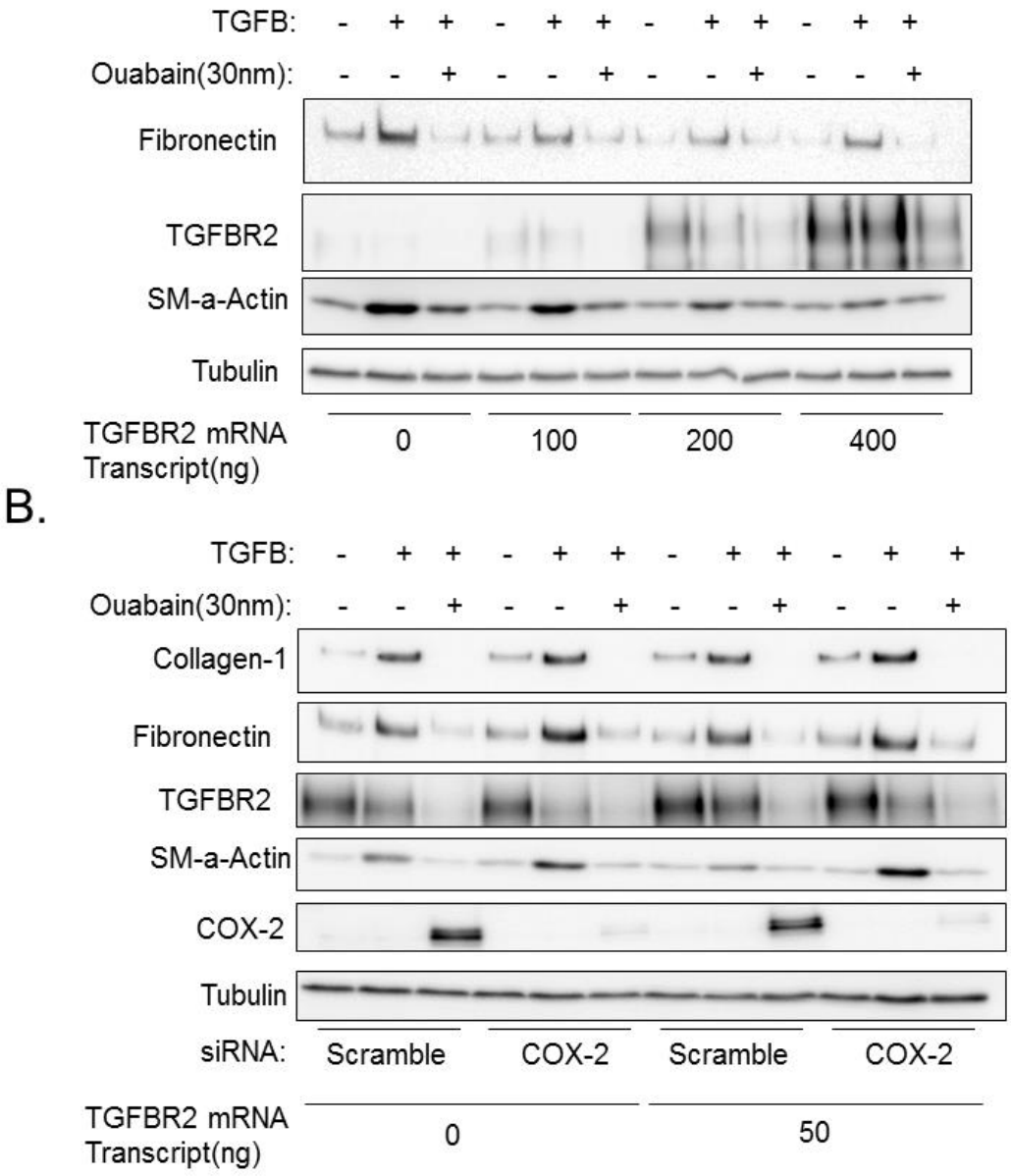

Figure 3.7. Overexpression of TGFβR2 via mRNA does not rescue the effects of ouabain.

A, TGFβR2 mRNA was transfected into HLF. Cells were starved 5 hours after transfection and immediately treated with both ouabain and TGFβ1 overnight. **B.** HLF were transfected with scramble or COX-2 siRNA for 24 hours followed by transfection of TGFβR2 mRNA for 5 hours. Cells were then starved and treated with TGFβ1 and ouabain overnight. All cells were lysed and analyzed via Western blotting

400 ng of TGFβR2 mRNA transcript blocked TGFβ1-induced myofibroblast differentiation to basal levels, indicating increased TGFβR2 over basal levels may inhibit differentiation (Figure 3.7A). Importantly, our previous studies have shown ouabain treatment dramatically upregulated COX-2 expression, the rate limiting enzyme for PGE2 synthesis (La et al., 2016). Taking into account COX-2 expression may inhibit SRF activity, a target downstream of Smad-dependent gene transcription, the lack of rescue by TGFβR2 overexpression may be due to the additional inhibition of the SRF pathway by ouabain. To investigate this hypothesis, we explored if both TGFβR2 overexpression and downregulation COX-2 expression could reverse the inhibition of myofibroblast differentiation by ouabain. Given the higher doses of TGFβR2 mRNA blocked myofibroblast differentiation, we lowered the transfected dose of TGFβR2 mRNA to 50ng. At this concentration, there was a slight increase of TGFβR2 protein over basal levels after transfection. Ouabain at 30 nM profoundly upregulated COX-2 expression and COX-2 siRNA completely abolished this upregulation. However, ouabain treatment, with or without COX-2 siRNA and TGFβR2 overexpression, resulted in both the downregulation of differentiation makers and TGFβR2 protein (Figure 3.7B).

Overexpression of Smad2 does not rescue the effects of ouabain. Previously our lab demonstrated the overexpression of Smad2 (via plasmid transfection), a protein phosphorylated and activated by TGFβR1, drove the induction of the SBE-luciferase reporter gene. Therefore, we explored if Smad2 overexpression could rescue to effects of ouabain on myofibroblast activation.

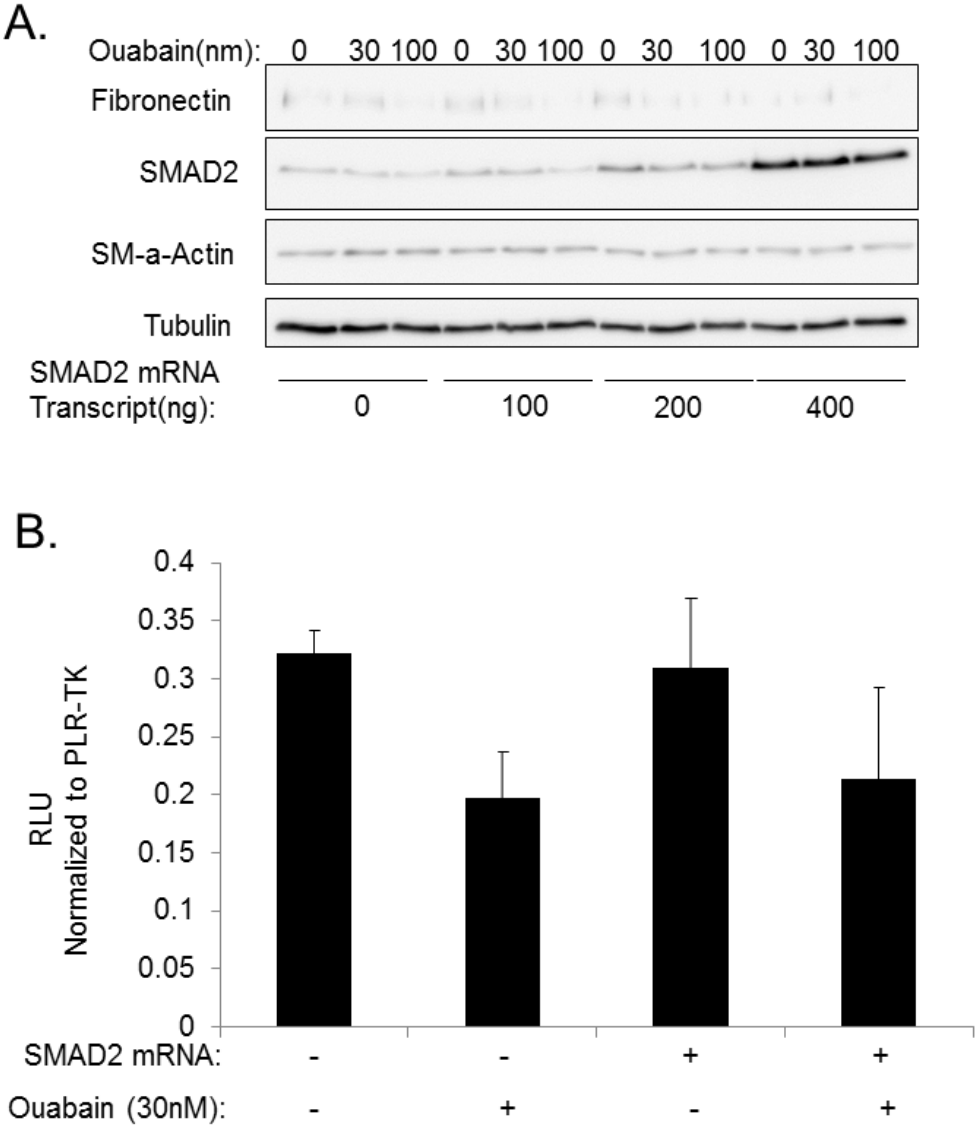

Figure 3.8. Smad2 Overexpression does not Induce Myofibroblast Differentiation or Drive SBE-Luciferase Reporter Gene.
A. HLF transfected with Smad2 mRNA then treated with ouabain overnight. Cell were lysed and then analyzed for protein via Western blotting. **B**. HLF were transiently transfected the SBE-luciferase reporter, along with thymidine kinase-driven renilla (TK-RL) control reporter, and then transfected with Smad2 mRNA. The activity of luciferase was then measured in cell lysates and normalized to the activity of renilla. Data represent the results of at least three experiments performed in triplicate (*$P < 0.05$).

Smad2 mRNA transfection successfully overexpressed Smad2 in a dose dependent manner; however there was no change in differentiation markers, indicating lack of differentiation (Figure 3.8A). Furthermore, unlike overexpression of Smad2 via plasmid transfection, overexpression of Smad2 via mRNA transfection does not drive the SBE-luciferase reporter gene (Figure 3.8B).

Knockdown of the α1 or β1 subunit does not recapitulate the effects of cardiac glycosides. We have demonstrated cardiac glycosides and K^+-free media potently attenuated TGFβ1 stimulated myofibroblast differentiation in vitro. As a result, we investigated if TGFβ1 controls myofibroblast differentiation by modulating the Na^+/K^+-ATPase subunit expression. Given ATP1A1 and ATP1B1 are the most abundantly expressed isoform in lung tissue (Orlowski and Lingrel, 1988), a time course of TGFβ1 treatment was performed to investigate how TGFβ1 effects ATP1A1 and ATP1B1 expression. qPCR analysis showed that TGFβ1 induced a sustained upregulation of ATP1B1 mRNA but not ATP1A1 (Figure 3.9A), suggesting TGFβ1 may regulate ATP1B1 transcription. Furthermore, examination of the ATP1B1 promoter revealed the promoter contains a perfect putative Smad-binding site identical to the established Smad target gene, Smad7, indicating ATP1B1 may be regulated via Smad-dependent gene transcription (Figure 3.9C). In parallel with increased mRNA levels, ATP1B1 protein was also upregulated upon TGFβ1 stimulation in vitro (Figure 3.10A). In vivo, mouse lung homogenate exhibited increased ATP1B1 expression and collagen deposition in response to bleomycin injury (Figures 3.9B and 3.9C).

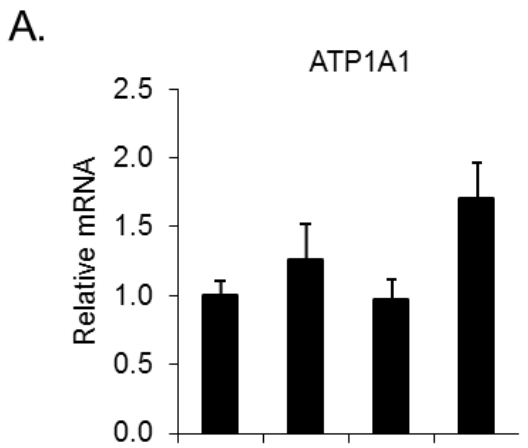

C

5'GTGCAGATATTGTTGCCTGGG**GTCTAGAC**TGGCCTGAGTCTCAATTGGTTTCTACGGGACAACTC
ACTGCGGGCTACCGCCCTGGGTGGGTTTGGCAATTGTCCTGCTCGAGGTGGTTCAGGCCGCCCAC
AAGGGGCACAGCCGGGCAGTCAGGAACCGGGGCTGCCGGCTGGGCTGGCCTGCAAAGAAGAGGG
AAGGGCCGGAACTGCAACCGCAGTGGCGGGGAGTGCGAGGGGGCGGCAGGTGCAGGAGCGGGA
GGCGGGGCGGAGCTGGGCAGAGTCCTCGCCAGTCCGGCGTCCCGGAGTGACCTTCCCCCACCCC
GCCAGCGCCCAGGAGGGGTGGACCCACAGCCCAGGGAGGCCGAAAGCGCGGGCGGGCAGGCAG
AGGCGTGGAGGCTGGGCCAGGACTGCCGGGCTGGGGTCCTCGAGGCTCCGGGCGACCCAGGTG
CGGATCCCCCAGCCACGGAAGGGGCGGTTCACGCCCAGCCGGGAGCTGGGAGGGGGCTGCGCG
GCGCTGCCTGCGCGTCCCTCACCGCCGCCCCCGCCTCCTCCTCGCCCCGCGCCCAACGCCCCGC
GCCCAGCGATCCAAGCGGCCCCTCTAGCCCCGGCGGCTCCTTTGTGCCGGCCCCGAACCCGCCCT
CTCGGGCCGAGTCCCTGCCCCTGGCGCCGGCGATTGGCCACCGGGCCGCTAGAGGGCGGGGCG
CACGGCCGCCGGGGCGCGGTATATAGTAAAGGTAGGGCGGGCGCAGCCAATTCCTCGGCTCCTG
GCGGGAGTGCCGGTGGCGCCCCGCAGTCCGCTTGTCCGTCCTTCCCTCTCTGACTCTCCTACCCC
GGGCCTGTCTCTGCAGAGGTCAGGGGAGGCGGGGGCCCAGCACACGTCCCCAGTGGCAGCGGGA
GCGGCAGCTACGGGTTCGCGGAGCCCCCGACCCCCCAAGGGCTAGAGGAGCGCTC3'

Figure 3.9. TGFβ1 Induces ATP1B1 but not ATP1A1 mRNA, and the ATP1B1 Promoter Contains a Smad Binding Element.

A and **B**. Quiescent lung were stimulated with TGFβ1 for 1, 2, and 3 days. mRNA was extracted and qPCR was performed to analyze ATP1A1 and ATP1B1 mRNA levels. **C**. The ATP1B1 promoter is about 1200 bp upstream of the transcription start site (underlined). The palindromic sequence GTCTAGAC (bold) is identical to the Smad binding element found in the Smad7 promoter.

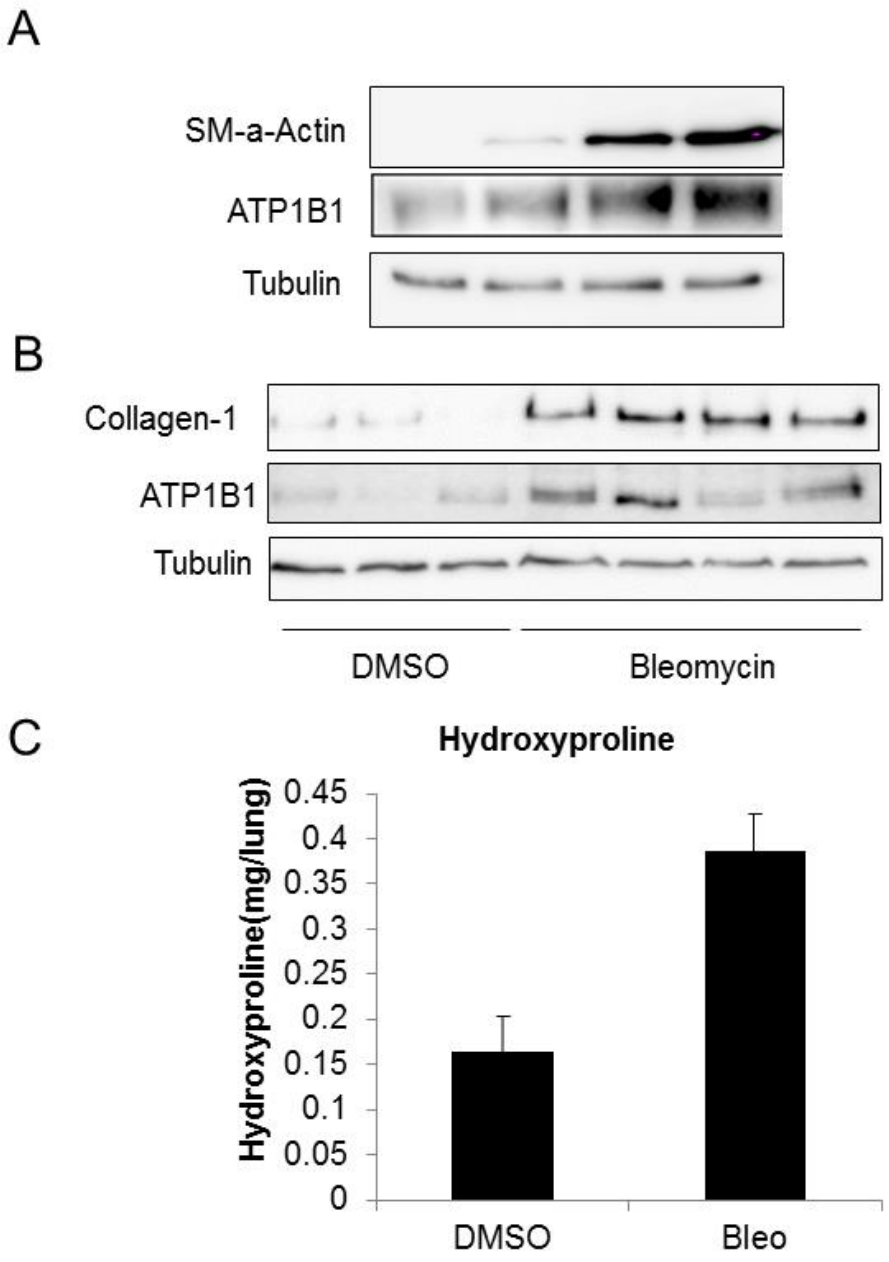

Figure 3.10. TGFβ1 Stimulates ATP1B1 Protein Expression and Fibrotic Mouse Lungs Exhibit Increased ATP1B1 expression. **A**, Serum starved HLF were stimulated with TGFβ1 for 1, 2, and 3 days. Cell were lysed and analyzed via Western blotting. **B**, Right and left lungs were extracted from control and bleomycin injured mice and homogenized in PBS. Lung homogenate was run on a Western blot and analyzed for collagen and ATP1B1 protein. **C**, Right and left lung homogenates were extracted and analyzed for collagen via hydroxyproline assay.

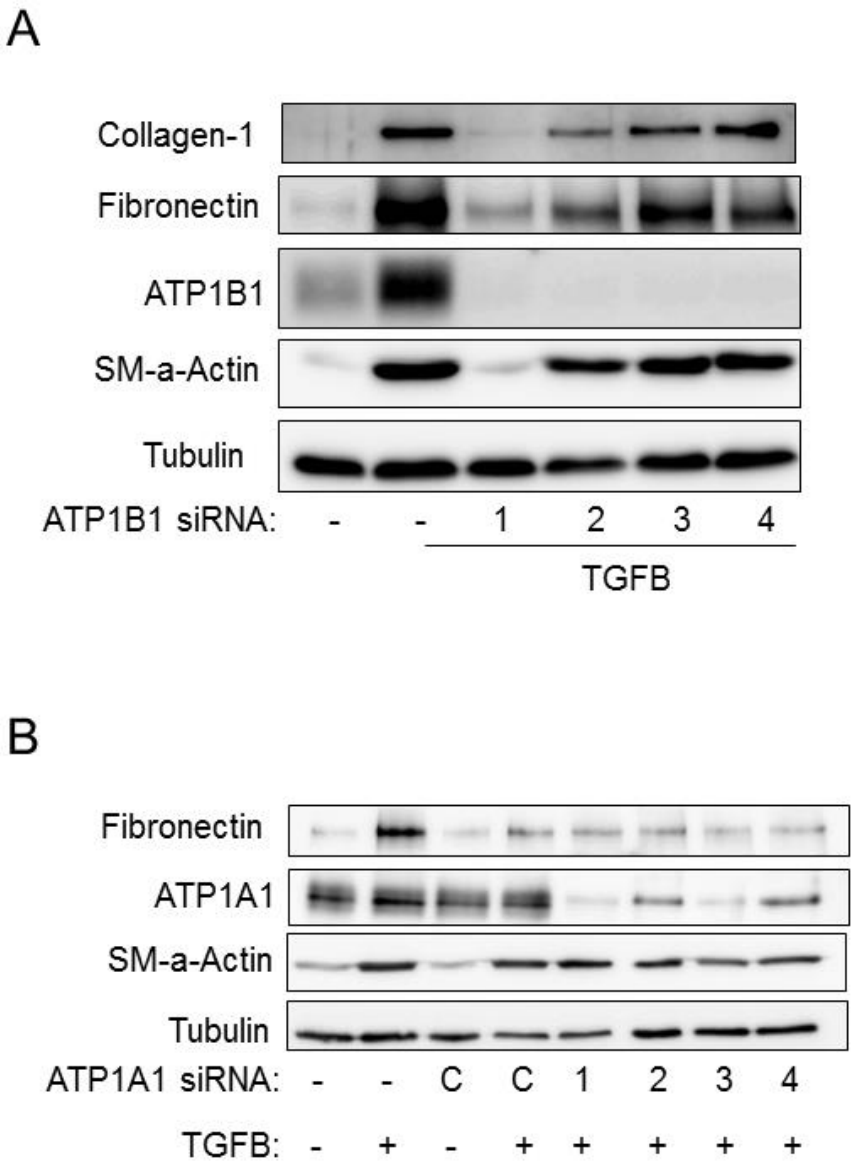

Figure 3.11. siRNA Knockdown of ATP1B1 and ATP1A1 does not Recapitulate the Effects of Cardiac Glycosides.
A and **B.** HLF were subjected to siRNA knockdown of ATP1B1 **(A)** and ATP1A1 **(B)** using 4 different siRNAs. Cells were then stimulated with TGFβ1 for 48 hours. Cells were lysed and analyzed via Western blotting.

Given the upregulation of ATP1B1 is highly associated with induction of myofibroblast differentiation, we investigate if knockdown of ATP1B1 would be sufficient to inhibit differentiation. Four siRNA constructs were used separately to knockdown ATP1B1 in HLF. siRNA-ATP1B1 #1 efficiently knocked-down ATP1B1 and inhibited myofibroblast differentiation in response to TGFβ1. However, the remaining siRNA constructs also effectively downregulated ATP1B1 protein, but did not display any anti-fibrotic properties (Figure 3.11A), suggesting si-RNA#1 may have non-specific targets that effect myofibroblast differentiation. Furthermore, siRNA to ATP1A1, the catalytic subunit of the Na^+/K^+ ATPase, did not demonstrate any anti-fibrotic effects either (Figure 3.10B).

Isolated $\alpha1^{S/S}$ mouse lung fibroblasts are sensitive to ouabain and treatment

of ouabain and treatment of ouabain attenuated fibrosis in the bleomycin model of pulmonary fibrosis. Given the potency of inhibition of myofibroblast differentiation by ouabain, we explored the anti-fibrotic effects of cardiac glycosides in vivo. Wild-type rodents are not sensitive to cardiac glycosides; as a result α1-sensitive ($\alpha1^{S/S}$) knock-in mice in the C57B6 background were used in the bleomycin model, to test if the administration of ouabain displayed anti-fibrotic properties in vivo. The mutant mouse was generated by introducing two amino acid substitutions in the α1 isoform of the Na^+/K^+-ATPase, deeming this subunit sensitive to cardiac glycosides. To test if mutant mice respond to cardiac glycosides, mouse lung fibroblasts from both wild-type and $\alpha1^{S/S}$ mice were isolated and subjected to ouabain treatment.

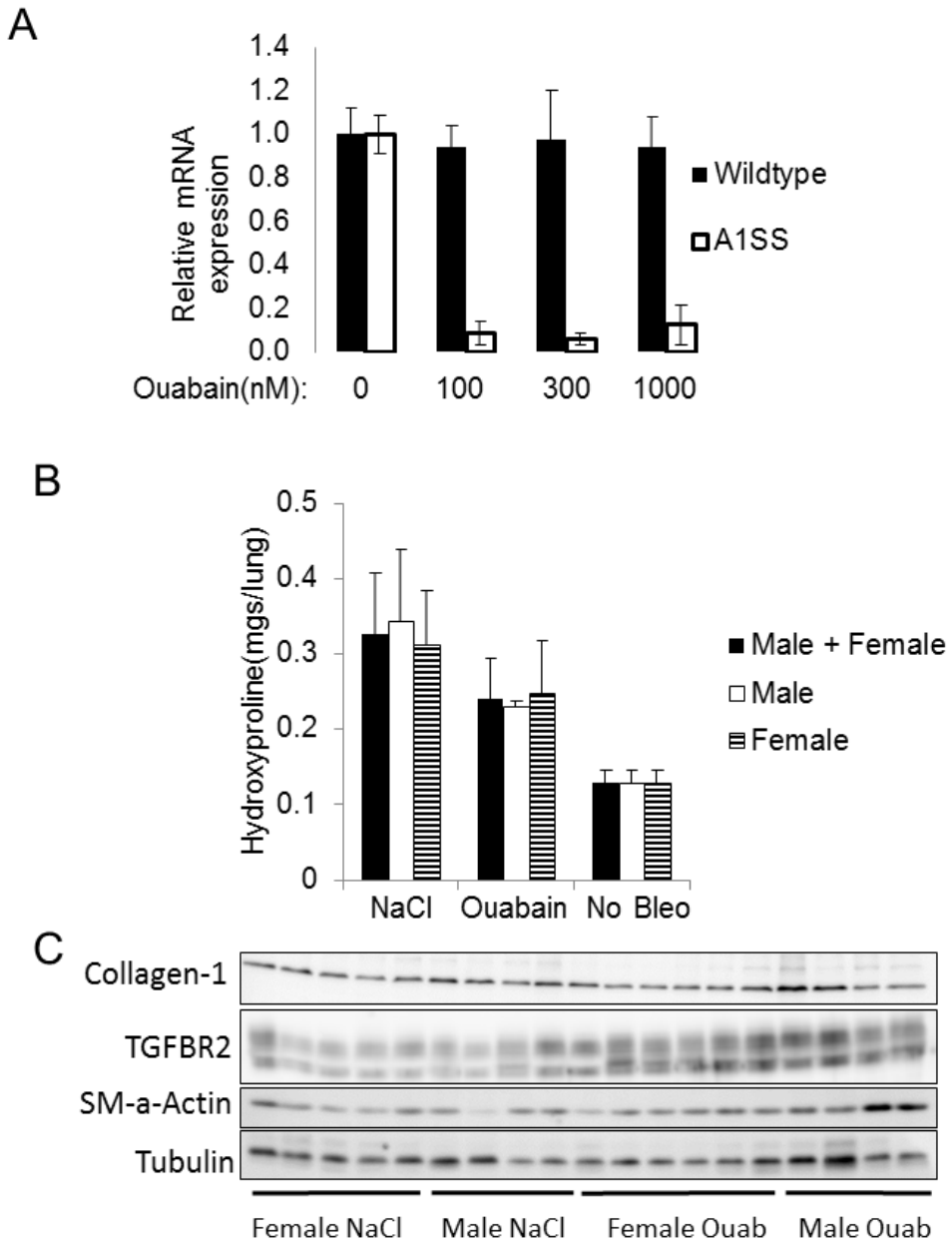

Figure 3.12. Isolated α1$^{S/S}$ Mouse Lung Fibroblasts are Sensitive to ouabain, but treatment of ouabain (1ug/kg) does not Significantly Reduce Collagen Deposition in the Bleomycin Model.

A. Mouse lung fibroblasts (MLF) isolated from wildtype and α1$^{S/S}$ mice were treated with or without 100, 300, and 1000nm of ouabain for 24 hours. qPCR analysis was used to visualize TGFβR2 mRNA levels. **B and C.** Mice were injected IP with ouabain (1 ug/kg) or NaCl daily for 14 days a week after intratracheal instillation of bleomycin. After 14 days of treatment mice were sacrificed and whole long homogenate was analyzed for collagen via hydroxyproline assay (**B**) and Western blotting(**C**).

Isolated wild-type mouse lung fibroblasts demonstrated no change in TGFβR2 mRNA in response to ouabain, while $\alpha1^{S/S}$ lung fibroblasts dramatically downregulated TGFβR2 mRNA in the presence of ouabain (Figure 3.12A), further indicating the downregulation of TGFβR2 by ouabain is Na^+/K^+-ATPase dependent. After confirming the sensitivity of these mice to cardiac glycosides, we examined if ouabain exhibited anti-fibrotic effects in vivo. Given gender plays a role in bleomycin sensitivity, male and female mice were administered 1.26 and 1.4 units/kg of bleomycin respectively, and analyzed separately. Mice were treated daily (intraperitoneal) with PBS or ouabain at 1 ug/kg, 7 days after intratracheal instillation of bleomycin. After 2 weeks of treatment, mice were sacrificed and lungs were analyzed for collagen deposition. Although there was a trend towards less collagen deposition in the lungs in both the male and female ouabain treated mice, ouabain did not significantly reduced collagen deposition in comparison to saline controls (Figure 3.12B and C). To rule out the possibility that the dose given may be too low for therapeutic use in mice, we performed a dose response in vivo. Mice were injected with ouabain ranging from 0-400 µg/kg ouabain for 3-14 days. Doses above 100µg/kg resulted in death; however, doses below 100µg/kg were well tolerated. To increase the likelihood of reaching a therapeutic dose without lethal side effects, we chose a new dose of 50 µg/kg of ouabain for our next in vivo studies. However, treatment with 50 µg/kg of ouabain did not demonstrate anti-fibrotic effects in vivo (Figures 3.13 A and B). Considering the delivery of a single bolus of ouabain may result in inefficient drug distribution to the lungs, we decided to change our mode of administration from IP injections to a constant infusion of ouabain via osmotic mini-pumps.

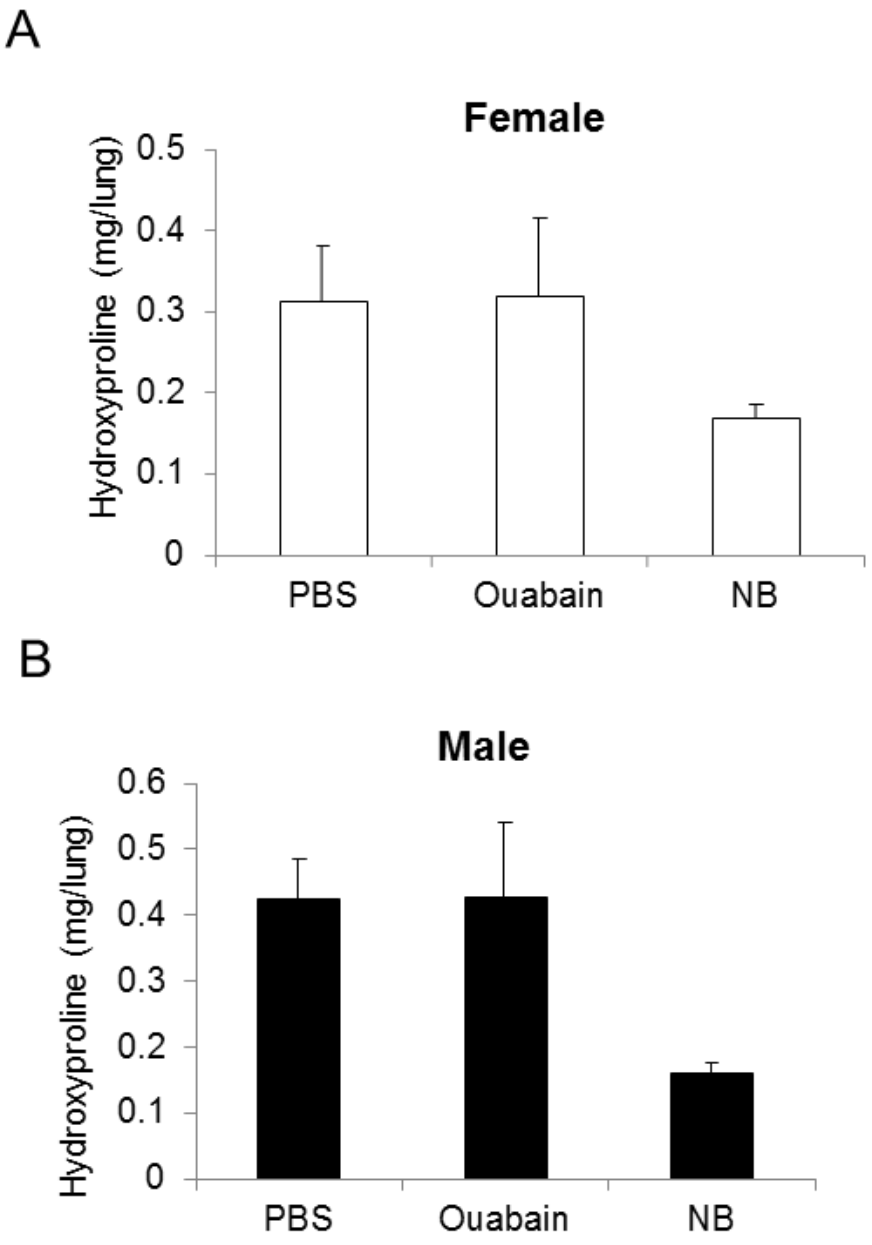

Figure 3.13. Effect of Ouabain on Bleomycin-Induced Pulmonary Fibrosis in $\alpha 1^{S/S}$ mice.

Male and female mice were injected IP with ouabain (50 ug/kg) or PBS daily, for 14 days, on the day of bleomycin instillation (males at 1.26 units/kg and females at 1.4 units/kg). After 14 days of treatment mice were sacrificed and whole long homogenates were analyzed for collagen via hydroxyproline assay.

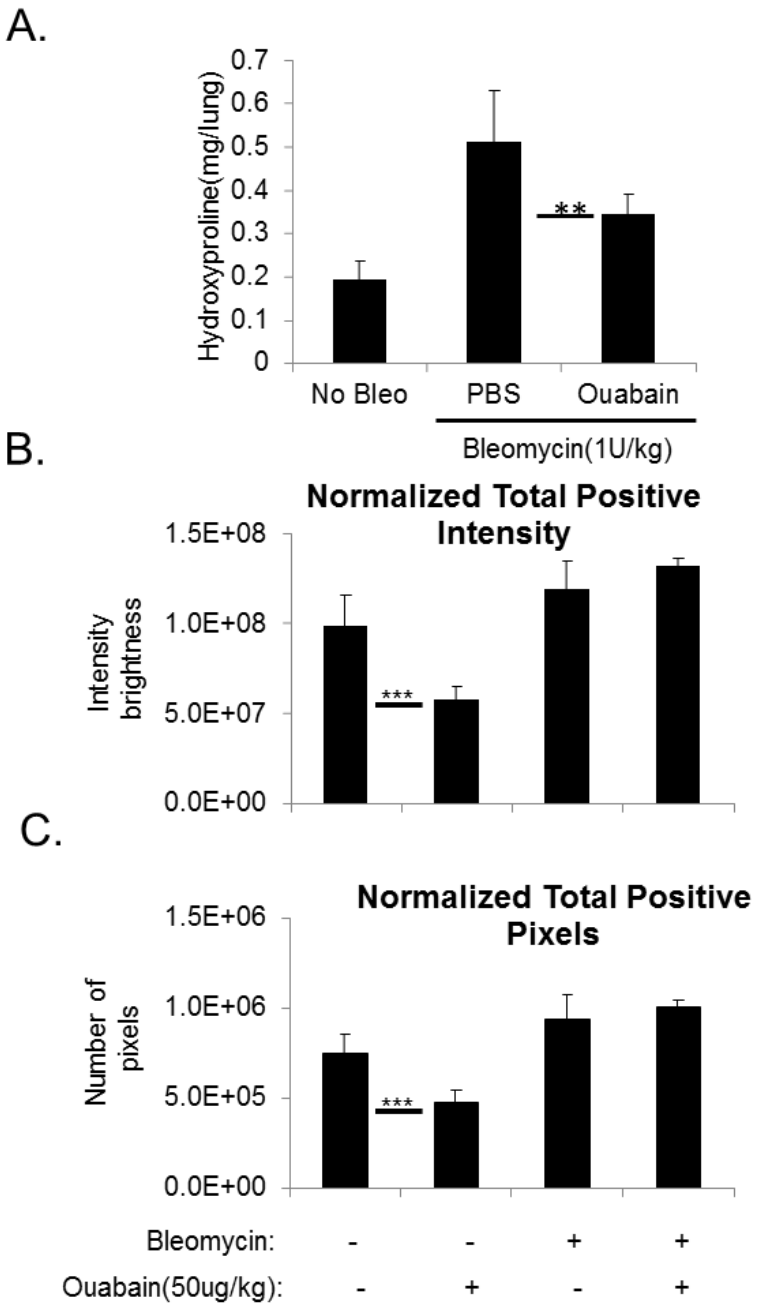

Figure 3.14. Ouabain Treatment at Via Osmotic Pumps Show Protective Effects in the Bleomycin Model of Pulmonary Fibrosis.

Male $\alpha 1^{S/S}$ mice were intratracheally instilled with 1 unit/kg of bleomycin. 48 hours following bleomycin injury, mice were treated with a constant dose of 50ug/kg per day of ouabain using osmotic mini-pumps for 14 days. Whole lungs were homogenized and analyzed for collagen deposition via the hydroxyproline assay (**A**) or whole lungs were formalin fixed and paraffin embedded, and the lung sections were stained with Masson's Trichrome stain. The average of total intensity of positive blue pixels and the total number of positive blue pixels normalized to surface area for each group are plotted. *Error bars*, S.E.; ** $p < 0.005$, *** $p < 0.0005$

Male mice were infused with PBS or 50 µg/kg of ouabain per day 2 days after bleomycin instillation. After 14 days of ouabain treatment mice were sacrificed. Whole lung homogenates from non-injured mice and bleomycin injured mice (treated with PBS or ouabain (50 µg/kg per day)), were used to analyze collagen deposition via hydroxyproline assay. Mice with bleomycin injury showed significantly more collagen deposition than non-injured controls. Importantly, mice treated with ouabain displayed a significant decrease in collagen deposition as compared to PBS treated mice (Figure 3.14A). Whole lungs were also formalin fixed and paraffin embedded, and the lung sections were stained with Masson's Trichrome stain. Quantification of total positive blue pixel intensities and total positive blue pixels, normalized to lung surface area, revealed that bleomycin injured mice treated with ouabain had similar amounts of collagen deposition as compared to bleomycin saline controls (Figure 3.14B and C). Given the 5 micron lung slice represents less than 1% of the whole lung, it may not be a true representative of the whole lung fibrosis. Furthermore, bleomycin results in more centralized fibrosis, therefore more lung slices from different sections of the lung may be required to get a better representation.

Chapter 4

Summary and Discussion

Overall Summary

Multiple studies have demonstrated IPF patients have low COX-2 expression and thus a lower capacity to synthesize PGE2. Considering COX-2 and PGE2 exhibit anti-fibrotic effects in vitro and in vivo, the lack of COX-2 and PGE2 in IPF lung is thought to play a role in the onset and progression of pulmonary fibrosis. PGE2 inhibited myofibroblast differentiation in vitro and attenuated pulmonary fibrosis in the bleomycin model. Therefore, inducing COX-2 expression in fibrotic lungs, thus driving PGE2 synthesis, could be a potential therapeutic for pulmonary fibrosis. A microarray study revealed the use of cardiac glycoside, ouabain, promoted COX-2 expression in multiple cells lines, therefore we investigated if ouabain can induce COX-2 expression in human lung fibroblasts. Our preliminary data demonstrated ouabain treatment profoundly upregulated COX-2 expression, which drove the activation of PKA, a potent inhibitor of myofibroblast differentiation. In addition, ouabain also dramatically downregulated TGFβR2 mRNA and protein levels in a dose and time dependent manner. The use of K^+-free media, an alternative mechanism of inhibiting the Na^+/K^+-ATPase, recapitulated the upregulation of COX-2 and the downregulation of TGFβR2 by ouabain, strongly suggesting these effects are Na^+/K^+-ATPase-dependent. Therefore, we hypothesized that the impedance of the Na^+/K^+-ATPase activity by cardiac glycosides would regulate myofibroblast differentiation through a dual mechanism of activating PKA and downregulating TGFβR2. To test this hypothesis, we proposed the following specific aims:

Specific Aim # 1. Examine the mechanism of by which cardiac glycoside induced COX-2 expression regulate myofibroblast activation in vitro.

Specific Aim #2. Examine the mechanism of by which cardiac glycosides regulate myofibroblast activation through the downregulation of TGFβR2. Within this aim, I will also explore the effect of ouabain administration on the development and progression of pulmonary fibrosis in the bleomycin mouse model of disease.

Studies in specific AIM1 demonstrated for the first time the inhibition of the Na^+/K^+-ATPase by ouabain dramatically upregulated COX-2 protein in pulmonary fibroblasts. Given COX-2 protein is an essential enzyme for the synthesis of PGE2, a potent activator of PKA, we explored the effects of ouabain on PKA activation and myofibroblast differentiation. We found the treatment of fibroblasts with ouabain induced PKA activation in a COX-2-dependent manner. Both enzymatic inhibition of COX-2 by NS-398 or COX-2 knockdown by siRNA resulted in the loss of ouabain stimulated PKA activation. Interestingly, ouabain also blocked TGFβ1-induced myofibroblast differentiation, which was tightly coupled to the change in the intracellular sodium and potassium levels and the induction of COX-2 expression by ouabain. To test if the upregulation of COX-2 expression was responsible for the suppression of myofibroblast differentiation by ouabain, we co-treated human lung fibroblasts with TGFβ1 and ouabain, with or without NS-398 or COX-2 siRNA. The inhibition of COX-2 enzymatic activity by NS-398 and the knockdown of COX-2 by siRNA were unable to rescue the effects of ouabain on myofibroblast differentiation.

Studies performed for specific AIM2 demonstrated the inhibition of the Na^+/K^- ATPase by ouabain potently downregulates TGFβR2 mRNA and protein levels in a

time-dependent manner in human lung fibroblast and A459 cells. Given the importance of TGFβR2 in the initiation of TGFβ1 signaling, we investigated the role of ouabain/ K^+-free media on the canonical TGFβ1 pathway. Ouabain/ K^+-free media inhibited TGFβ1-induced Smad2 phosphorylation and SBE luciferase. Furthermore, the downregulation of TGFβR2 was accompanied with the suppression of TGFβ1-induced myofibroblast differentiation and epithelial to mesenchymal transition. Although the downregulation of TGFβR2 was tightly associated with inhibition of myofibroblast differentiation, the overexpression of TGFβR2 failed to abolish the inhibitory actions of ouabain. Nonetheless, the impedance of the Na^+/K^-ATPase activity strongly inhibited TGFβ1-stimulated myofibroblast activation, and as a result we explored the potential anti-fibrotic properties of ouabain in the bleomycin model. Mice administered with ouabain at 50 μg/kg per day via osmotic mini-pumps had less collagen deposition in their lung as compared to PBS controls after bleomycin injury.

Discussion of Chapter 2

The present study describes two major findings. (i) We demonstrated the use of cardiac glycosides or K^+-free media, which inhibited the Na^+/K^+-ATPase and elevated the intracellular $[Na^+]/[K^+]$ ratio, profoundly induced COX-2 expression and PKA activation; and this effect was largely dependent on the increase of the intracellular Ca^{2+} concentration, induced by the reverse transport of the Na^+/Ca^{2+} exchanger. (ii) Inhibition of Na^+/K^+-ATPase by ouabain resulted in the attenuation of TGFβ1 induced fibrotic signaling (Rho activation, stress fiber formation and SRF activation) and the expression of myofibroblast differentiation markers, demonstrating a novel function of the Na^+/K^+-ATPase in the control of the fibroblast phenotype. However, the inhibition of COX-2 or

of the Na^+/Ca^{2+} exchanger failed to reverse the inhibitory effect of ouabain on TGFβ1-induced fibrotic signaling and myofibroblast differentiation. This may suggest that either the anti-fibrotic effects of ouabain are independent of COX-2, or COX-2 expression and PKA activation are not sufficient for inhibition of the fibrotic effects of TGFβ1 by ouabain, but may act together with other mechanisms yet to be identified. Given the previously established anti-fibrotic role of COX-2 and PKA (Dackor et al., 2011; Kach et al., 2013, 2014; Lovgren et al., 2006; Zhu et al., 2010), the latter possibility is plausible.

Our results show for the first time that cardiac glycosides suppress TGFβ1-induced fibrotic signaling (Rho activation, stress fiber formation and SRF activation (Figures 2.5, 2.8) as well as myofibroblast differentiation in HLFs, (expression of collagen-1, fibronectin and smooth muscle-α-actin) (Figure 2.4) without any impact on their survival (Figure 2.3B). Similarly to cardiac glycosides, we demonstrated that TGFβ1-induced myofibroblast differentiation is also blocked by sustained inhibition of the Na^+/K^+-ATPase in K^+-free medium (Figure 2.6). The inhibition of myofibroblast differentiation by ouabain was tightly associated with the increased intracellular $[Na^+]/[K^+]$ ratio (Figure 2.7), strongly suggesting that cardiac glycosides inhibit myofibroblast differentiation via a Na_i^+/K_i^+-dependent mechanism. It is noteworthy to mention that the actions of cardiac glycosides on fibrotic responses may be cell-specific. It was shown that certain inhibitors of Na^+/K^+-ATPase increase collagen synthesis in cultured rat cardiac fibroblasts, human dermal fibroblasts, or rat vascular smooth muscle cells (Elkareh et al., 2007, 2009; El-Okdi et al., 2008; Fedorova et al., 2015). However, these studies have not rigorously examined the effect of these compounds on 1. the expression of myofibroblast differentiation markers, 2. the magnitude of their

effect relative to that of TGFβ1, 3.TGFβ1-induced myofibroblast differentiation, or 4. collagen synthesis relative to the $[Na^+]_i/[K^+]_i$ ratio. Furthermore, these studies have largely employed marinobufagenin, which, distinct from ouabain, causes structural changes in the α1 subunit of Na^+/K^+ -ATPase (Klimanova et al., 2015) and may act through Na_i^+/K_i^+-independent mechanisms (Elkareh et al., 2009).

Previous studies have shown the increase in the $[Na^+]_i/[K^+]_i$ ratio affects the expression of genes via $Ca^{2+}{}_i$ mediated and $Ca^{2+}{}_i$-independent mechanisms (Orlov and Hamet, 2015). We found that COX-2 expression in ouabain-treated HLF is abolished by KB-R7943, a potent inhibitor of Na^+/Ca^{2+} exchanger, suggesting the elevation of the $[Na^+]_i/[K^+]_i$ ratio triggers COX-2 expression via Ca_i^{2+}- mediated signaling pathways. It should be noted, however, that along with inhibition of the three isoforms of the Na^+/Ca^{2+} exchanger (NCX1-NCX3) (Billman, 2001), KB-R7943 also affects other molecules/processes, including the ATP-dependent K^+ current (Abramochkin and Vornanen, 2014), nonselective cation channels (Pezier et al., 2009), and the mitochondrial permeability transition pore (Wiczer et al., 2014). Thus, additional experiments should be performed to examine the role of intracellular Ca^{2+} in the expression of COX-2, as well as to identify other transcriptomic changes contributing to the suppression of myofibroblast differentiation by cardiac glycosides.

The anti-fibrotic actions of COX-2, prostaglandins, and PKA are well established (Dackor et al., 2011; Kach et al., 2013, 2014; Zhu et al., 2010). It was shown that genetic disruption or pharmacological inhibition of COX-2 induced an exaggerated accumulation of myofibroblasts in mouse models of pulmonary fibrosis (Bonner et al., 2002; Giri and Hyde, 1987; Huang et al., 2008; Keerthisingam et al., 2001). Our data

demonstrated the anti-fibrotic action from the elevated $[Na^+]_i/[K^+]_i$ ratio parallels with the increase in COX-2 expression and PKA activation. Treatment of HLF with cardiac glycosides (ouabain or digoxin) or with K^+-free medium sharply augmented the content of COX-2 mRNA and protein, as well as the activity of PKA as assessed by VASP mobility shift (Figures 2.1, 2.4, 2.6). Furthermore, ouabain blocked TGFβ1 induced Rho activation (Figure 2.7), stress fiber formation, and SRF activation (Figure 2.5), all of which are critical processes for myofibroblast differentiation known to be regulated by PKA (Sandbo et al., 2009, 2011). We also showed that the COX-2 inhibitor, NS-398, and siRNA COX-2 knockdown completely abolished VASP shift seen in ouabain treated HLF (Figure 2.1). However, neither COX-2 inhibitor NS-398, nor the knockdown of this enzyme reversed the inhibitory action of ouabain on Rho activation and myofibroblast differentiation in HLF in response to TGFβ1. This may suggest that the anti-fibrotic effects of ouabain are independent of COX-2. However, given the established anti-fibrotic role of COX-2 (Dackor et al., 2011; Kach et al., 2013, 2014; Zhu et al., 2010), we propose that the elevated COX-2 expression, by the rise in the $[Na^+]_i/[K^+]_i$ ratio, may be an important but not sufficient mechanism on the inhibition of myofibroblast differentiation. Further, our data shows that inhibition of myofibroblast differentiation by ouabain is not mediated by the increase in $[Ca^{2+}]_i$, as it was not reversed by inhibition of Na^+/Ca^{2+} exchanger (Figure 2.8C), which largely contributed to the increase in $[Ca^{2+}]_i$ in response to ouabain (Figure 2.2A). Thus, unknown potential actions of the elevated $[Na^+]_i/[K^+]_i$ ratio may be responsible for the regulation of myofibroblast differentiation by cardiac glycosides.

Although this study focused on TGFβ1-induced myofibroblast differentiation, the myofibroblast phenotype and function depend on many other factors, including matrix stiffness (Liu et al., 2010; Marinković et al., 2012). Thus, it would be important to determine if cardiac glycosides affect myofibroblast differentiation driven by other factors, especially given that myofibroblast differentiation induced by a stiff matrix is associated with a decreased COX-2 expression and prostaglandin E2 synthesis (Liu et al., 2010). Further, while this study proposes the inhibition of Rho/stress fiber/SRF pathway as a potential anti-fibrotic mechanism of cardiac glycosides, their effect on other mechanosensitive signaling pathways that also contribute to myofibroblast differentiation should be examined, including the YAP/TAZ pathway (Liu et al., 2015). Finally, it would be fundamentally and practically important to demonstrate the anti-fibrotic effect of cardiac glycosides in vivo. However, numerous studies have demonstrated that the α1 subunit of the Na^+/K^+-ATPase in rodents require significantly higher concentrations of cardiac glycosides for enzyme inhibition than other mammals, whereas the affinities of rodent α2- and α3-subunits for cardiac glycosides are similar to those in other mammals (Schoner and Scheiner-Bobis, 2007). Given that the α1 subunit is the predominant isoform expressed in mouse lung fibroblasts (data not shown), wild type rodents could not be utilized for evaluating the anti-fibrotic effects of cardiac glycosides in vivo. The resistance to cardiac glycosides is caused by the presence of glutamine and asparagine as opposed to arginine and aspartate at positions 111 and 122 respectively. Based on this, Lingrel and co-workers have generated a mouse with a knock-in of ouabain-sensitive α1 isoform ($\alpha1^{s/s}$) of the Na^+/K^+-ATPase and have used it to delineate the role of α1 in blood pressure regulation, cardiac and skeletal muscle

contraction, and renal salt handling (Lingrel, 2010). These mice can be also used for elucidation of the anti-fibrotic effect of cardiac glycosides in vivo in the models of pulmonary fibrosis.

Discussion of Chapter 3

Cardiac glycosides have been used extensively for treatment of cardiac arrhythmias and heart failure due to its positive inotropic effects of the heart. Our study for the first time demonstrates (i) the inhibition of the Na^+/K^+-ATPase by cardiac glycosides promote a profound downregulation of TGFβR2 mRNA and protein levels in human lung fibroblasts and A549 cells; (ii) inhibition of the Na^+/K^+-ATPase results in the loss of TGFβ1-induced Smad2 phosphorylation, myofibroblast differentiation, and EMT; and (iii) Ouabain exhibits anti-fibrotic effects in the bleomycin model of pulmonary fibrosis.

Our results showed the inhibition of the Na^+/K^+-ATPase, via the employment of multiple mechanisms, downregulates TGFβR2 mRNA and protein levels (Figures 3.1 and 3.2). The loss of TGFβR2 was apparent in a number of IPF and non-IPF primary fibroblast, suggesting this is a general effect on fibroblasts (Figure 3.1C). Considering TGFβ1 is a major player in the activation of myofibroblasts and the progression of pulmonary fibrosis (Bartram and Speer, 2004; Broekelmann et al., 1991; Fernandez and Eickelberg, 2012; Wolters et al., 2014), inhibiting TGFβ1 signaling could be a potential approach to treating IPF. Numerous studies have demonstrated blocking the initiation of TGFβ1 signaling inhibits myofibroblast differentiation and pulmonary fibrosis. Expression of kinase-defective TGFβR2 alone was sufficient to suppress TGFβ1-dependent tenascin and fibronectin production in rat lung fibroblasts (Zhao, 1999) and

treatment with soluble-TGFβR2 attenuated liver fibrosis in Sprague-Dawley rats (George et al., 1999). Given this, we tested the effect of ouabain on TGFβ1-induced Smad phosphorylation, myofibroblast differentiation, and EMT. The downregulation of TGFβR2 by cardiac glycosides was tightly coupled with the suppression of these effects (Figures 3.3 and 3.4). Interestingly, a recently published paper revealed digoxin blocked myofibroblast differentiation in several fibroblast cell lines, further supporting the role of the Na^+/K^+-ATPase in the fibroblast phenotype (Coleman et al., 2016).

Myofibroblasts are thought to be crucial pathogenic cells in pulmonary fibrosis, and are hypothesized to be responsible for the progressive nature of this disorder. The high contractile force and extracellular matrix proteins generated by the myofibroblast has proven to be beneficial during wound healing, contributing to wound closure and tissue remodeling; however, the continued and long term presence and activation of the myofibroblasts leads to fibrotic diseases. Therefore, hindering myofibroblasts activation can potentially alleviate progressive fibrosis, a characteristic presented in IPF. The sources of myofibroblasts have been extensively studied and there is evidence to support fibroblasts arise from resident fibroblasts and EMT (Phan, 2008; Wynn, 2011). It has been well established that resident pulmonary fibroblasts are capable of differentiating into myofibroblasts. We and others have shown primary lung fibroblasts differentiate into myofibroblasts upon stimulation with TGFβ1 (Kach et al., 2014; Sandbo et al., 2011; Thannickal et al., 2003). Importantly, the inhibition of the Na^+/K^+-ATPase by ouabain/ K^+-free media blocks TGFβ1-induced myofibroblast differentiation (Figure 3.4), alluding to possible anti-fibrotic effects in vivo, given resident fibroblasts are the dominating source of fibroblasts for myofibroblast activation in the lung. The role of EMT

as source of lung myofibroblast has been controversial. However, we and others have demonstrated A549 cells, a human alveolar epithelial cell line, expressed increased mesenchymal markers, n-cadherin and vimentin, in response to TGFβ1, suggesting lung epithelial cells have the capacity for EMT. Furthermore, the presence of ouabain inhibited TGFβ1-induced Smad2 phosphorylation and mesenchymal markers in A459 cells. Limiting the pool of available fibroblasts in the lung would inhibit further myofibroblast activation.

Adenoviral infection of ad-LacZ and ad-TGFβR2 slightly abolished the effects of ouabain on the inhibition of myofibroblast differentiation, suggesting non-specific effects of adenovirus on differentiation (Figure 3.6B). To avoid the use of adenovirus, we transfected HLF with TGFβR2 mRNA transcripts, as a new method of homogenous overexpression. The overexpression of TGFβR2 via mRNA transcripts did not reverse the inhibitory actions of ouabain. In fact, increasing amounts of TGFβR2 blocked TGFβ1-induced myofibroblast differentiation (Figure 3.7A). A possible explanation for this observation may be that the overexpression of TGFβR2 results in a higher TGFβR2:TGFβR1 ratio on the cell membrane, thus decreasing the chance of TGFβR2 heterodimerizing with TGFβR1 to initiate signaling; however, this further depicts TGFβ1 signaling as necessary for myofibroblast differentiation (Figure 4.1). Therefore, overexpression of both TGFβR2 and TGFβR1 may be required to rescue the effects of ouabain on TGFβ1-induced myofibroblast differentiation.

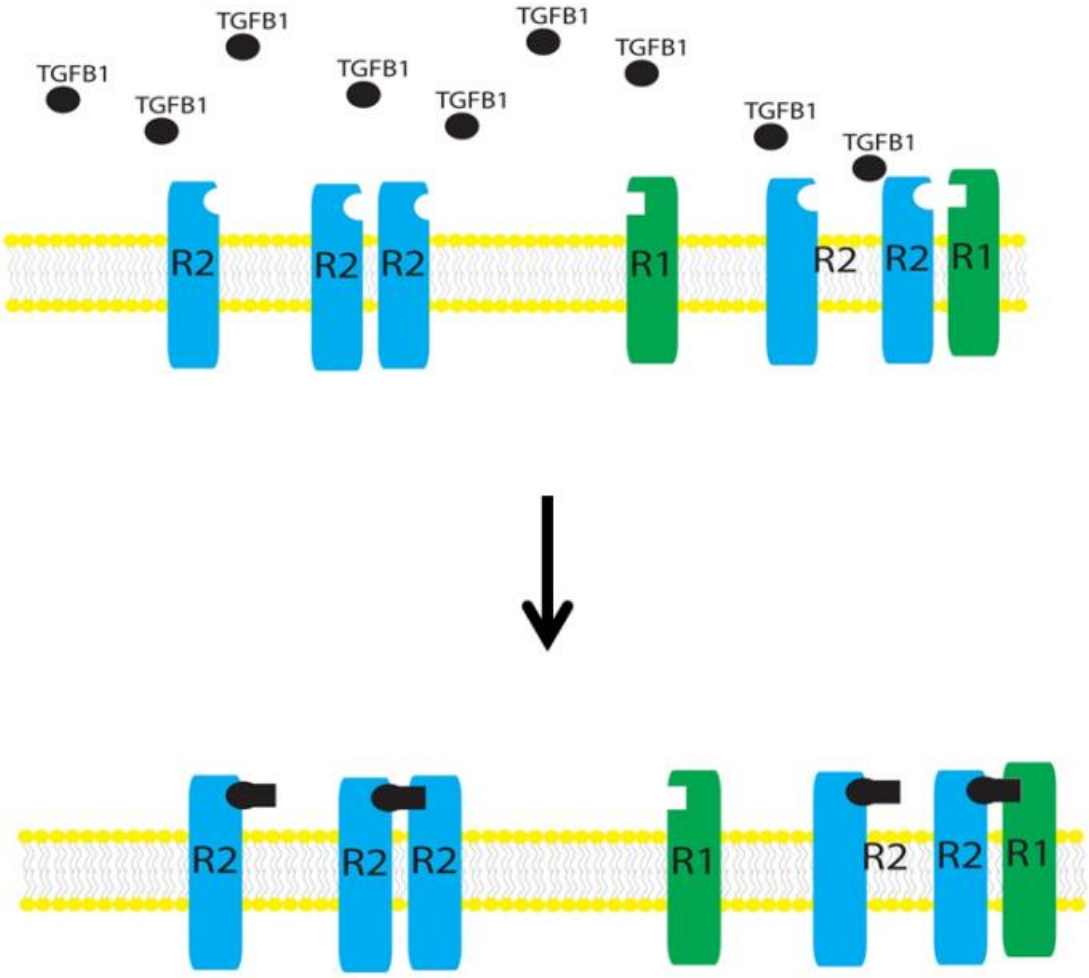

Figure 4.1 TGFβR2 Overexpression May Inhibit TGFβ1 signaling.
TGFβR2 overexpression increases the ratio of TGFβR2: TGFβR1. This decreases the likelihood of TGFβR2 binding to TGFβR1 after binding of ligand, thus inhibiting TGFβ1 signaling.

The transforming growth factor receptors are internalized via both clathrin coated pits and lipid rafts/caveolae, resulting in the induction of TGFβ1 signaling or receptor degradation respectively (Di Guglielmo et al., 2003). It is well established that depleting intracellular potassium disrupts clathrin formation by 80-90% (Larkin et al., 1983, 1985). Interestingly, a previous study demonstrated that the use of K^+-free media blocked clathrin-mediated TGFβ receptor internalization, and thus inhibited TGFβ1 signaling (Penheiter et al., 2002). Taking into account both K^+-free media and cardiac glycosides hinder the activity of the Na^+/K^+-ATPase and therefore reduces the intracellular potassium levels (La et al., 2016), cardiac glycosides may mimic the effect of K^+-free media on clathrin coated pit formation. Thus, assuming cardiac glycosides blocks TGFβ receptor internalization; the overexpression of TGFβR2 would not abolish the inhibitory actions of ouabain on TGFβ1-induced myofibroblast differentiation (Figure 4.2). Further, reduction of endocytosis by clathrin coated pits shifts the equilibrium towards increased internalization of TGFβ receptors by lipid rafts/caveolae, leading to receptor degradation (Di Guglielmo et al., 2003), which may contribute to the observed downregulation of TGFβR2 protein by ouabain. Given this, it is important to investigate whether cardiac glycosides inhibit clathrin formation and explore if this mechanism is important in the suppression of myofibroblast differentiation by cardiac glycosides. Considering cardiac glycosides may inhibit receptor internalization, we investigated if overexpression Smad2 protein, which we have shown to drive the SBE-luciferase reporter gene (data not shown), could be used as an alternative method to induced TGFβ1 signaling downstream of receptor endocytosis.

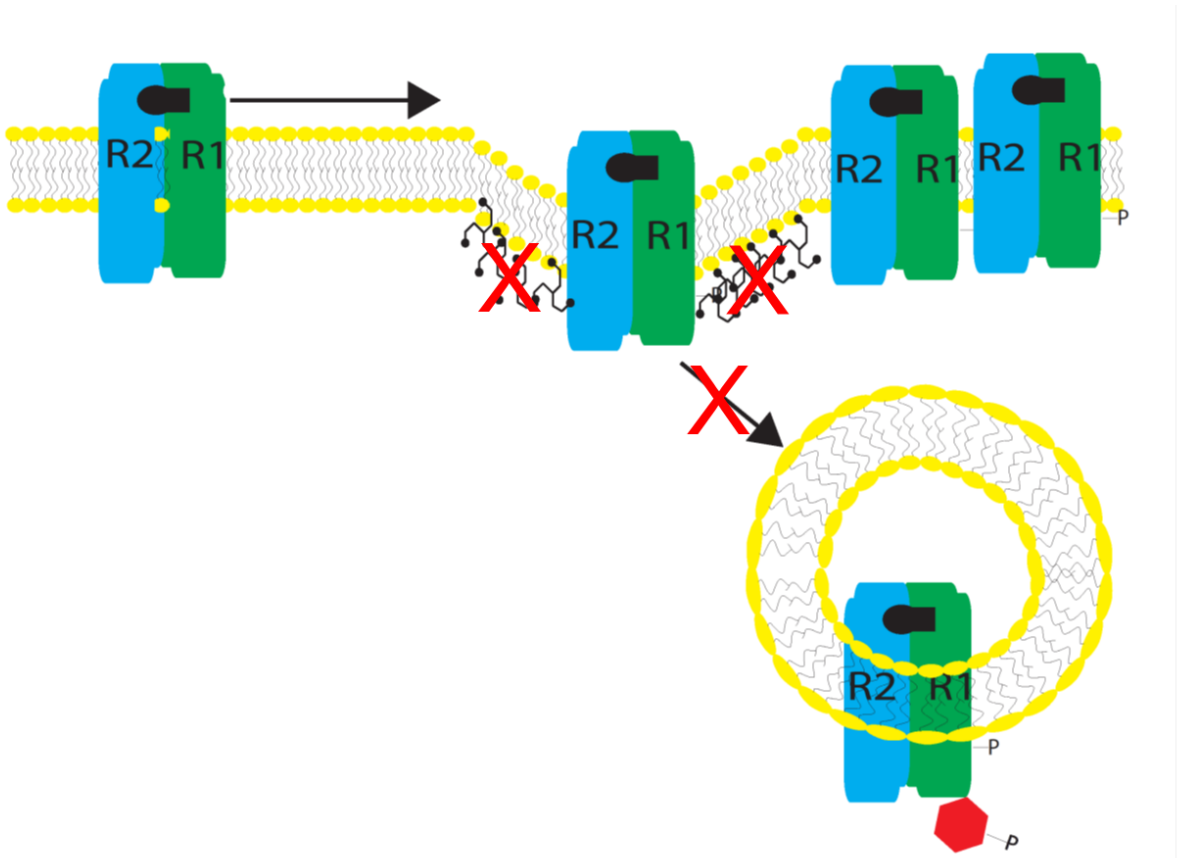

Figure 4.2 Alternative Mechanism of blocking TGFβ1 signaling by inhibiting the Na/K ATPase.
Similarly to potassium free media, it is proposed that cardiac glycosides could also prevent clathrin coated pit dependent endocytosis, a process required for the initiation of TGFβ1 signaling. Therefore, cardiac glycosides may block the initiation of TGFβ1 signaling by hindering clathrin mediated endocytosis of the TGFβ receptors after ligand binding.

Transfection of Smad2 mRNA successfully promoted Smad2 protein expression; however, it did not induce myofibroblast differentiation or drive SBE-luciferase in vitro (Figure 3.8).

Our previous study demonstrated the inhibition of the Na^+/K^+-ATPase dramatically upregulated COX-2-dependent PKA activity (La et al., 2016), which has been shown to exhibit anti-fibrotic properties by regulating the SRF axis (a signaling pathway downstream of Smad activation). However, inhibition of COX-2 enzymatic activity or COX-2 knockdown was unable to rescue the effects of ouabain on myofibroblast differentiation. Given ouabain both dramatically downregulates TGFβR2 and profoundly upregulates COX-2, we explored if both TGFβR2 overexpression and knockdown of COX-2 are required for abolishing the inhibitory actions of ouabain. We found the overexpression of TGFβR2 and knockdown of COX-2 does not reverse the inhibition of myofibroblast differentiation by ouabain (Figure 3.7B). Together, these data suggests the anti-fibrotic effects of ouabain are independent of TGFβR2 downregulation, COX-2 expression, and PKA activation, or the downregulation of TGFβR2, COX-2 expression, and PKA activation are not sufficient for inhibition of the fibrotic effects of TGFβ1 by ouabain.

Considering the strong effect of ouabain/K^+ free media on TGFβ1-induced myofibroblast differentiation, we investigated if TGFβ1 controls myofibroblast differentiation by manipulating the expression or function of the Na^+/K^+-ATPase. As previously mentioned, the Na^+/K^+-ATPase consists of the catalytic α-subunit (required for enzymatic activity of the protein) and regulatory β-subunit (required for appropriate localization and stabilization of the α-subunit). We found 1. TGFβ1 induced a profound

and sustained expression of the ATP1B1 (β1-subunit) mRNA and protein, and 2. the ATP1B1 promoter contained a putative SmS-binding site identical to the established SMAD target gene, Smad7 (Nagarajan et al., 1999), suggesting ATP1B1 may be a novel target of TGFβ1 as a mechanism to regulate myofibroblast differentiation (Figure 3.9). To explore if increased ATP1B1 expression by TGFβ1 is required for myofibroblast differentiation, we examined if knockdown of ATP1B1 would block TGFβ1-induced myofibroblast differentiation. Knockdown of ATP1B1 or ATP1A1 was not sufficient to inhibit TGFβ1-induced myofibroblast differentiation (Figure 3.11). Given many isoforms of both the α and β units exist in mammals, the knockdown of one isoform may be compensated by another isoform. Measuring the change in intracellular Na^+ and K^+ concentration after siRNA knockdown of each isoform needs to be performed to confirm possible compensatory functions by other isozymes.

The family of cardiac glycosides has been well established as inhibitors of the Na^+/K^+-ATPase, and both digoxin and ouabain are clinically used for heart failure and cardiac arrhythmias. For the first time, we showed that cardiac glycosides have anti-fibrotic effects in vivo. Because wild-type mice are insensitive to cardiac glycosides, we used $\alpha1^{S/S}$ knock-in mice to test the effects of ouabain on pulmonary fibrosis in vivo. Mouse lung fibroblasts isolated from the mutant mice, but not wild-type mice, showed a dramatic downregulation of TGFβR2 mRNA in response to ouabain treatment (Figure 3.12A), further suggesting that the inhibition of Na^+/K^+-ATPase leads to the downregulation of TGFβR2. However in vivo, treatment of ouabain via IP injections did not significantly reduce pulmonary collagen levels in the bleomycin model (Figures 3.12 and 3.13).

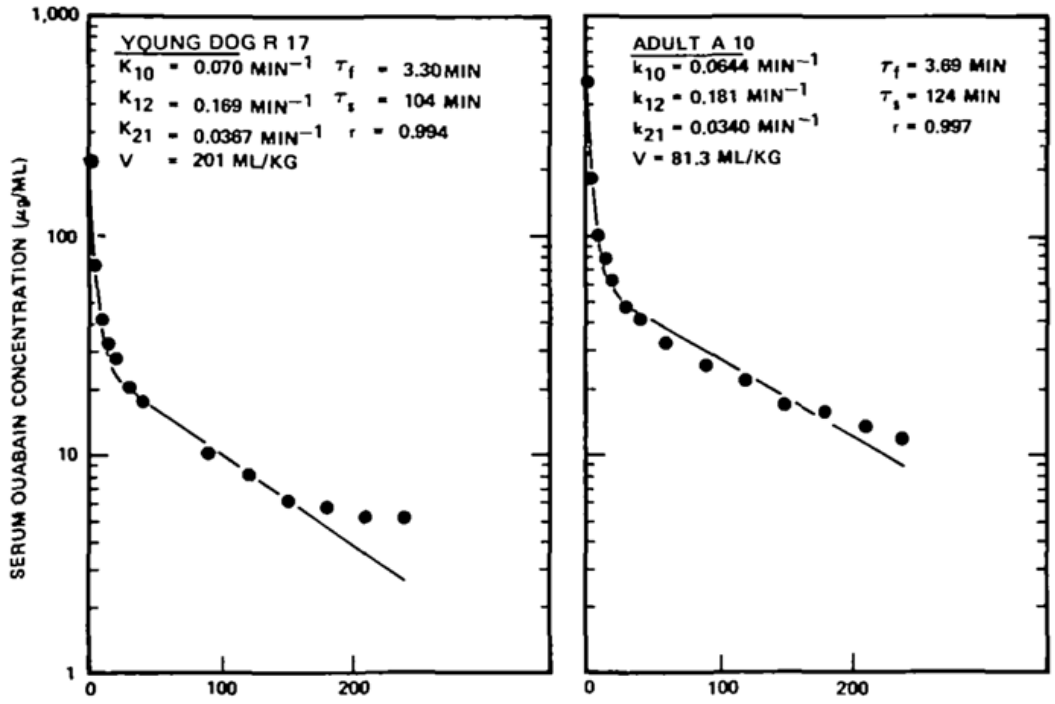

TABLE 1 *Serum Ouabain Concentrations*

	Serum ouabain concentration (ng/ml)								
	Adult dogs			Young dogs				Weights*	
Time (min)	*n*	Mean	SE	*n*	Mean	SE	*P*†	Adult dogs	Young dogs
1	16	478	16.9	18	248	13.3	0.000	0.0125	0.00343
5	18	148	6.54	18	70.5	5.08	0.000	0.0740	0.0235
10	20	84.3	6.28	21	39.4	2.14	0.000	0.0722	0.113
15	18	53.5	3.73	19	30.6	2.14	0.000	0.227	0.125
20	20	46.3	2.96	22	26.1	1.80	0.000	0.325	0.154
30	20	35.3	2.47	22	20.3	1.32	0.000	0.467	0.286
40	15	31.6	2.54	17	18.1	1.23	0.000	0.589	0.419
60	15	24.5	2.32	17	14.2	1.14	0.001	0.704	0.493
90	15	19.1	2.22	17	10.7	0.984	0.002	0.768	0.662
120	10	15 4	1.91	12	8.50	0.884	0.003	1.55	1.16
150	10	12.5	1.63	12	7.17	0.891	0.004	2.14	1.15
180	9	10.7	1.79	12	5.73	0.600	0.013	1.97	2.53
210	10	9.60	1.55	12	5.06	0.592	0.009	2.36	2.59
240	10	8.54	1.45	12	4.26	0 461	0.008	2.73	4.29

* If all points were weighted equally, each weight would be 1.

† To test the hypothesis that adult concentrations are greater than young dog concentrations, we used a one-tail *t*-test SPSS reports exact *P* values, rounded to three decimal places. Thus 0.000 indicates $P < 0.0005$.

Figure 4.3. Serum Ouabain Concentration in Young and Adult Dog. Data for these two typical dogs show that the linear two-compartment model accurately predicts the observed biexponenlial drop in serum ouabain concentration in both adult and young dogs. Note, however, that late in the experiment the predicted curve systematically falls below the observations in both cases (Glantz et al).

TABLE 1
Tissue Distribution of Ouabain-H^3

	Rat %/. dose/100g 16 min	Rat %/. dose/100g 6 hrs	Guinea Pig %/. dose/100g 16 min
Atrium	2.41	0.18	4.82
Ventricle	7.59	0.37	8.89
Liver	25.20	0.93	2.41
Spleen	1.00	0.18	1.71
Adrenal	2.95	1.85	1.10
Kidney	6.22	1.11	15.95
Ovary	4.54	0.18	2.02
Skeletal Muscle	5.57	1.73	0.40
Eye	2.59	0.28	0.50
Pituitary	40.87	5.46	6.36
Hypothalamus	2.33	1.11	0.10
Cortex	0.37	0.09	0.10
Lung	2.41	1.11	1.71
Uterine Muscle	3.61	0.81	1.82
Fat	1.01	2.78	1.52 *
Blood	3.33	0.09	1.41

* Two Animals

Figure 4.4. Tissue Distribution of Ouabain in Rats and Guinea Pigs.

Rats and Guinea pigs were administered 46ug/kg of Ouabain-H^3 intravenously and sacrificed 16 minutes later for analysis of ouabain distribution in the indicated tissues. Numbers represent percent of dose per 100g of tissue. (Dutta and Marks, 1966)

Given the half-life of ouabain in blood plasma of dogs is about 5 minutes, the lack of efficacy from a single daily dose of ouabain maybe be due to poor distribution of drug to the lungs (Glantz et al., 1976) (Figure 4.3). A study on the volume of distribution of ouabain demonstrated that the majority of ouabain is absorbed by the pituitary and the liver, 16 minutes post IV injection. Importantly, some drug does end up in the lungs (Dutta and Marks, 1966) (Figure 4.4). Constant infusion of drug at a slow steady rate, as opposed to a daily bolus of drug, will provide a steady supply of free drug in the blood for delivery to the lungs. As a result, we inserted osmotic pumps (infusion rate of 26ul) filled with PBS or ouabain (50µg/kg per day), into $\alpha1^{S/S}$ mice 2 days post bleomycin injury. Mice treated with ouabain via osmotic mini-pump exhibited less collagen deposition in the lung as compared to their sex-matched controls when quantifying whole lung homogenate via hydroxyproline assay (Figure 3.14A). Given the mutant mouse Na^+/K^+-ATPase may not be as sensitive as human Na^+/K^+-ATPase to cardiac glycosides, the current clinical dose of 3.4-5.1 µg/kg of digoxin may be adequate for inhibiting myofibroblast differentiation. A previous study showed three healthy males ranging between 73-82 kg, injected with ouabain at 0.5mg IV (6.1-6.8ng/kg), had ouabain plasma concentration above 30 nM for over 50 hours post IV injection (Selden and Smith, 1972). Considering the volume of distribution between blood and lung are similar (Dutta and Marks, 1966) and 30 nM ouabain was sufficient to inhibit myofibroblast differentiation in vitro (Figure 3.4D), the amount of ouabain delivered to the lung at clinical doses may be sufficient to suppress myofibroblast differentiation in vivo. Thus, cardiac glycosides may be repurposed and used as a potential therapeutic for pulmonary fibrosis.

Chapter 5

Materials and Methods for Chapter 2

Isolation and culture of primary human lung fibroblasts. Human lung fibroblasts were isolated as described previously (Sandbo et al., 2009). Briefly, tissue samples from explanted lungs from patients undergoing lung transplantation were obtained and placed in Dulbecco's Modified Eagle Medium (DMEM) with 100 U/ml streptomycin, 250 ng/ml amphotericin B, and 100 U/ml penicillin. Lung tissue was minced, washed in PBS, and plated on 10-cm plates in growth media containing DMEM supplemented with 10% FBS, 2 mM L-glutamine, 100 U/ml streptomycin, 250 ng/ml amphotericin B, and 100 U/ml penicillin. The media was changed every two days. After ~2 weeks, the explanted and amplified fibroblasts were cleared from the tissue pieces, trypsinized, and further amplified as passage 1. For experiments, cells were grown in 12-well plates at a density of 1×10^5cells/well in a growth medium (DEME containing 20% heat inactivated FBS, antibiotics, and L-glutamine) for 24 hours, starved in DMEM containing filtered bovine serum albumin at 0.1% for 24 hours, and treated with desired drugs for various times. All primary cultures were used from passage 3 to 10.

Transfection and Luciferase Assay. Subconfluent cells were co-transfected with desired firefly luciferase reporter plasmid, and thymidine kinase (TK) promoter-driven Renilla luciferase plasmid (TK-Rl). Briefly, desired amount of plasmid (300ng/well in 24 well plate) and thymidine kinase promoter-driven Renilla luciferase plasmid (20ng/well in 24 well plate) was diluted in DMEM containing HEPES and glutamine. GeneDrill reagent was also diluted in the same media (1.5ul of GeneDrill per well in 24 well plate). Plasmid and GeneDrill mixture was mixed together in a 1:1 ratio for 15 minutes.

Meanwhile, the cell media was replaced with fresh full serum media before transfection. Plasmid and genedrill mixture was introduced to the cells for 5 hours. Cells were serum-starved, followed by stimulation with desired agonists. Cells were washed and then lysed in protein extraction reagent. Lysates were assayed for firefly and Renilla luciferase activity using the dual luciferase assay kit (Promega). To account for differences in transfection efficiency, firefly luciferase activity of each sample was normalized to Renilla luciferase activity.

Knockdown of COX-2. For COX-2 knockdown, the following siRNA was used: 5'-UAGGGCUUCAGCAUAAAGCGU-3' (Qiegen, Valencia, CA). COX siRNA or scrambled RNA were transfected using use Lipofectamine® RNAiMAX transfection reagent (Life Technologies, Grand Island, NY) following manufacture's standard protocol. Briefly, siRNA (30pM final concentration in well) was diluted in optimem buffer and RNAiMAX (3ul/ well per 12 well dish) was also diluted in optimem buffer. siRNA and RNAiMAX solutions were combined in a 1:1 ratio and sat for 5 minutes. Cells were transfected with combined mixture for 24 hours before cells were starved. Afterwards cells were subjected to desired drug treatment for specified amount of time. Cells were lysed in ripa buffer then subjected to Western blotting.

Cell lysis and Western blotting. After stimulation of cells with desired agonists, cells were lysed in the radioimmunoprecipitation (RIPA) buffer containing 25 mM HEPES (pH 7.5), 150 mM NaCl, 1% Triton X-100, 0.1% SDS, 2 mM EDTA, 2 mM EGTA, 10% glycerol, 1 mM NaF, 200 μM sodium orthovanadate, and protease inhibitor cocktail (Sigma). Cells were scraped, sonicated, a sample taken for the measurement of protein concentration, and the remainder boiled in Laemmli buffer for 5 min. The samples were

normalized to the protein content, subjected to polyacrylamide gel electrophoresis, analyzed by Western blotting with desired primary antibodies and corresponding horseradish peroxidase- conjugated secondary antibodies, and developed by an enhanced chemilumeniscence reaction (Pierce). The digital chemilumeniscent pictures were imaged by a Luminescent Image Analyzer LAS-4000 (Fujifilm).

Reverse transcription-quantitative real-time PCR. RNA STAT-60 (TEL-Test) was used to isolate total RNA following the manufacturer's protocol. RNA was randomly primed and reverse transcribed using the iScript cDNA synthesis kit (Bio-Rad, Hercules, USA) according to the manufacturer's protocols. Real-time PCR analysis was performed using iTaq SYBR Green supermix with ROX (Bio-Rad) in a MyIQ single-color real-time PCR detection system (Bio-Rad) The COX-2 primers were: AGAAAACTGCTCAACACCGGA (forward) and CAAGGGAGTCGGGCAATCAT (reverse).

Fluorescent microscopy of stress fibers. For visualization of stress fibers, cells grown on cover slips were fixed in 4% paraformaldehyde in PBS followed by permeabilization with 0.2% Triton X-100 in PBS. Cells were then incubated in 2% BSA in PBS, followed by incubation rhodamine-conjugated phalloidin (Life Technologies, Grand Island, NY) for 1 hour at room temperature. Cells were then washed 5 times with PBS and coverslips were mounted using Vectashield mounting medium containing DAPI nuclear stain (Vector Laboratories, Burlingame, CA). Fluorescence images were obtained using an Olympus 1X71 fluorescent microscope.

In vitro isolation of stress fibers. Stress fibers were isolated as previously described (Sandbo et al., 2011). All the procedures were performed on ice using the buffers

containing protease inhibitor cocktail (Sigma). After stimulation with desired agonists, cells were washed with PBS, and then extracted with a buffer containing 2.5mM triethanolamine (pH 8.2) for 30 minutes with 6 buffer changes, followed by extraction with 0.05% NP-40 (pH 7.2) for 5 minutes, and subsequent extraction with 0.5% Triton X-100 (pH 7.2) for additional 5 minutes. Cells were then immediately washed with cold PBS, scraped, and suspended in PBS, followed by centrifugation at 100,000 g for 1 hr. Supernatant was removed, and the pellet was 5 sonicated in 0.5% TX100, 50 mM NaCl, 20 mM Hepes (pH 7.0), 1 mM EDTA. Laemmli buffer was added and samples were boiled for 5 minutes prior to further Western blot analysis as described above.

Intracellular content of monovalent ions. Intracellular K^+ and Na^+ content was measured as the steady-state distribution of extra- and intracellular ^{86}Rb and ^{22}Na, respectively. To establish isotope equilibrium, cells growing in 12-well plates were preincubated for 3 hours in control or K^+ -free medium (Sp-DMEM+Ca) containing 0.5 µCi/ml $^{86}RbCl$ or ^{4} µCi/ml ^{22} NaCl with high concentration ouabain added for the next 3 hours. To test the action of K^+ -free medium, the cells were washed twice with ice-cold Sp-DMEM+Ca. Then, cells were transferred to Sp-DMEM+Ca medium containing NaCl. After 3 hours, cells were transferred on ice, washed 4 times with 2 mls of ice-cold medium W containing 100 mM $MgCl_2$ and 10 mM HEPES-tris buffer (pH 7.4). The washing medium was aspirated and the cells lysed with 1% SDS and 4 mM EDTA solution. Radioactivity of the incubation media and cell lysates was quantified, and intracellular cation content was calculated as A/am, where A was the radioactivity of the samples (cpm), “a” was the specific radioactivity of ^{86}Rb (K^+) or ^{22} Na (cpm/nmol), and “m” was protein content (mg). For more details, see Akimova et al., 2005.

$^{45}Ca^{2+}$ influx. Confluent, quiescent cultures of HLF seeded in 12-well plates were treated as indicated in Fig. 2.6A legend, washed twice at room temperature with 2-ml aliquots of medium containing 150 mM NaCl and 10 mM HEPES-Tris (pH 7.4) and 0.5 ml of medium containing 140 mM NaCl, 5 mM KCl, 1 mM $MgCl_2$, 0.1 mM $CaCl_2$, 5 mM glucose, 20 mM, HEPES-Tris 20 (pH 7.4), ^{4} mCi/ml ^{45} Ca ± 1 µM nicardipine or 3 µM KB-R4943 was added to each well. After 5 minutes, isotope uptake was terminated by the addition of 2.5 ml ice-cold medium W. The dishes were transferred onto ice, and the cells were washed 5 times with 2.5 ml of ice-cold medium W. The cells were lysed with 1 ml of 4 mM EDTA/1% sodium dodecyl sulfate, and radioactivity was quantified by liquid scintillation counting. ^{45}Ca influx was calculated as A/am, where “A” is radioactivity in the cell lysate (cpm), “a” is specific radioactivity of the incubation medium (cpm/pmol), and ” m” is the protein content per well (mg). The activity of L-type Ca2+ channel and Na^{+}/Ca^{2+} exchanger was quantified as nicardipine- and KB-R7943-sensitive components of the rate of ^{45}Ca influx, respectively. For more details, see (Orlov et al., 1993, 1996b) .

Cytotoxicity assay. Cytotoxicity of drugs was measured by a release of lactate dehydrogenase (LDH) using colorimetric CytoTox 96® Non-Radioactive Cytotoxicity Assay kit (Promega) and following the manufacturer's protocol. Cells were split into a 96 well dish and grown overnight. Afterwards cells were starved for 24 hours then stimulated with drugs for the specified amount of time. 50 ul of supernatant from the wells post treatment was transferred to a new 96 well dish (plate a) for reading. 50ul of low serum media was added back to the wells and cells were then subjected to cell lysis using the lysis buffer from the kit. Supernatant from lysed cells were transferred to the

plate for reading. Amount of LDH release was measured using a standard curve. The percent of LDH released was calculated by amount of LDH released after treatment/(LDH released after treatment + LDH released after lysis).

Reagents. TGF-β1 and VASP antibodies were from EMD Millipore (Billerica, MA). COX-2 antibodies were from Cell Signaling Technology (Danvers, MA); collagen-1 antibodies were from Cedarlane (Burlington, NC); fibronectin antibodies were from BD Biosciences (San Jose, CA). Ouabain, digoxin, nicardipine and antibodies against SM α-actin and β-tubulin were provided by Sigma-Aldrich (St. Louis, MO). ^{22} NaCl, ^{86} RbCl and ^{45} CaCl2 were obtained from PerkinElmer (Waltham, MA).

Materials and Methods for Chapter 3

Primary Culture of Human and Mouse Lung Fibroblasts. Human lung fibroblasts were cultured as described previously as described above. Mouse lung fibroblasts were cultured in a similar manner. For experiments, cells were grown in 12-well plates at a density of 1×10^5cells/well in a growth medium (DEME containing 20% heat inactivated FBS, antibiotics, and L-glutamine) for 24 hours, starved in DMEM containing filtered bovine serum albumin at 0.1% for 24 hours, then treated with desired drugs for various times. All primary cultures were used from passage 3 to 10.

Reverse transcription-quantitative real-time PCR. Zymoresearch Isolate Kit was used to isolate RNA (Direct-zol™ RNA Kits). RNA was randomly primed and reverse transcribed using the iScript cDNA synthesis kit (Bio-Rad, Hercules, USA) according to the manufacturer's protocols. Real-time PCR analysis was performed using iTaq SYBR Green supermix with ROX (Bio-Rad) in a MyIQ single-color real-time PCR detection system (Bio-Rad), the hTGFβR2 primers were: GGAGTTTCCTGTTTCCCCCG

(forward) and ATGTCTCAGTGGATGGGCAG (reverse), the hATP1B1 primers were: CGGGAAAGCCAAGGAGGAG (forward) and GGCCACTCGGTCCTGATATG (reverse), the hATP1A1 primers were: AGCTGCTCTGTGCTTTTCTCT (forward) and TGTTAATCCCCGGCTCAAGT (reverse).

Cell Lysis and Western Blotting. Cells were lysed in urea buffer containing 8 M deionized urea, 1% SDS, 10% glycerol, 60mM Tris ph 6.8, 0.01% pyronin Y, and 5% BME. Lysates were sonicated for 5 seconds. Samples were then subjected to polyacrylamide gel electrophoresis and Western blotting with desired primary antibodies and corresponding horseradish peroxidase (HRP)-conjugated secondary antibodies, and developed by chemiluminescence reaction (Pierce). Digital chemiluminescent images below the saturation level were obtained with a LAS-4000 analyzer, and the light intensity was quantified using Multi Gauge software (Fujifilm).

Transfection and Luciferase Assay. Subconfluent cells were co-transfected with desired firefly luciferase reporter plasmid, and thymidine kinase (TK) promoter-driven Renilla luciferase plasmid (TK-Rl) as described above. Briefly, desired amount of plasmid and thymidine kinase promoter-driven Renilla luciferase plasmid was diluted in DMEM containing HEPES and glutamine. GeneDrill reagent was also diluted in the same media. Plasmid and GeneDrill mixture was mixed together in a 1:1 ratio for 15 minutes. Meanwhile, the cell media was replaced with fresh full serum media before transfection. Plasmid and genedrill mixture was introduced to the cells for 5 hours. Cells were serum-starved, followed by stimulation with desired agonists. Cells were washed and then lysed in protein extraction reagent. Lysates were assayed for firefly and Renilla luciferase activity using the dual luciferase assay kit (Promega). To account for

differences in transfection efficiency, firefly luciferase activity of each sample was normalized to Renilla luciferase activity.

Knockdown of ATP1B1 and ATP1A1. For ATP1B1 and ATP1A1 knockdown, the following siRNAs were used: ATP1B1#1 5'- AACCGAGTTCTAGGCTTCAAA-3', ATP1B1#2 5'- CCCAGTGAACCGAAAGAACGA-3', ATP1B1#3 5'- ATCCTTCTATTCTACGTAATA-3', ATP1B1#4 5'- CCGGTGGCAGTTGGTTTAAGA-3', ATP1A1#1 5'-CCCGGAAAGACTGAAAGAATA-3', ATP1A1 #2 5'- CACCTCTTTCTGCCAGATGAA-3' , ATP1A1 #3 5'-ATCCATGAAGCTGATACGACA-3, ATP1A1#4 5'-CTTGATGAACTTCATCGTAAA-3' (Qiegen, Valencia, CA). ATP1A1/ATP1B1 siRNA or scrambled RNA were transfected using use Lipofectamine® RNAiMAX transfection reagent (Life Technologies, Grand Island, NY) following manufacture's standard protocol. Briefly, siRNA was diluted in optimem buffer and RNAiMAX (3ul/ well per 12 well dish) was also diluted in optimem buffer. siRNA and RNAiMAX solutions were combined in a 1:1 ratio and sat for 5 minutes. Cells were transfected with combined mixture for 24 hours before cells were starved. Afterwards cells were subjected to desired drug treatment for specified amount of time. Cells were lysed in urea buffer then subjected to western blotting.

Adenoviral infection. Adenovirus-mediated gene transduction was performed by incubating desired virus concentrations with GeneJammer reagent (Stratagene, La Jolla, CA) for 5 minutes. Virus and GeneJammer mixture was introduced to subconfluent cells for 24 hours. Afterwards cells were starved in 0.1% BSA for 24 hours then treated with desired drugs for the specified amount of time.

De Novo synthesis of TGFβR2 and SMAD2 mRNA. TGFβR2 and SMAD2 mRNA were made following the mMESSAGE mMACHINE T7 Transcription Kit. Briefly, TGFβR2 and SMAD2 cDNA was cloned downstream of the T7 promoter in the pcDNA3.1+ vector. T7- TGFβR2 and T7-SMAD2 cDNA was amplified then the PCR template was subjected to gel extraction purification using the QIAquick gel extraction kit. PCR template concentrations fell between 100-200ng/ul. 150ng of template was used to synthesize mRNA following the manual's steps. Synthesized mRNA was recovered using the MEGAclear kit.

Transfection of mRNA. mRNA was transfected based on the Lipofectamine MessengerMAX Transfection protocol. Desired concentration of synthesized mRNA was diluted in opti-MEM buffer and the MessengerMAX reagent (3ul/well in 12 well dish) was also separately diluted in opti-MEM buffer. mRNA and MessengerMAX mixture was combined in a 1:1 ratio for 5 minutes then introduced to the cells for 24 hours. Afterwards, cells were starved for 24 hours then treated with desired drugs for the specified amount of time. Cells were lysed in urea buffer and cell lysates were subjected to Western blotting.

Bleomycin-induced Pulmonary Fibrosis. Alpha1-sensitive ($\alpha1^{S/S}$) mice were kindly provided by Dr. John N. Lingrel (University of Cincinnati, OH, USA) and bred in house for in vivo studies. 8–13 week old $\alpha1^{S/S}$ mice were intratracheally instilled with 1 unit/kg bleomycin (BLEOmycin, Teva). Ouabain was administered IP daily (7 days after bleomycin) or via mini-pumps (Alzet, Model 1002) with a dose of 50μg/kg per day (2 days after bleomycin). Lungs were removed 14 days after ouabain administration. Whole lungs were homogenized to analyze hydroxyproline content or formalin-fixed and

paraffin embedded, and immunohistochemistry was performed on lung sections. Images of the stained sections were obtained on a CRi Pannoramic whole slide scanner.

Hydroxyproline Assay. The hydroxyproline assay was performed as described previously (Kach et al., 2013). Briefly, whole lungs were homogenized in 2mls of PBS. 12N hydrocholoric acid was added to homogenate in a 1:1 ratio and was hydrolyzed overnight at 110 °C. A 10 ul aliquot was evaporated, resuspended in 100ul of citrate-acetate buffer (5% citric acid, 1.2% glacial acetic acid, 7.24% sodium acetate, 3.4% NaOH, In dH2O pH 6.0) with chloramine T (0.282 g Chloramine T, 2mL n-Propanol, 2mL dH2O, Add citrate-acetate buffer to 20mL line) and left at room temperature for 20 minutes. Afterwards 100ul of fresh Ehrlich's solution (4.5g dimethylaminobenzaldehyde, 18.6ml n-propanol, 7.8mL 70% perchloric acid) was then added, and samples were heated at 65 °C for 15 min. Absorbance was measured at 550 nm. Hydroxyproline content was determined against a standard curve generated from pure hydroxyproline.

Histology Quantification. Whole lungs were formalin-fixed and paraffin embedded, and immunohistochemistry was performed on lung sections. Images of the Masson Trichrome stained sections were obtained on a CRi Pannoramic whole slide scanner. Slides were analyzed using the Aperio ImageScope program. Briefly, the lung sections were traced using the pen tool. The positive pixel count algorithm (parameters: hue width of 0.33 and ISP low of 50) was used to quantify the blue pixel intensities and blue pixel numbers as a way to sum total collagen in the lung. The sum of the positive total intensity and the sum of the total number of blue pixels was normalized to the lung surface area.

Reagents. Ouabain Octahydrate was from Sigma-Aldrich. TGFβ1 was from EMD Millipore (billerica, MA). Pharmaceutical grade bleomycin (BLEOmycin) was from TEVA (lot#: 31314497B). Antibodies for western blotting against SM α-actin, β-actin, and α-tubulin were from Sigma-Aldrich; collagen-1 and transforming growth factor-β type 2 receptor antibodies were from Santa Cruz. SiRNA was ordered from Qiagen. Hydroxyproline was from sigma. Osmotic mini pumps are from Alzet (model 1002).

Statistical Analysis. Quantitative data from three independent experiments were analyzed by Student's t-test. Values of $p < 0.05$ were considered statistically significant.

References

Abramochkin, D.V., and Vornanen, M. (2014). Inhibition of the cardiac ATP-dependent potassium current by KB-R7943. Comp. Biochem. Physiol. A. Mol. Integr. Physiol. 175, 38–45.

Ackermann, U., and Geering, K. (1990). Mutual dependence of Na,K-ATPase alpha- and beta-subunits for correct posttranslational processing and intracellular transport. FEBS Lett. 269, 105–108.

Akimova, O., Tremblay, J., Hamet, P., and Orlov, S.N. (2006). The Na+/K+-ATPase as [K+]o sensor: Role in cardiovascular disease pathogenesis and augmented production of endogenous cardiotonic steroids. Pathophysiology 13, 209–216.

Akimova, O.A., Bagrov, A.Y., Lopina, O.D., Kamernitsky, A.V., Tremblay, J., Hamet, P., and Orlov, S.N. (2005). Cardiotonic steroids differentially affect intracellular Na+ and [Na+]i/[K+]i-independent signaling in C7-MDCK cells. J. Biol. Chem. 280, 832–839.

Alberts, B., Johnson, A., Lewis, J., Raff, M., Roberts, K., and Walter, P. (2002). Molecular Biology of the Cell (Garland Science).

Annes, J.P., Chen, Y., Munger, J.S., and Rifkin, D.B. (2004). Integrin αVβ6-mediated activation of latent TGF-β requires the latent TGF-β binding protein-1. J. Cell Biol. 165, 723–734.

Aperia, A. (2007). New roles for an old enzyme: Na,K-ATPase emerges as an interesting drug target. J. Intern. Med. 261, 44–52.

Aronow, W.S., and Aranow, W.S. (1992). Clinical use of digitalis. Compr. Ther. 18, 38–41.

B Moore, B., Lawson, W.E., Oury, T.D., Sisson, T.H., Raghavendran, K., and Hogaboam, C.M. (2013). Animal models of fibrotic lung disease. Am. J. Respir. Cell Mol. Biol. 49, 167–179.

Bartram, U., and Speer, C.P. (2004). The role of transforming growth factor beta in lung development and disease. Chest 125, 754–765.

Baumgartner, K.B., Samet, J.M., Stidley, C.A., Colby, T.V., and Waldron, J.A. (1997). Cigarette smoking: a risk factor for idiopathic pulmonary fibrosis. Am. J. Respir. Crit. Care Med. 155, 242–248.

Biernacka, A., Dobaczewski, M., and Frangogiannis, N.G. (2011). TGF-β signaling in fibrosis. Growth Factors Chur Switz. 29, 196–202.

Billman, G.E. (2001). KB-R7943. Kanebo. Curr. Opin. Investig. Drugs Lond. Engl. 2000 2, 1740–1745.

Blaustein, M.P., and Lederer, W.J. (1999). Sodium/calcium exchange: its physiological implications. Physiol. Rev. 79, 763–854.

Bonner, J.C., Rice, A.B., Ingram, J.L., Moomaw, C.R., Nyska, A., Bradbury, A., Sessoms, A.R., Chulada, P.C., Morgan, D.L., Zeldin, D.C., et al. (2002). Susceptibility of cyclooxygenase-2-deficient mice to pulmonary fibrogenesis. Am. J. Pathol. 161, 459–470.

Bonniaud, P., Margetts, P.J., Kolb, M., Schroeder, J.A., Kapoun, A.M., Damm, D., Murphy, A., Chakravarty, S., Dugar, S., Higgins, L., et al. (2005). Progressive transforming growth factor beta1-induced lung fibrosis is blocked by an orally active ALK5 kinase inhibitor. Am. J. Respir. Crit. Care Med. 171, 889–898.

Borok, Z., Gillissen, A., Buhl, R., Hoyt, R.F., Hubbard, R.C., Ozaki, T., Rennard, S.I., and Crystal, R.G. (1991). Augmentation of functional prostaglandin E levels on the respiratory epithelial surface by aerosol administration of prostaglandin E. Am. Rev. Respir. Dis. 144, 1080–1084.

Briones-Orta, M.A., Tecalco-Cruz, A.C., Sosa-Garrocho, M., Caligaris, C., and Macías-Silva, M. (2011). Inhibitory Smad7: emerging roles in health and disease. Curr. Mol. Pharmacol. 4, 141–153.

Broekelmann, T.J., Limper, A.H., Colby, T.V., and McDonald, J.A. (1991). Transforming growth factor beta 1 is present at sites of extracellular matrix gene expression in human pulmonary fibrosis. Proc. Natl. Acad. Sci. U. S. A. 88, 6642–6646.

de Caestecker, M.P., Piek, E., and Roberts, A.B. (2000). Role of transforming growth factor-beta signaling in cancer. J. Natl. Cancer Inst. 92, 1388–1402.

Chaldakov, D.G.N., Nabika, T., Nara, Y., and Yamori, Y. (1989). Cyclic AMPand cytochalasin B-induced arborization in cultured aortic smooth muscle cells: its cytopharmacological characterization. Cell Tissue Res. 255, 435–442.

Chen, J., Ghorai, M.K., Kenney, G., and Stubbe, J. (2008). Mechanistic studies on bleomycin-mediated DNA damage: multiple binding modes can result in double-stranded DNA cleavage. Nucleic Acids Res. 36, 3781–3790.

Clements, J.A. (1997). LUNG SURFACTANT: A Personal Perspective. Annu. Rev. Physiol. 59, 1–21.

Coalson, J.J. (1982). The ultrastructure of human fibrosing alveolitis. Virchows Arch. A Pathol. Anat. Histol. 395, 181–199.

Coleman, D.T., Gray, A.L., Stephens, C.A., Scott, M.L., and Cardelli, J.A. (2016). Repurposed drug screen identifies cardiac glycosides as inhibitors of TGF-β-induced cancer-associated fibroblast differentiation. Oncotarget.

Coultas, D.B., Zumwalt, R.E., Black, W.C., and Sobonya, R.E. (1994). The epidemiology of interstitial lung diseases. Am. J. Respir. Crit. Care Med. 150, 967–972.

Coward, W.R., Watts, K., Feghali-Bostwick, C.A., Knox, A., and Pang, L. (2009). Defective histone acetylation is responsible for the diminished expression of cyclooxygenase 2 in idiopathic pulmonary fibrosis. Mol. Cell. Biol. 29, 4325–4339.

Dackor, R.T., Cheng, J., Voltz, J.W., Card, J.W., Ferguson, C.D., Garrett, R.C., Bradbury, J.A., DeGraff, L.M., Lih, F.B., Tomer, K.B., et al. (2011). Prostaglandin E2 protects murine lungs from bleomycin-induced pulmonary fibrosis and lung dysfunction. Am. J. Physiol. - Lung Cell. Mol. Physiol. 301, L645–L655.

Darby, I.A., Laverdet, B., Bonté, F., and Desmoulière, A. (2014). Fibroblasts and myofibroblasts in wound healing. Clin. Cosmet. Investig. Dermatol. 7, 301–311.

Davis, A., Hogarth, K., Fernandes, D., Solway, J., Niu, J., Kolenko, V., Browning, D., Miano, J.M., Orlov, S.N., and Dulin, N.O. (2003). Functional significance of protein kinase A activation by endothelin-1 and ATP: negative regulation of SRF-dependent gene expression by PKA. Cell. Signal. 15, 597–604.

Degryse, A.L., and Lawson, W.E. (2011). Progress toward improving animal models for idiopathic pulmonary fibrosis. Am. J. Med. Sci. 341, 444–449.

Derynck, R., and Zhang, Y.E. (2003). Smad-dependent and Smad-independent pathways in TGF-beta family signalling. Nature 425, 577–584.

Desmoulière, A., Redard, M., Darby, I., and Gabbiani, G. (1995). Apoptosis mediates the decrease in cellularity during the transition between granulation tissue and scar. Am. J. Pathol. 146, 56–66.

Desmoulière, A., Chaponnier, C., and Gabbiani, G. (2005). Tissue repair, contraction, and the myofibroblast. Wound Repair Regen. Off. Publ. Wound Heal. Soc. Eur. Tissue Repair Soc. 13, 7–12.

Di Guglielmo, G.M., Le Roy, C., Goodfellow, A.F., and Wrana, J.L. (2003). Distinct endocytic pathways regulate TGF-beta receptor signalling and turnover. Nat. Cell Biol. 5, 410–421.

Dutta, S., and Marks, B.H. (1966). Distribution of ouabain and digoxin in the rat and guinea pig. Life Sci. 5, 915–920.

Elkareh, J., Kennedy, D.J., Yashaswi, B., Vetteth, S., Shidyak, A., Kim, E.G.R., Smaili, S., Periyasamy, S.M., Hariri, I.M., Fedorova, L., et al. (2007). Marinobufagenin stimulates fibroblast collagen production and causes fibrosis in experimental uremic cardiomyopathy. Hypertens. Dallas Tex 1979 49, 215–224.

Elkareh, J., Periyasamy, S.M., Shidyak, A., Vetteth, S., Schroeder, J., Raju, V., Hariri, I.M., El-Okdi, N., Gupta, S., Fedorova, L., et al. (2009). Marinobufagenin induces

increases in procollagen expression in a process involving protein kinase C and Fli-1: implications for uremic cardiomyopathy. Am. J. Physiol. - Ren. Physiol. 296, F1219–F1226.

El-Okdi, N., Smaili, S., Raju, V., Shidyak, A., Gupta, S., Fedorova, L., Elkareh, J., Periyasamy, S., Shapiro, A.P., Kahaleh, M.B., et al. (2008). Effects of cardiotonic steroids on dermal collagen synthesis and wound healing. J. Appl. Physiol. Bethesda Md 1985 105, 30–36.

Evans, I.C., Barnes, J.L., Garner, I.M., Pearce, D.R., Maher, T.M., Shiwen, X., Renzoni, E.A., Wells, A.U., Denton, C.P., Laurent, G.J., et al. (2016). Epigenetic regulation of cyclooxygenase-2 by methylation of c8orf4 in pulmonary fibrosis. Clin. Sci. Lond. Engl. 1979 130, 575–586.

Fedorova, O.V., Emelianov, I.V., Bagrov, K.A., Grigorova, Y.N., Wei, W., Juhasz, O., Frolova, E.V., Marshall, C.A., Lakatta, E.G., Konradi, A.O., et al. (2015). Marinobufagenin-induced vascular fibrosis is a likely target for mineralocorticoid antagonists. J. Hypertens. 33, 1602–1610.

Fehrenbach, H. (2001). Alveolar epithelial type II cell: defender of the alveolus revisited. Respir. Res. 2, 33–46.

Feng, X.-H., and Derynck, R. (2005). Specificity and versatility in tgf-beta signaling through Smads. Annu. Rev. Cell Dev. Biol. 21, 659–693.

Fernandez, I.E., and Eickelberg, O. (2012). The Impact of TGF-β on Lung Fibrosis. Proc. Am. Thorac. Soc. 9, 111–116.

Gabbiani, G. (2003). The myofibroblast in wound healing and fibrocontractive diseases. J. Pathol. 200, 500–503.

Gabbiani, G., Ryan, G.B., and Majno, G. Presence of modified fibroblasts in granulation tissue and their possible role in wound contraction. Experientia 27, 549–550.

Gauldie, J. (2002). Inflammatory Mechanisms Are a Minor Component of the Pathogenesis of Idiopathic Pulmonary Fibrosis. Am. J. Respir. Crit. Care Med. 165, 1205–1206.

Geering, K. (2001). The functional role of beta subunits in oligomeric P-type ATPases. J. Bioenerg. Biomembr. 33, 425–438.

Geering, K., Theulaz, I., Verrey, F., Häuptle, M.T., and Rossier, B.C. (1989). A role for the beta-subunit in the expression of functional Na+-K+-ATPase in Xenopus oocytes. Am. J. Physiol. 257, C851-858.

Geering, K., Beggah, A., Good, P., Girardet, S., Roy, S., Schaer, D., and Jaunin, P. (1996). Oligomerization and maturation of Na,K-ATPase: functional interaction of the

cytoplasmic NH2 terminus of the beta subunit with the alpha subunit. J. Cell Biol. 133, 1193–1204.

George, J., Roulot, D., Koteliansky, V.E., and Bissell, D.M. (1999). In vivo inhibition of rat stellate cell activation by soluble transforming growth factor beta type II receptor: a potential new therapy for hepatic fibrosis. Proc. Natl. Acad. Sci. U. S. A. 96, 12719–12724.

von Gersdorff, G., Susztak, K., Rezvani, F., Bitzer, M., Liang, D., and Böttinger, E.P. (2000). Smad3 and Smad4 mediate transcriptional activation of the human Smad7 promoter by transforming growth factor beta. J. Biol. Chem. 275, 11320–11326.

Giri, S.N., and Hyde, D.M. (1987). Increases in severity of lung damage and mortality by treatment with cyclo and lipoxygenase inhibitors in bleomycin and hyperoxia model of lung injury in hamsters. Pathology (Phila.) 19, 150–158.

Glantz, S.A., Kernoff, R., and Goldman, R.H. (1976). Age-related changes in ouabain pharmacology. Ouabain exhibits a different volume of distribution in adult and young dogs. Circ. Res. 39, 407–414.

Gross, N.J. (1977). Pulmonary effects of radiation therapy. Ann. Intern. Med. 86, 81–92.

Gross, T.J., and Hunninghake, G.W. (2001). Idiopathic Pulmonary Fibrosis. N. Engl. J. Med. 345, 517–525.

Hay, J., Shahzeidi, S., and Laurent, G. (1991). Mechanisms of bleomycin-induced lung damage. Arch. Toxicol. 65, 81–94.

Hilberg, F., Roth, G.J., Krssak, M., Kautschitsch, S., Sommergruber, W., Tontsch-Grunt, U., Garin-Chesa, P., Bader, G., Zoephel, A., Quant, J., et al. (2008). BIBF 1120: triple angiokinase inhibitor with sustained receptor blockade and good antitumor efficacy. Cancer Res. 68, 4774–4782.

Hinz, B. (2006). Masters and servants of the force: the role of matrix adhesions in myofibroblast force perception and transmission. Eur. J. Cell Biol. 85, 175–181.

Hinz, B., Celetta, G., Tomasek, J.J., Gabbiani, G., and Chaponnier, C. (2001). Alpha-smooth muscle actin expression upregulates fibroblast contractile activity. Mol. Biol. Cell 12, 2730–2741.

Hinz, B., Phan, S.H., Thannickal, V.J., Galli, A., Bochaton-Piallat, M.-L., and Gabbiani, G. (2007). The myofibroblast: one function, multiple origins. Am. J. Pathol. 170, 1807–1816.

Hirano, A., Kanehiro, A., Ono, K., Ito, W., Yoshida, A., Okada, C., Nakashima, H., Tanimoto, Y., Kataoka, M., Gelfand, E.W., et al. (2006). Pirfenidone modulates airway responsiveness, inflammation, and remodeling after repeated challenge. Am. J. Respir. Cell Mol. Biol. 35, 366–377.

Hla, T., and Neilson, K. (1992). Human cyclooxygenase-2 cDNA. Proc. Natl. Acad. Sci. U. S. A. 89, 7384–7388.

Hogarth, D.K., Sandbo, N., Taurin, S., Kolenko, V., Miano, J.M., and Dulin, N.O. (2004). Dual role of PKA in phenotypic modulation of vascular smooth muscle cells by extracellular ATP. Am. J. Physiol. Cell Physiol. 287, C449-456.

Huang, S., Wettlaufer, S.H., Hogaboam, C., Aronoff, D.M., and Peters-Golden, M. (2007). Prostaglandin E(2) inhibits collagen expression and proliferation in patient-derived normal lung fibroblasts via E prostanoid 2 receptor and cAMP signaling. Am. J. Physiol. Lung Cell. Mol. Physiol. 292, L405-413.

Huang, S.K., Wettlaufer, S.H., Chung, J., and Peters-Golden, M. (2008). Prostaglandin E2 inhibits specific lung fibroblast functions via selective actions of PKA and Epac-1. Am. J. Respir. Cell Mol. Biol. 39, 482–489.

Huang, S.K., White, E.S., Wettlaufer, S.H., Grifka, H., Hogaboam, C.M., Thannickal, V.J., Horowitz, J.C., and Peters-Golden, M. (2009). Prostaglandin E2 induces fibroblast apoptosis by modulating multiple survival pathways. FASEB J. 23, 4317–4326.

Huaux, F., Louahed, J., Hudspith, B., Meredith, C., Delos, M., Renauld, J.C., and Lison, D. (1998). Role of interleukin-10 in the lung response to silica in mice. Am. J. Respir. Cell Mol. Biol. 18, 51–59.

Hubbard, R., Lewis, S., Richards, K., Johnston, I., and Britton, J. (1996). Occupational exposure to metal or wood dust and aetiology of cryptogenic fibrosing alveolitis. Lancet Lond. Engl. 347, 284–289.

Iwai, K., Mori, T., Yamada, N., Yamaguchi, M., and Hosoda, Y. (1994). Idiopathic pulmonary fibrosis. Epidemiologic approaches to occupational exposure. Am. J. Respir. Crit. Care Med. 150, 670–675.

Iyer, S.N., Wild, J.S., Schiedt, M.J., Hyde, D.M., Margolin, S.B., and Giri, S.N. (1995). Dietary intake of pirfenidone ameliorates bleomycin-induced lung fibrosis in hamsters. J. Lab. Clin. Med. 125, 779–785.

Iyer, S.N., Margolin, S.B., Hyde, D.M., and Giri, S.N. (1998). Lung fibrosis is ameliorated by pirfenidone fed in diet after the second dose in a three-dose bleomycin-hamster model. Exp. Lung Res. 24, 119–132.

Izbicki, G., Segel, M.J., Christensen, T.G., Conner, M.W., and Breuer, R. (2002). Time course of bleomycin-induced lung fibrosis. Int. J. Exp. Pathol. 83, 111–119.

Jakowlew, S.B. (2006). Transforming growth factor-beta in cancer and metastasis. Cancer Metastasis Rev. 25, 435–457.

Janick-Buckner, D., Ranges, G.E., and Hacker, M.P. (1989). Alteration of bronchoalveolar lavage cell populations following bleomycin treatment in mice. Toxicol. Appl. Pharmacol. 100, 465–473.

Jonk, L.J., Itoh, S., Heldin, C.H., ten Dijke, P., and Kruijer, W. (1998). Identification and functional characterization of a Smad binding element (SBE) in the JunB promoter that acts as a transforming growth factor-beta, activin, and bone morphogenetic protein-inducible enhancer. J. Biol. Chem. 273, 21145–21152.

Kach, J., Sandbo, N., Sethakorn, N., Williams, J., Reed, E.B., La, J., Tian, X., Brain, S.D., Rajendran, K., Krishnan, R., et al. (2013). Regulation of myofibroblast differentiation and bleomycin-induced pulmonary fibrosis by adrenomedullin. Am. J. Physiol. Lung Cell. Mol. Physiol. 304, L757-764.

Kach, J., Sandbo, N., La, J., Denner, D., Reed, E.B., Akimova, O., Koltsova, S., Orlov, S.N., and Dulin, N.O. (2014). Antifibrotic effects of noscapine through activation of prostaglandin E2 receptors and protein kinase A. J. Biol. Chem. 289, 7505–7513.

Kaplan, J.H. (2002). Biochemistry of Na,K-ATPase. Annu. Rev. Biochem. 71, 511–535.

Kasai, H., Allen, J.T., Mason, R.M., Kamimura, T., and Zhang, Z. (2005). TGF-β1 induces human alveolar epithelial to mesenchymal cell transition (EMT). Respir. Res. 6, 56.

Kasper, M., and Haroske, G. (1996). Alterations in the alveolar epithelium after injury leading to pulmonary fibrosis. Histol. Histopathol. 11, 463–483.

Katzenstein, A.L., and Myers, J.L. (1998). Idiopathic pulmonary fibrosis: clinical relevance of pathologic classification. Am. J. Respir. Crit. Care Med. 157, 1301–1315.

Kawanami, O., Ferrans, V.J., and Crystal, R.G. (1982). Structure of alveolar epithelial cells in patients with fibrotic lung disorders. Lab. Investig. J. Tech. Methods Pathol. 46, 39–53.

Keerthisingam, C.B., Jenkins, R.G., Harrison, N.K., Hernandez-Rodriguez, N.A., Booth, H., Laurent, G.J., Hart, S.L., Foster, M.L., and McAnulty, R.J. (2001). Cyclooxygenase-2 deficiency results in a loss of the anti-proliferative response to transforming growth factor-beta in human fibrotic lung fibroblasts and promotes bleomycin-induced pulmonary fibrosis in mice. Am. J. Pathol. 158, 1411–1422.

Keogh, B.A., and Crystal, R.G. (1982). Alveolitis: the key to the interstitial lung disorders. Thorax 37, 1–10.

Khalil, N., O'Connor, R.N., Flanders, K.C., and Unruh, H. (1996). TGF-beta 1, but not TGF-beta 2 or TGF-beta 3, is differentially present in epithelial cells of advanced pulmonary fibrosis: an immunohistochemical study. Am. J. Respir. Cell Mol. Biol. 14, 131–138.

King, T.E., Schwarz, M.I., Brown, K., Tooze, J.A., Colby, T.V., Waldron, J.A., Flint, A., Thurlbeck, W., and Cherniack, R.M. (2001). Idiopathic pulmonary fibrosis: relationship between histopathologic features and mortality. Am. J. Respir. Crit. Care Med. 164, 1025–1032.

King Jr, T.E., Pardo, A., and Selman, M. (2011). Idiopathic pulmonary fibrosis. The Lancet 378, 1949–1961.

Klimanova, E.A., Petrushanko, I.Y., Mitkevich, V.A., Anashkina, A.A., Orlov, S.N., Makarov, A.A., and Lopina, O.D. (2015). Binding of ouabain and marinobufagenin leads to different structural changes in Na,K-ATPase and depends on the enzyme conformation. FEBS Lett. 589, 2668–2674.

Kolodsick, J.E., Peters-Golden, M., Larios, J., Toews, G.B., Thannickal, V.J., and Moore, B.B. (2003). Prostaglandin E2 inhibits fibroblast to myofibroblast transition via E. prostanoid receptor 2 signaling and cyclic adenosine monophosphate elevation. Am. J. Respir. Cell Mol. Biol. 29, 537–544.

La, J., Reed, E.B., Koltsova, S., Akimova, O., Hamanaka, R.B., Mutlu, G.M., Orlov, S.N., and Dulin, N.O. (2016). Regulation of myofibroblast differentiation by cardiac glycosides. Am. J. Physiol. Lung Cell. Mol. Physiol. 310, L815-823.

Lama, V., Moore, B.B., Christensen, P., Toews, G.B., and Peters-Golden, M. (2002). Prostaglandin E2 synthesis and suppression of fibroblast proliferation by alveolar epithelial cells is cyclooxygenase-2-dependent. Am. J. Respir. Cell Mol. Biol. 27, 752–758.

Larkin, J.M., Brown, M.S., Goldstein, J.L., and Anderson, R.G. (1983). Depletion of intracellular potassium arrests coated pit formation and receptor-mediated endocytosis in fibroblasts. Cell 33, 273–285.

Larkin, J.M., Donzell, W.C., and Anderson, R.G. (1985). Modulation of intracellular potassium and ATP: effects on coated pit function in fibroblasts and hepatocytes. J. Cell. Physiol. 124, 372–378.

Laursen, M., Yatime, L., Nissen, P., and Fedosova, N.U. (2013). Crystal structure of the high-affinity Na+,K+-ATPase–ouabain complex with Mg2+ bound in the cation binding site. Proc. Natl. Acad. Sci. 110, 10958–10963.

Leask, A., and Abraham, D.J. (2004). TGF-beta signaling and the fibrotic response. FASEB J. Off. Publ. Fed. Am. Soc. Exp. Biol. 18, 816–827.

Levenson, R. (1994). Isoforms of the Na,K-ATPase: family members in search of function. Rev. Physiol. Biochem. Pharmacol. 123, 1–45.

Ley, B., Collard, H.R., and King, T.E. (2011). Clinical Course and Prediction of Survival in Idiopathic Pulmonary Fibrosis. Am. J. Respir. Crit. Care Med. 183, 431–440.

Lingrel, J.B. (2010). The physiological significance of the cardiotonic steroid/ouabain-binding site of the Na,K-ATPase. Annu. Rev. Physiol. 72, 395–412.

Lingrel, J.B., Argüello, J.M., Van Huysse, J., and Kuntzweiler, T.A. (1997). Cation and cardiac glycoside binding sites of the Na,K-ATPase. Ann. N. Y. Acad. Sci. 834, 194–206.

Liu, J., and Xie, Z.-J. (2010). The sodium pump and cardiotonic steroids-induced signal transduction protein kinases and calcium-signaling microdomain in regulation of transporter trafficking. Biochim. Biophys. Acta 1802, 1237–1245.

Liu, F., Mih, J.D., Shea, B.S., Kho, A.T., Sharif, A.S., Tager, A.M., and Tschumperlin, D.J. (2010). Feedback amplification of fibrosis through matrix stiffening and COX-2 suppression. J. Cell Biol. 190, 693–706.

Liu, F., Lagares, D., Choi, K.M., Stopfer, L., Marinković, A., Vrbanac, V., Probst, C.K., Hiemer, S.E., Sisson, T.H., Horowitz, J.C., et al. (2015). Mechanosignaling through YAP and TAZ drives fibroblast activation and fibrosis. Am. J. Physiol. Lung Cell. Mol. Physiol. 308, L344-357.

Liu, H., Drew, P., Gaugler, A.C., Cheng, Y., and Visner, G.A. (2005). Pirfenidone inhibits lung allograft fibrosis through L-arginine-arginase pathway. Am. J. Transplant. Off. J. Am. Soc. Transplant. Am. Soc. Transpl. Surg. 5, 1256–1263.

Lok, S.S., Stewart, J.P., Kelly, B.G., Hasleton, P.S., and Egan, J.J. (2001). Epstein-Barr virus and wild p53 in idiopathic pulmonary fibrosis. Respir. Med. 95, 787–791.

Lovgren, A.K., Jania, L.A., Hartney, J.M., Parsons, K.K., Audoly, L.P., Fitzgerald, G.A., Tilley, S.L., and Koller, B.H. (2006). COX-2-derived prostacyclin protects against bleomycin-induced pulmonary fibrosis. Am. J. Physiol. Lung Cell. Mol. Physiol. 291, L144-156.

MacKenzie, K.F., Clark, K., Naqvi, S., McGuire, V.A., Nöehren, G., Kristariyanto, Y., van den Bosch, M., Mudaliar, M., McCarthy, P.C., Pattison, M.J., et al. (2013). PGE(2) induces macrophage IL-10 production and a regulatory-like phenotype via a protein kinase A-SIK-CRTC3 pathway. J. Immunol. Baltim. Md 1950 190, 565–577.

Marinković, A., Mih, J.D., Park, J.-A., Liu, F., and Tschumperlin, D.J. (2012). Improved throughput traction microscopy reveals pivotal role for matrix stiffness in fibroblast contractility and TGF-β responsiveness. Am. J. Physiol. Lung Cell. Mol. Physiol. 303, L169-180.

Mason, R.J., Schwarz, M.I., Hunninghake, G.W., and Musson, R.A. (1999). NHLBI Workshop Summary. Pharmacological therapy for idiopathic pulmonary fibrosis. Past, present, and future. Am. J. Respir. Crit. Care Med. 160, 1771–1777.

Massagué, J. (1992). Receptors for the TGF-beta family. Cell 69, 1067–1070.

Massagué, J. (2008). TGFbeta in Cancer. Cell 134, 215–230.

Massagué, J. (2012). TGFβ signalling in context. Nat. Rev. Mol. Cell Biol. 13, 616–630.

McDonald, T.F., Pelzer, S., Trautwein, W., and Pelzer, D.J. (1994). Regulation and modulation of calcium channels in cardiac, skeletal, and smooth muscle cells. Physiol. Rev. 74, 365–507.

Menger, L., Vacchelli, E., Kepp, O., Eggermont, A., Tartour, E., Zitvogel, L., Kroemer, G., and Galluzzi, L. (2013). Trial watch: Cardiac glycosides and cancer therapy. Oncoimmunology 2, e23082.

Midgley, A.C., Rogers, M., Hallett, M.B., Clayton, A., Bowen, T., Phillips, A.O., and Steadman, R. (2013). Transforming growth factor-β1 (TGF-β1)-stimulated fibroblast to myofibroblast differentiation is mediated by hyaluronan (HA)-facilitated epidermal growth factor receptor (EGFR) and CD44 co-localization in lipid rafts. J. Biol. Chem. 288, 14824–14838.

Miralles, F., Posern, G., Zaromytidou, A.-I., and Treisman, R. (2003). Actin dynamics control SRF activity by regulation of its coactivator MAL. Cell 113, 329–342.

Miyazono, K., Olofsson, A., Colosetti, P., and Heldin, C.H. (1991). A role of the latent TGF-beta 1-binding protein in the assembly and secretion of TGF-beta 1. EMBO J. 10, 1091–1101.

Moore, B.B., and Hogaboam, C.M. (2008). Murine models of pulmonary fibrosis. Am. J. Physiol. Lung Cell. Mol. Physiol. 294, L152-160.

Muggia, F.M., Louie, A.C., and Sikic, B.I. (1983). Pulmonary toxicity of antitumor agents. Cancer Treat. Rev. 10, 221–243.

Munger, J.S., Huang, X., Kawakatsu, H., Griffiths, M.J., Dalton, S.L., Wu, J., Pittet, J.F., Kaminski, N., Garat, C., Matthay, M.A., et al. (1999). The integrin alpha v beta 6 binds and activates latent TGF beta 1: a mechanism for regulating pulmonary inflammation and fibrosis. Cell 96, 319–328.

Nagarajan, R.P., Zhang, J., Li, W., and Chen, Y. (1999). Regulation of Smad7 Promoter by Direct Association with Smad3 and Smad4. J. Biol. Chem. 274, 33412–33418.

Nakao, S., Ogata, Y., Modéer, T., Segawa, M., Furuyama, S., and Sugiya, H. (2001). Bradykinin induces a rapid cyclooxygenase-2 mRNA expression via Ca2+mobilization in human gingival fibroblasts primed with interleukin-1 β. Cell Calcium 29, 446–452.

Nakayama, T., Mutsuga, N., Yao, L., and Tosato, G. (2006). Prostaglandin E2 promotes degranulation-independent release of MCP-1 from mast cells. J. Leukoc. Biol. 79, 95–104.

Noble, P.W., Albera, C., Bradford, W.Z., Costabel, U., Glassberg, M.K., Kardatzke, D., King Jr, T.E., Lancaster, L., Sahn, S.A., Szwarcberg, J., et al. (2011). Pirfenidone in patients with idiopathic pulmonary fibrosis (CAPACITY): two randomised trials. The Lancet 377, 1760–1769.

Noguchi, S., Mishina, M., Kawamura, M., and Numa, S. (1987). Expression of functional (Na+ + K+)-ATPase from cloned cDNAs. FEBS Lett. 225, 27–32.

O'Banion, M.K., Sadowski, H.B., Winn, V., and Young, D.A. (1991). A serum- and glucocorticoid-regulated 4-kilobase mRNA encodes a cyclooxygenase-related protein. J. Biol. Chem. 266, 23261–23267.

Oku, H., Shimizu, T., Kawabata, T., Nagira, M., Hikita, I., Ueyama, A., Matsushima, S., Torii, M., and Arimura, A. (2008). Antifibrotic action of pirfenidone and prednisolone: different effects on pulmonary cytokines and growth factors in bleomycin-induced murine pulmonary fibrosis. Eur. J. Pharmacol. 590, 400–408.

Orlov, S.N., and Hamet, P. (2015). Salt and gene expression: evidence for [Na+]i/[K+]i-mediated signaling pathways. Pflüg. Arch. Eur. J. Physiol. 467, 489–498.

Orlov, S., Resink, T.J., Bernhardt, J., Ferracin, F., and Buhler, F.R. (1993). Vascular smooth muscle cell calcium fluxes. Regulation by angiotensin II and lipoproteins. Hypertens. Dallas Tex 1979 21, 195–203.

Orlov, S.N., Tremblay, J., and Hamet, P. (1996a). Cell volume in vascular smooth muscle is regulated by bumetanide-sensitive ion transport. Am. J. Physiol. 270, C1388-1397.

Orlov, S.N., Tremblay, J., and Hamet, P. (1996b). cAMP signaling inhibits dihydropyridine-sensitive Ca2+ influx in vascular smooth muscle cells. Hypertens. Dallas Tex 1979 27, 774–780.

Orlowski, J., and Lingrel, J.B. (1988). Tissue-specific and developmental regulation of rat Na,K-ATPase catalytic alpha isoform and beta subunit mRNAs. J. Biol. Chem. 263, 10436–10442.

Penheiter, S.G., Mitchell, H., Garamszegi, N., Edens, M., Jules J. E. Doré, J., and Leof, E.B. (2002). Internalization-Dependent and -Independent Requirements for Transforming Growth Factor β Receptor Signaling via the Smad Pathway. Mol. Cell. Biol. 22, 4750–4759.

Petkova, D.K., Clelland, C.A., Ronan, J.E., Lewis, S., and Knox, A.J. (2003). Reduced expression of cyclooxygenase (COX) in idiopathic pulmonary fibrosis and sarcoidosis. Histopathology 43, 381–386.

Pezier, A., Bobkov, Y.V., and Ache, B.W. (2009). The Na+/Ca2+ exchanger inhibitor, KB-R7943, blocks a nonselective cation channel implicated in chemosensory transduction. J. Neurophysiol. 101, 1151–1159.

Phan, S.H. (2008). Biology of Fibroblasts and Myofibroblasts. Proc. Am. Thorac. Soc. 5, 334–337.

Pubchem (2016). ouabain | C29H44O12 - PubChem.

Raghu, G., Nyberg, F., and Morgan, G. (2004). The epidemiology of interstitial lung disease and its association with lung cancer. Br. J. Cancer 91, S3–S10.

Raghu, G., Weycker, D., Edelsberg, J., Bradford, W.Z., and Oster, G. (2006a). Incidence and prevalence of idiopathic pulmonary fibrosis. Am. J. Respir. Crit. Care Med. 174, 810–816.

Raghu, G., Freudenberger, T.D., Yang, S., Curtis, J.R., Spada, C., Hayes, J., Sillery, J.K., Pope, C.E., and Pellegrini, C.A. (2006b). High prevalence of abnormal acid gastro-oesophageal reflux in idiopathic pulmonary fibrosis. Eur. Respir. J. 27, 136–142.

Raghu, G., Collard, H.R., Egan, J.J., Martinez, F.J., Behr, J., Brown, K.K., Colby, T.V., Cordier, J.-F., Flaherty, K.R., Lasky, J.A., et al. (2011). An official ATS/ERS/JRS/ALAT statement: idiopathic pulmonary fibrosis: evidence-based guidelines for diagnosis and management. Am. J. Respir. Crit. Care Med. 183, 788–824.

Rahaman, S.O., Grove, L.M., Paruchuri, S., Southern, B.D., Abraham, S., Niese, K.A., Scheraga, R.G., Ghosh, S., Thodeti, C.K., Zhang, D.X., et al. (2014). TRPV4 mediates myofibroblast differentiation and pulmonary fibrosis in mice. J. Clin. Invest. 124, 5225–5238.

Redente, E.F., Jacobsen, K.M., Solomon, J.J., Lara, A.R., Faubel, S., Keith, R.C., Henson, P.M., Downey, G.P., and Riches, D.W.H. (2011). Age and sex dimorphisms contribute to the severity of bleomycin-induced lung injury and fibrosis. Am. J. Physiol. Lung Cell. Mol. Physiol. 301, L510-518.

Ricciotti, E., and FitzGerald, G.A. (2011). Prostaglandins and Inflammation. Arterioscler. Thromb. Vasc. Biol. 31, 986–1000.

Richeldi, L., Costabel, U., Selman, M., Kim, D.S., Hansell, D.M., Nicholson, A.G., Brown, K.K., Flaherty, K.R., Noble, P.W., Raghu, G., et al. (2011). Efficacy of a Tyrosine Kinase Inhibitor in Idiopathic Pulmonary Fibrosis. N. Engl. J. Med. 365, 1079–1087.

Richeldi, L., du Bois, R.M., Raghu, G., Azuma, A., Brown, K.K., Costabel, U., Cottin, V., Flaherty, K.R., Hansell, D.M., Inoue, Y., et al. (2014). Efficacy and Safety of Nintedanib in Idiopathic Pulmonary Fibrosis. N. Engl. J. Med. 370, 2071–2082.

Rifkin, D.B. (2005). Latent Transforming Growth Factor-β (TGF-β) Binding Proteins: Orchestrators of TGF-β Availability. J. Biol. Chem. 280, 7409–7412.

Sandbo, N., Kregel, S., Taurin, S., Bhorade, S., and Dulin, N.O. (2009). Critical role of serum response factor in pulmonary myofibroblast differentiation induced by TGF-beta. Am. J. Respir. Cell Mol. Biol. 41, 332–338.

Sandbo, N., Lau, A., Kach, J., Ngam, C., Yau, D., and Dulin, N.O. (2011). Delayed stress fiber formation mediates pulmonary myofibroblast differentiation in response to TGF-β. Am. J. Physiol. Lung Cell. Mol. Physiol. 301, L656-666.

Sanjabi, S., Zenewicz, L.A., Kamanaka, M., and Flavell, R.A. (2009). Anti-inflammatory and pro-inflammatory roles of TGF-beta, IL-10, and IL-22 in immunity and autoimmunity. Curr. Opin. Pharmacol. 9, 447–453.

Schatzmann, H.J., and Räss, B. (1965). [Inhibition of the active Na-K-transport and Na-K-activated membrane ATP-ase of erythrocyte stroma by ouabain]. Helv. Physiol. Pharmacol. Acta 65, C47-49.

Scheiner-Bobis, G., and Schoner, W. (2001). A fresh facet for ouabain action. Nat. Med. 7, 1288–1289.

Schoner, W., and Scheiner-Bobis, G. (2007). Endogenous and exogenous cardiac glycosides: their roles in hypertension, salt metabolism, and cell growth. Am. J. Physiol. Cell Physiol. 293, C509-536.

Schrier, D.J., Kunkel, R.G., and Phan, S.H. (1983). The role of strain variation in murine bleomycin-induced pulmonary fibrosis. Am. Rev. Respir. Dis. 127, 63–66.

Selden, R., and Smith, T.W. (1972). Ouabain pharmacokinetics in dog and man. Determination by radioimmunoassay. Circulation 45, 1176–1182.

Selman, M., King, T.E., Pardo, A., American Thoracic Society, European Respiratory Society, and American College of Chest Physicians (2001). Idiopathic pulmonary fibrosis: prevailing and evolving hypotheses about its pathogenesis and implications for therapy. Ann. Intern. Med. 134, 136–151.

Serini, G., Bochaton-Piallat, M.-L., Ropraz, P., Geinoz, A., Borsi, L., Zardi, L., and Gabbiani, G. (1998). The Fibronectin Domain ED-A Is Crucial for Myofibroblastic Phenotype Induction by Transforming Growth Factor-β1. J. Cell Biol. 142, 873–881.

Silverman, M.E. (1989). William Withering and an account of the foxglove. Clin. Cardiol. 12, 415–418.

Sime, P.J., Xing, Z., Graham, F.L., Csaky, K.G., and Gauldie, J. (1997). Adenovector-mediated gene transfer of active transforming growth factor-beta1 induces prolonged severe fibrosis in rat lung. J. Clin. Invest. 100, 768–776.

Sisson, T.H., Mendez, M., Choi, K., Subbotina, N., Courey, A., Cunningham, A., Dave, A., Engelhardt, J.F., Liu, X., White, E.S., et al. (2010). Targeted injury of type II alveolar epithelial cells induces pulmonary fibrosis. Am. J. Respir. Crit. Care Med. 181, 254–263.

Sisson, T.H., Ajayi, I.O., Subbotina, N., Dodi, A.E., Rodansky, E.S., Chibucos, L.N., Kim, K.K., Keshamouni, V.G., White, E.S., Zhou, Y., et al. (2015). Inhibition of

myocardin-related transcription factor/serum response factor signaling decreases lung fibrosis and promotes mesenchymal cell apoptosis. Am. J. Pathol. 185, 969–986.

Slingerland, M., Cerella, C., Guchelaar, H.J., Diederich, M., and Gelderblom, H. (2013). Cardiac glycosides in cancer therapy: from preclinical investigations towards clinical trials. Invest. New Drugs 31, 1087–1094.

Smith, W.L., Garavito, R.M., and DeWitt, D.L. (1996). Prostaglandin Endoperoxide H Synthases (Cyclooxygenases)-1 and −2. J. Biol. Chem. 271, 33157–33160.

Stenkvist, B. (1999). Is digitalis a therapy for breast carcinoma? Oncol. Rep. 6, 493–496.

Stenkvist, B., Bengtsson, E., Eriksson, O., Holmquist, J., Nordin, B., and Westman-Naeser, S. (1979). Cardiac glycosides and breast cancer. Lancet Lond. Engl. 1, 563.

Stenkvist, B., Bengtsson, E., Dahlqvist, B., Eriksson, O., Jarkrans, T., and Nordin, B. (1982). Cardiac glycosides and breast cancer, revisited. N. Engl. J. Med. 306, 484.

Stubbe, J., and Kozarich, J.W. (1987). Mechanisms of bleomycin-induced DNA degradation. Chem. Rev. 87, 1107–1136.

Sugimoto, Y., and Narumiya, S. (2007). Prostaglandin E Receptors. J. Biol. Chem. 282, 11613–11617.

Taipale, J., Miyazono, K., Heldin, C.H., and Keski-Oja, J. (1994). Latent transforming growth factor-beta 1 associates to fibroblast extracellular matrix via latent TGF-beta binding protein. J. Cell Biol. 124, 171–181.

Taniguchi, H., Ebina, M., Kondoh, Y., Ogura, T., Azuma, A., Suga, M., Taguchi, Y., Takahashi, H., Nakata, K., Sato, A., et al. (2010). Pirfenidone in idiopathic pulmonary fibrosis. Eur. Respir. J. 35, 821–829.

Thannickal, V.J., Lee, D.Y., White, E.S., Cui, Z., Larios, J.M., Chacon, R., Horowitz, J.C., Day, R.M., and Thomas, P.E. (2003). Myofibroblast Differentiation by Transforming Growth Factor-β1 Is Dependent on Cell Adhesion and Integrin Signaling via Focal Adhesion Kinase. J. Biol. Chem. 278, 12384–12389.

Thannickal, V.J., Toews, G.B., White, E.S., Lynch, J.P., and Martinez, F.J. (2004). Mechanisms of pulmonary fibrosis. Annu. Rev. Med. 55, 395–417.

Thomas, P.E., Peters-Golden, M., White, E.S., Thannickal, V.J., and Moore, B.B. (2007). PGE2 inhibition of TGF-β1-induced myofibroblast differentiation is Smad-independent but involves cell shape and adhesion-dependent signaling. Am. J. Physiol. Lung Cell. Mol. Physiol. 293, L417–L428.

Tiitto, L., Bloigu, R., Heiskanen, U., Pääkkö, P., Kinnula, V.L., and Kaarteenaho-Wiik, R. (2006). Relationship between histopathological features and the course of idiopathic pulmonary fibrosis/usual interstitial pneumonia. Thorax 61, 1091–1095.

Tobin, R.W., Pope, C.E., Pellegrini, C.A., Emond, M.J., Sillery, J., and Raghu, G. (1998). Increased prevalence of gastroesophageal reflux in patients with idiopathic pulmonary fibrosis. Am. J. Respir. Crit. Care Med. 158, 1804–1808.

Tokhtaeva, E., Clifford, R.J., Kaplan, J.H., Sachs, G., and Vagin, O. (2012). Subunit isoform selectivity in assembly of Na,K-ATPase α-β heterodimers. J. Biol. Chem. 287, 26115–26125.

Tomasek, J.J., Gabbiani, G., Hinz, B., Chaponnier, C., and Brown, R.A. (2002). Myofibroblasts and mechano-regulation of connective tissue remodelling. Nat. Rev. Mol. Cell Biol. 3, 349–363.

Tsukamoto, K., Hayakawa, H., Sato, A., Chida, K., Nakamura, H., and Miura, K. (2000). Involvement of Epstein-Barr virus latent membrane protein 1 in disease progression in patients with idiopathic pulmonary fibrosis. Thorax 55, 958–961.

Tsukazaki, T., Chiang, T.A., Davison, A.F., Attisano, L., and Wrana, J.L. (1998). SARA, a FYVE domain protein that recruits Smad2 to the TGFbeta receptor. Cell 95, 779–791.

Ueda, T., Ohta, K., Suzuki, N., Yamaguchi, M., Hirai, K., Horiuchi, T., Watanabe, J., Miyamoto, T., and Ito, K. (1992). Idiopathic pulmonary fibrosis and high prevalence of serum antibodies to hepatitis C virus. Am. Rev. Respir. Dis. 146, 266–268.

Vaughan, M.B., Howard, E.W., and Tomasek, J.J. (2000). Transforming growth factor-beta1 promotes the morphological and functional differentiation of the myofibroblast. Exp. Cell Res. 257, 180–189.

Wahl, S.M. (1992). Transforming growth factor beta (TGF-beta) in inflammation: a cause and a cure. J. Clin. Immunol. 12, 61–74.

Wiczer, B.M., Marcu, R., and Hawkins, B.J. (2014). KB-R7943, a plasma membrane Na+/Ca2+ exchanger inhibitor, blocks opening of the mitochondrial permeability transition pore. Biochem. Biophys. Res. Commun. 444, 44–49.

Wilborn, J., Crofford, L.J., Burdick, M.D., Kunkel, S.L., Strieter, R.M., and Peters-Golden, M. (1995). Cultured lung fibroblasts isolated from patients with idiopathic pulmonary fibrosis have a diminished capacity to synthesize prostaglandin E2 and to express cyclooxygenase-2. J. Clin. Invest. 95, 1861–1868.

Williams, M.C. (2003). Alveolar Type I Cells: Molecular Phenotype and Development. Annu. Rev. Physiol. 65, 669–695.

Willis, B.C., Liebler, J.M., Luby-Phelps, K., Nicholson, A.G., Crandall, E.D., du Bois, R.M., and Borok, Z. (2005). Induction of epithelial-mesenchymal transition in alveolar

epithelial cells by transforming growth factor-beta1: potential role in idiopathic pulmonary fibrosis. Am. J. Pathol. 166, 1321–1332.

Witschi, H. (1990). Responses of the lung to toxic injury. Environ. Health Perspect. 85, 5–13.

Wolters, P.J., Collard, H.R., and Jones, K.D. (2014). Pathogenesis of idiopathic pulmonary fibrosis. Annu. Rev. Pathol. 9, 157–179.

Wynn, T.A. (2011). Integrating mechanisms of pulmonary fibrosis. J. Exp. Med. 208, 1339–1350.

Wynn, T.A., and Ramalingam, T.R. (2012). Mechanisms of fibrosis: therapeutic translation for fibrotic disease. Nat. Med. 18, 1028–1040.

Xie, Z., and Askari, A. (2002). Na(+)/K(+)-ATPase as a signal transducer. Eur. J. Biochem. FEBS 269, 2434–2439.

Yata, Y., Gotwals, P., Koteliansky, V., and Rockey, D.C. (2002). Dose-dependent inhibition of hepatic fibrosis in mice by a TGF-beta soluble receptor: implications for antifibrotic therapy. Hepatol. Baltim. Md 35, 1022–1030.

Yatime, L., Laursen, M., Morth, J.P., Esmann, M., Nissen, P., and Fedosova, N.U. (2011). Structural insights into the high affinity binding of cardiotonic steroids to the Na+,K+-ATPase. J. Struct. Biol. 174, 296–306.

Yu, Y., and Chadee, K. (1998). Prostaglandin E2 stimulates IL-8 gene expression in human colonic epithelial cells by a posttranscriptional mechanism. J. Immunol. Baltim. Md 1950 161, 3746–3752.

Zawel, L., Le Dai, J., Buckhaults, P., Zhou, S., Kinzler, K.W., Vogelstein, B., and Kern, S.E. (1998). Human Smad3 and Smad4 Are Sequence-Specific Transcription Activators. Mol. Cell 1, 611–617.

Zhao, Y. (1999). Transforming growth factor-beta (TGF-beta) type I and type II receptors are both required for TGF-beta-mediated extracellular matrix production in lung fibroblasts. Mol. Cell. Endocrinol. 150, 91–97.

Zhu, Y., Hua, P., Rafiq, S., Waffner, E.J., Duffey, M.E., and Lance, P. (2002). Ca2+- and PKC-dependent stimulation of PGE2 synthesis by deoxycholic acid in human colonic fibroblasts. Am. J. Physiol. Gastrointest. Liver Physiol. 283, G503-510.

Zhu, Y., Liu, Y., Zhou, W., Xiang, R., Jiang, L., Huang, K., Xiao, Y., Guo, Z., and Gao, J. (2010). A prostacyclin analogue, iloprost, protects from bleomycin-induced pulmonary fibrosis in mice. Respir. Res. 11, 34.

(2000a). Idiopathic Pulmonary Fibrosis: Diagnosis and Treatment. Am. J. Respir. Crit. Care Med. 161, 646–664.

(2000b). American Thoracic Society. Idiopathic pulmonary fibrosis: diagnosis and treatment. International consensus statement. American Thoracic Society (ATS), and the European Respiratory Society (ERS). Am. J. Respir. Crit. Care Med. 161, 646–664.